The Structural Geology, Kinematics and Timing of Deformation at the Superior craton margin, Gull Rapids, Manitoba

by

Matthew W. Downey

A thesis
presented to the University of Waterloo
in fulfillment of the
thesis requirement for the degree of
Master of Science
in
Earth Sciences

Waterloo, Ontario, Canada, 2005

AUTHOR'S DECLARATION FOR ELECTRONIC SUBMISSION OF A THESIS

I hereby declare that I am the sole author of this thesis. This is a true copy of the thesis, including any required final revisions, as accepted by my examiners.

I understand that my thesis may be made electronically available to the public.

Acknowledgements

Firstly, I would like to thank my advisor Dr. Shoufa Lin for his guidance, support, and patience throughout this work. His help and constructive criticisms were greatly appreciated throughout all aspects of this project. Secondly, I would like to thank my Gull Rapids colleagues, Dr. Christian Böhm of the Manitoba Geological Survey and Melissa Bowerman of the University of Alberta. Their advice and help on this thesis work was greatly appreciated and I could not have done without them. I would also like to thank my thesis and defence committee members Dr. Mario Coniglio, Dr. Bob Linnen, and Dr. Tom Edwards. Dr. Yvette Kuiper, Jen Parks, and Arjan Brem are thanked for their reading of the manuscript and providing useful suggestions and criticisms, and Dr. Larry Heaman and Dr. Russ Hartlaub, of the University of Alberta, for their advice and sharing of unpublished data. I would like to thank Lawrence Norquay and Bill Reynolds of Manitoba Hydro for logistical leadership in the field, and knowledge of Manitoba geology. This project would not be where it is without the support of Tim Corkery, Al Bailes, and Ric Syme of the Manitoba Geological Survey, and they are thanked for their vast knowledge of Manitoba geology and their enthusiasm towards the project. I also thank Sue Fisher for her tireless assistance in all graduate school matters.

Thanks to David Corrigan for providing the opportunity and funding for geochronology work at the Geological Survey of Canada, Ottawa, and special thanks to Nicole Rayner for taking the time to collect the data and go over the results with me. Tom Pestaj at the GSC is also thanked. Logistical field support was admirably supplied by Neill Brandson, Custom Helicopters, and the fantastic people from the Split Lake and Fox Lake Cree Bands. Trevor Allen, Drew Heasman, Tara Penner, Geoff Speers, Jenn Vinck, Tashia Dzikowski, and Todd Middleton provided tireless, and amusing, assistance in the field. The knowledge I have gained from all of these people has made me a much more experienced geologist, and a much better one, and I am truly grateful for it. Financial support was provided by Manitoba Hydro, Manitoba Geological Survey, and NSERC.

I could not have completed this project and gained so much experience without the support of all my friends in Waterloo and from all corners of this country. Their support, advice, humour, and worldly knowledge of all things helped me through graduate school and the ups and downs I have faced during this time, and I could not have done without them. Special thanks go to my old friends James and Mike from Toronto for all the great times we have had over the years; all the comedy and support kept me a laughing and happy guy. Also, to my roommates Katherine and Tiana for putting up with my antics (or lack thereof) day to day, and for helping me through all the rough times; I sincerely could not have got through them without your support. Lastly, special thanks go to my family for their complete and loving support throughout all the good and bad times.

Abstract

The Gull Rapids area, Manitoba, lies on the Superior craton margin and forms part of the Superior Boundary Zone (SBZ), a major collisional zone between the Archean Superior craton and the adjacent Paleoproterozoic Trans-Hudson Orogen. There are two main rock assemblages at Gull Rapids: orthogneisses (of possible Split Lake Block origin) and supracrustal rocks (metavolcanic and metasedimentary). Late, crosscutting felsic and mafic intrusive bodies (mostly dykes and sills) are used to constrain the relative and absolute timing of deformation and metamorphism.

The Gull Rapids area records a complex tectonic history. The area experienced four generations of Neoarchean ductile and brittle deformation (G1 – G4) and one of Paleoproterozoic ductile-brittle deformation (G5). G1 deformation produced the main foliation in the map area, as well as local isoclinal folding which may be related to an early shearing event. M1a prograde mid-amphibolite facies metamorphism is contemporaneous with the early stages of G1. Widespread, tight to isoclinal sheath folding during G2 was recorded in the supracrustal assemblage, and is the result of southwest-side-up, dextral shearing during the early shearing event. A ca. 2.68 Ga widespread phase of granitoid intrusion was emplaced late-G1 to early-G2, and is rich in metamorphic minerals that record conditions of M1b upper-amphibolite facies peak metamorphism. M1b metamorphism, late-G1 to early-G2 deformation, and intrusion of this felsic phase are contemporaneous. M2 retrograde metamorphism to mid-amphibolite facies was recorded sometime after M1b. G1 and G2 structures were re-folded during G3, which was then followed by G4 southwest-side-up, dextral and sinistral shearing, contemporaneous with late pegmatite intrusion at ca. 2.61 Ga. This was followed by mafic dyke emplacement at ca. 2.10 Ga, and then by G5 sinistral and dextral shearing and M3 greenschist facies metamorphism or hydrothermal alteration at ca. 1.80 Ga.

Deformation and metamorphism at Gull Rapids post-dates emplacement and deposition of gneissic and supracrustal rocks, respectively. This deformation and metamorphism, except for G5 and

M3, is Neoarchean (ca. 2.68–2.61 Ga), and represents a significant movement of crustal blocks: km-scale shearing of the supracrustal assemblage and consequent uplift of the Split Lake Block. Late deformation and metamorphism (G5, M3) may be related to the Paleoproterozoic Trans-Hudson orogeny. The Neoarchean and Paleoproterozoic zircon populations in the geochronological data suggest that the Gull Rapids area largely experienced Neoarchean deformation and metamorphism with a weak Paleoproterozoic overprint. All of the evidence presented above suggests that the Gull Rapids area lies in a part of the Superior Boundary Zone, yet does not lie at the exact margin of the Superior craton, and therefore does not mark the Archean-Proterozoic boundary proper in northeastern Manitoba.

Table of Contents

List of Figures

Map in back pocket

Detailed structural and geological map of the Gull Rapids area (1:5 000)

List of Tables

Chapter 1

GENERAL INTRODUCTION AND THESIS OUTLINE

1.1 GENERAL INTRODUCTION

The Superior Boundary Zone lies along the northern and western margins of the Superior Province in Manitoba, Ontario, and Quebec. In northeastern Manitoba, it lies along the northwestern margin of the Superior Province (Figure 1.1). It is a crustal-scale, complex transitional zone that separates Archean Superior Province crust from Paleoproterozoic crust of the Reindeer Zone (or internal zone) of the Trans-Hudson Orogen (Corkery 1985; Hoffman 1988, 1990; Bleeker 1990a; Weber 1990; White et al. 1999). The Superior Boundary Zone records evidence for both Archean and Proterozoic orogenic events, and portions of the Superior Boundary Zone are host to world-class nickel deposits (e.g. Thompson Nickel Belt in Manitoba, Cape Smith Belt in Quebec, and Labrador Trough in Labrador).

The Superior Boundary Zone is divided into five main segments in northeastern Manitoba: the Thompson Nickel Belt, the Split Lake Block, the Orr Lake Block, the Assean Lake Crustal Complex, and the Fox River Belt (Figure 1.2; Bleeker 1990a; Weber 1990; Böhm et al. 1999, 2000; White et al. 1999, 2002). Its width ranges from 10 km to 40 km. It is bound to the south by the Pikwitonei Granulite Domain of the Superior Province, and to the north by the Kisseynew Domain (Reindeer Zone) of the Trans-Hudson Orogen. The Superior craton margin (or Archean-Proterozoic contact) lies somewhere within the Superior Boundary Zone. The currently accepted location of the Superior craton margin in northeastern Manitoba is based mainly on lithological, metamorphic, structural, and geochronological constraints, but the exact location is complicated by an anastomosing network of high strain zones (e.g. the Assean Lake and Aiken River deformation zones) that bound and intersect the various crustal segments (Figure 1.2), and by a series of Archean and Proterozoic deformational and metamorphic overprinting events.

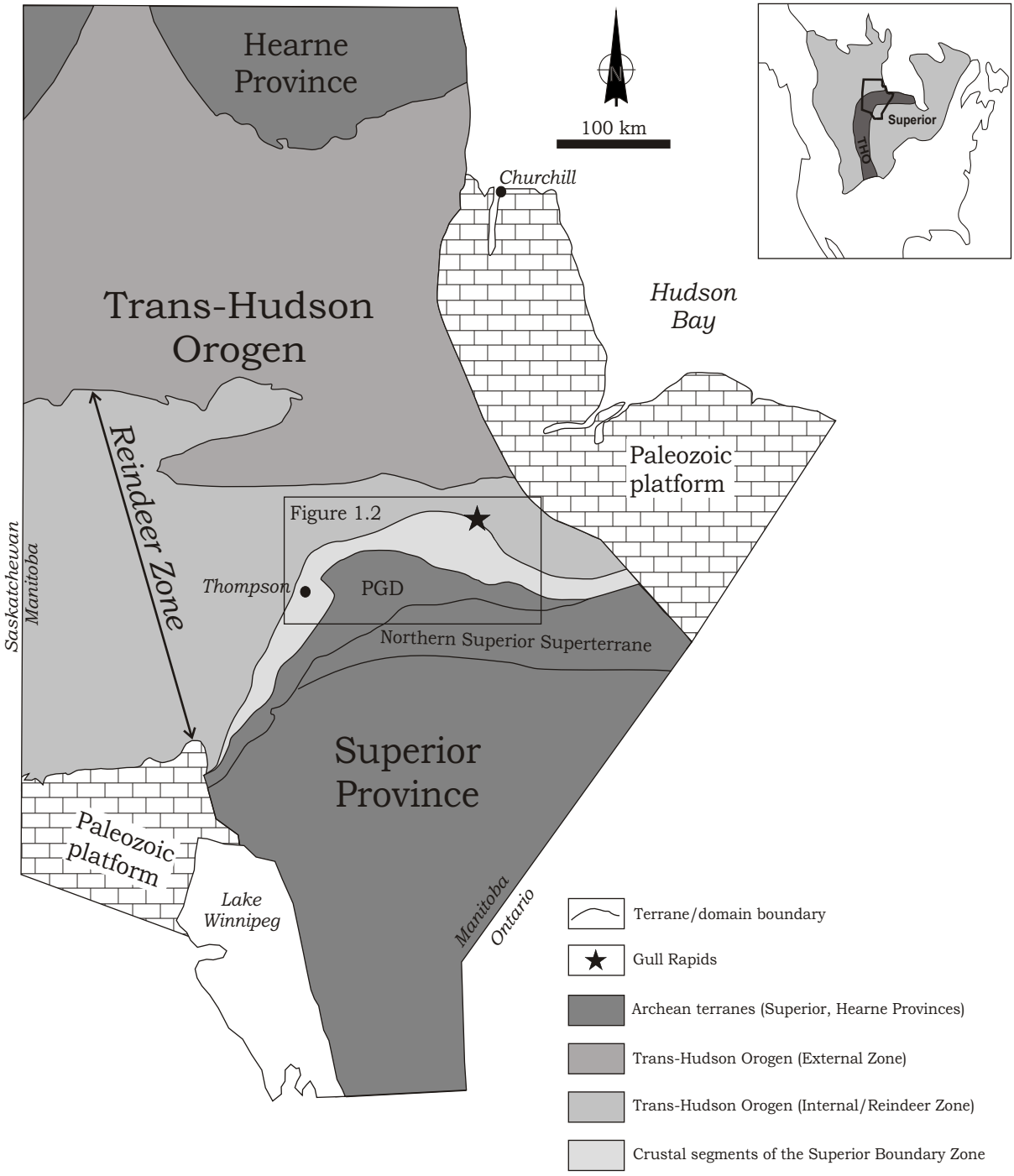

Figure 1.1. A generalized geological map of the northwestern Superior Province and the northwestern Trans-Hudson Orogen (showing the external and internal (Reindeer) zones), as well as the southeastern Hearne Province in Manitoba, showing major domain and terrane boundaries. PGD: Pikwitonei Granulite Domain. The Gull Rapids area is situated at the edge of the Split Lake Block, in the Superior Boundary Zone. The location of Figure 1.2 is indicated. Modified from Hoffman (1990), Lewry et al. (1990), Weber (1990), Zwanzig (1990), Corkery et al. (1992), Norman et al. (1995), White et al. (2002), and Parks et al. (*submitted*).

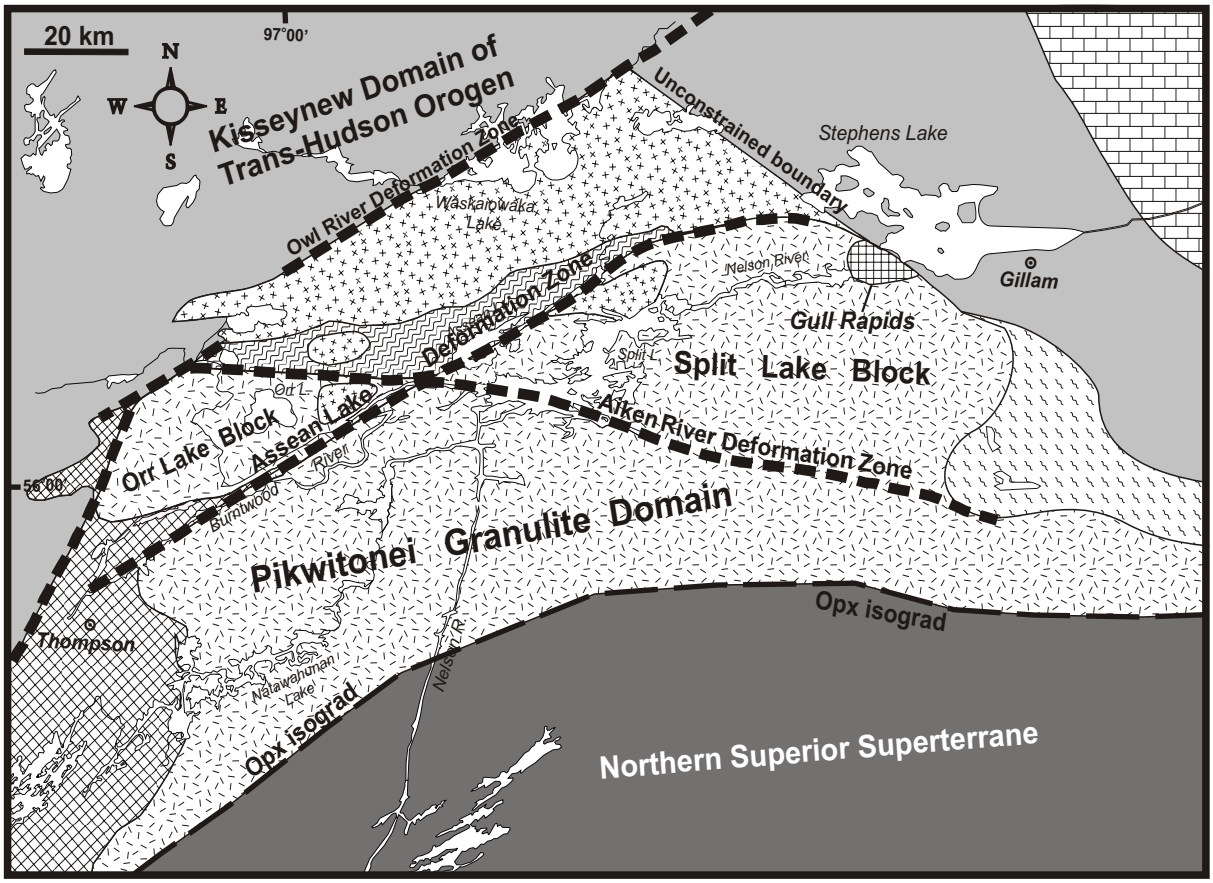

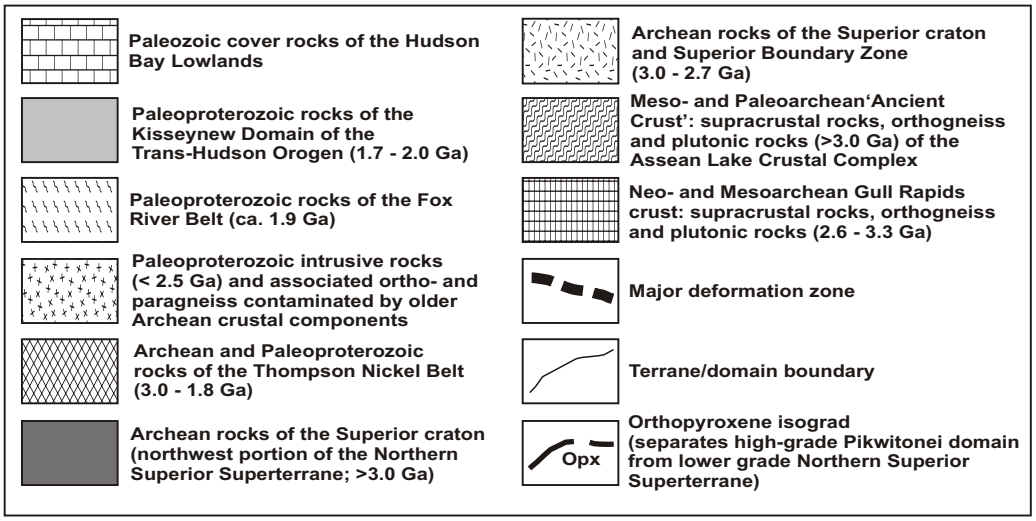

Figure 1.2. Geological map of the Superior Boundary Zone (SBZ). The Thompson Nickel Belt, Orr Lake Block, Split Lake Block, Assean Lake Crustal Complex, Gull Rapids domain, and Fox River Belt comprise the domains of the SBZ. Map includes the Pikwitonei Granulite Domain, a portion of the Northern Superior Superterrane of the Superior Province, and a portion of the Trans-Hudson Orogen. Modified after Corkery (1985), Weber (1990), Lindal (1992), Böhm et al. (1999, 2000, 2003d), and Kuiper et al. (2003).

The Thompson Nickel Belt is host to world-class nickel deposits, and historically has played an important role in the development of major concepts in the geology of this part of the Canadian Shield (Green et al. 1985; Bleeker 1990b). Exploration programs in the Fox River Belt and Assean Lake Crustal Complex have also delimited a potential for a variety of commodities including nickel, copper, platinum-group elements, and gold. In addition, ancient stable crust and crustal-scale sutures at the Superior craton margin enhance the possibility for diamondiferous kimberlites (Böhm et al. 2000, 2004). Locating the exact paleomargin of the Superior craton is therefore of importance for further and improved exploration in the area. The Gull Rapids area and the adjacent Split Lake Block are located along the same continental paleomargin as the economically important Superior Boundary Zone segments, and therefore a detailed study was conducted at Gull Rapids in order to determine the nature and location of the Superior craton margin in that area.

The Gull Rapids area is a part of the Superior Boundary Zone that lies on the northwestern margin of the Superior craton in northeastern Manitoba, sandwiched between Archean granulites of the Split Lake Block (northwestern Superior Province) and Paleoproterozoic amphibolite grade sedimentary and igneous rocks of the Kisseynew Domain (southern Trans-Hudson Orogen). It is host to a spectacularly exposed assemblage of multiply deformed and metamorphosed, Meso- to Neoarchean, upper amphibolite to granulite grade supracrustal and granitoid rocks (Figure 1.3). Previous authors have proposed that the Gull Rapids area represents a part of the Superior Boundary Zone, and in fact represents the Archean-Proterozoic contact (Haugh and Elphick 1968; Elphick 1970; Corkery 1975, 1985; Lindal 1992). This conclusion is based on a regional magnetic geophysical expression, and on the existence of the ‘Gull Rapids mylonite-cataclastic zone’, which lies just downstream of Gull Rapids in Stephens Lake (Haugh and Elphick 1968; Elphick 1970; Corkery 1975, 1985; Lindal 1992). This mylonite-cataclastic zone is no longer exposed, due to the widespread flooding of the area in 1974 by the production of Manitoba Hydro’s Kettle Rapids Hydroelectric Dam (Corkery 1985). Regardless, there is a noticeable change in the nature of the metasedimentary assemblages across the proposed Superior Province boundary at Gull Rapids, from

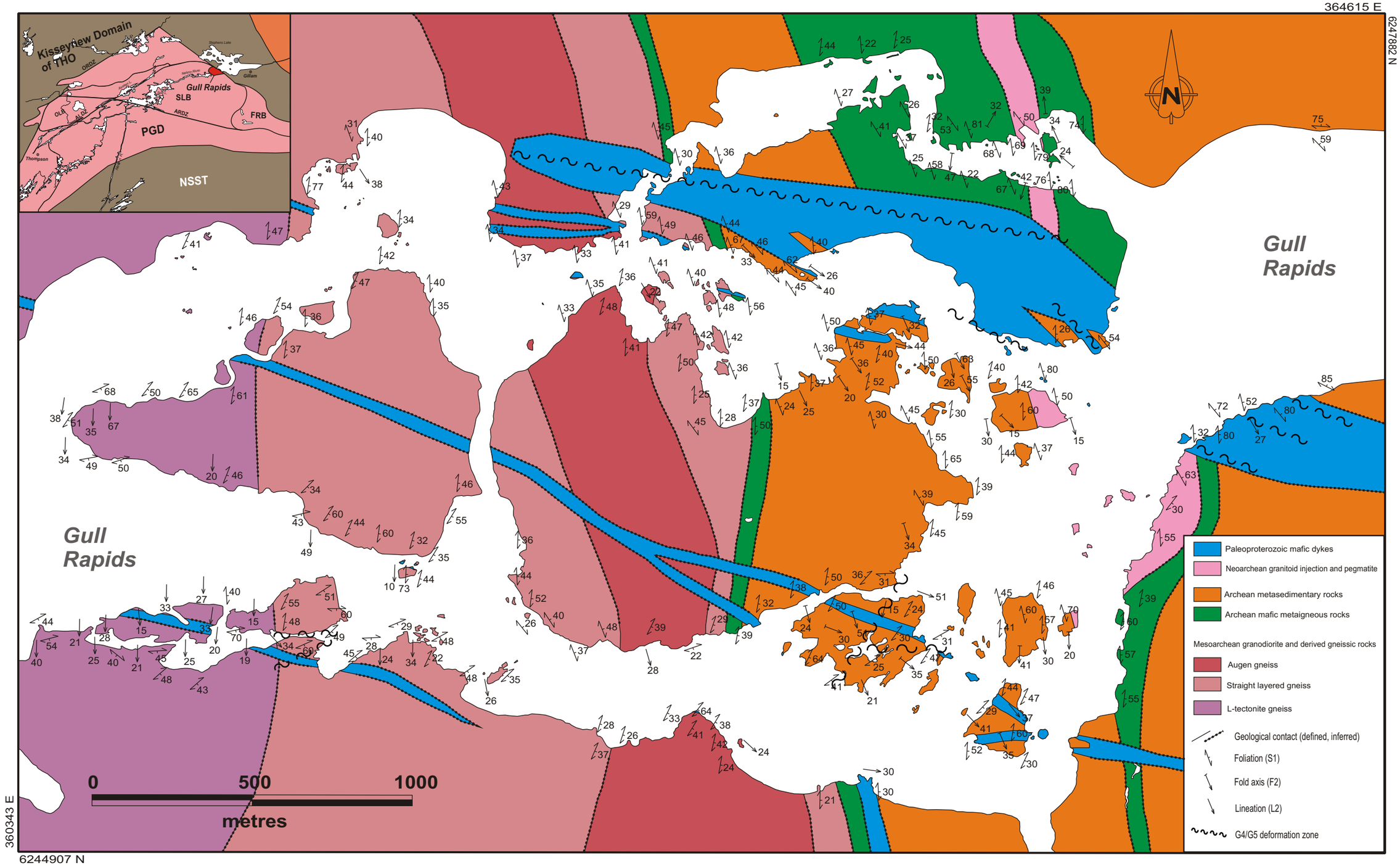

Figure 1.3. Geological map of the Gull Rapids area, showing all units, contacts (defined and inferred), and structures. Inset abbreviations: ALDZ: Assean Lake deformation zone; ARDZ: Aiken River deformation zone; FRB: Fox River Belt; NSST: Northern Superior superterrane; OLB: Orr Lake Block; ORDZ: Owl River deformation zone; PGD: Pikwitonei Granulite Domain; THO: Trans-Hudson Orogen.

typical Proterozoic Burntwood River Group metagreywacke to the north and east, to a mixed Archean assemblage at Gull Rapids, to a dominantly orthogneissic terrane in the Archean Split Lake Block to the south and west. This suggests that the Superior craton margin lies somewhere to the northeast of the Gull Rapids area.

The suggestion that the Superior craton margin lies somewhere to the northeast of the Gull Rapids area is strengthened by recent data from the Assean Lake deformation zone (Figure 1.2). This zone, as was the Gull Rapids area, was initially interpreted as being the Paleoproterozoic contact between the Archean Pikwitonei Granulite Domain (Superior Province) to the southeast and the Paleoproterozoic Kisseynew Domain (Trans-Hudson Orogen) to the northwest (Corkery 1985; Lindal 1992; Kuiper et al. 2003). However, the recent discovery of Mesoarchean (pre-3.5 Ga) crustal material in the Assean Lake Crustal Complex suggests that the actual Archean-Proterozoic contact lies further to the northwest (Böhm et al. 2000; Kuiper et al. 2003; Figure 1.2). This suggests that the Archean-Proterozoic contact in the Gull Rapids area most likely exists further to the northeast, in an area that is no longer exposed.

Understanding the structural evolution of the Gull Rapids area through studies on its structure and timing of deformation is key to comprehending the tectonic evolution of the Superior Boundary Zone and surrounding deformation zones, which in turn is important for understanding the evolution of the Superior craton margin. As well, this comprehension will provide additional insight into the exact location of the Superior craton margin, specifically in the Gull Rapids area but also in a more regional sense.

1.1.1 Objectives of the Study

This study is a part of the Manitoba Geological Survey's Superior craton margin program, a multidisciplinary project aimed at providing tools for identifying new Ni-Cu-PGE, Au, and diamond reserves and deposits in the Superior Boundary Zone. It is also aimed at understanding the complex deformational and metamorphic history of the Superior Boundary Zone, so as to develop a model for

the tectonic evolution of the Superior Boundary Zone, and for the Superior craton margin proper. The main purpose of this study is to document the previously unrecognized and/or poorly understood structural geology, kinematics, and timing of deformation and metamorphism at Gull Rapids. A better understanding of the structural evolution of the Gull Rapids area will put significant constraints on the tectonic evolution of the Superior craton margin.

This study provides accurate and detailed bedrock maps and structural data of the Gull Rapids area for Manitoba Hydro and other land-use clients. The structural study of this area is of importance to both Manitoba Hydro, for geological-engineering purposes (e.g., detailed fracture analysis required for the construction of a hydroelectric dam), and mineral-exploration companies. The completion of the structural study at Gull Rapids has provided a detailed geological framework to help guide future exploration programs along this portion of the Superior craton margin.

1.1.2 Location, Access, and Work done

The Gull Rapids area is a ten square kilometre package of exposed rocks that extends along the Nelson River in northern Manitoba, from the western edge of Stephens Lake to the eastern edge of Gull Lake (NTS 54 D/6; Figure 1.3). It is located at latitude 56º 20’ and longitude 96º 42’, approximately 30 km due west of the town of Gillam, and 55 km east of the town of Split Lake. The area is easily accessible by boat from Gillam, as the Nelson River provides access to most bedrock exposures and shorelines in the region. In the Gull Rapids area itself, access by boat is limited due to powerful and abundant rapids, and thus helicopters were also used in order to access islands, reefs, and river shorelines.

Geological mapping for the current project at Gull Rapids was done along shorelines and on river islands and reefs, where exposure was nearly 95%. The high level of exposure, and overall cleanliness of outcrop (e.g. free of lichens) is due to the turbulent water flow, fluctuations in water level (seasonal and hydroelectric dam-controlled), and seasonal ice movement. Inland outcrop

exposure in the region was nearly non-existent due to extensive forest re-growth and thick Pleistocene glacial sediment deposits, which reach up to 60 metres in thickness in some localities.

Mapping in the Gull Rapids area commenced in 2003 and continued through the 2004 field season, with collaborators from the University of Waterloo, University of Alberta, and Manitoba Hydro (Böhm et al. 2003a–d, 2004; Bowerman et al., 2004; Downey et al. 2004). Because of a proposed Manitoba Hydro hydroelectric dam site at Gull Rapids, a geological study was planned and carried out in order to recover geological information prior to extensive destruction of outcrop and flooding for dam construction. A geological engineering feasibility study was conducted in 2003 and 2004 by Manitoba Hydro, and diamond drill core from such work was used in conjunction with field mapping and sampling for this study.

During the current geological study at Gull Rapids, 1:5000, 1:1000, 1:500, and 1:200 scale detailed mapping was conducted. Detailed structural analyses, in conjunction with thin section and geochronological analyses, have been applied to unravel the structural evolution of the area. The high level of exposure at Gull Rapids allows for such a detailed study of structures and important crosscutting relationships, and helps in providing key clues as to the style and timing of deformation at this portion of the Superior craton margin.

A detailed structural map of the Gull Rapids area is enclosed in the pocket (scale 1:5000). A simplified version of this map is shown in Figure 1.3 and is referred to as the “map area” or “study area” throughout this thesis.

1.2 THESIS OUTLINE

This thesis is composed of five main body chapters (2-6). In Chapter 2, the regional geological setting is presented, including a discussion of the structural and metamorphic history of the Superior Boundary Zone. The local geological setting of the Gull Rapids area is presented in Chapter 3, and includes a discussion of the geochemistry and metamorphism of the rocks. A detailed structural

analysis is presented in Chapter 4. Here, ductile and brittle structures are described, as are the kinematics involved. Important crosscutting relationships between structures and intrusive phases are presented in Chapter 5, including discussions on the timing of deformation, metamorphism, and intrusive events. A geochronological analysis using absolute age dating is also presented here. A summary is presented in Chapter 6, and the study at Gull Rapids is put into a regional context.

Chapter 2

REGIONAL GEOLOGICAL SETTING

2.1 INTRODUCTION

The Superior Boundary Zone forms a part of the Circum-Superior Belt (Baragar and Scoates 1981), which extends from south central North America northward to central Canada, where it is exposed in the Canadian Shield in Manitoba and Ontario. From there it continues to the northeast underneath Hudson Bay, re-emerging in the Cape Smith Belt in northern Quebec and continuing down through the New Quebec Orogen (Baragar and Scoates 1981; Green et al. 1985; Bleeker 1990a; Hoffman 1988, 1990; Lewry and Collerson 1990; Weber 1990; White et al. 1999). The Superior Boundary Zone forms the northwestern margin of the Archean Superior craton in Manitoba (Green et al. 1985; Bleeker 1990a, b; Weber 1990; Machado et al. 1999; White et al. 1999, Zwanzig 1999, 2005; Corrigan 2004a, b). It is a complex transition zone containing Archean and Proterozoic rocks that separates rocks of the Pikwitonei Granulite Domain of the Archean Superior Province to the south from rocks of the Reindeer Zone of the Paleoproterozoic Trans-Hudson Orogen to the north (Figures 1.1 and 1.2). Rocks of the Superior Boundary Zone were affected by Neoarchean orogenesis, and then by Paleoproterozoic Hudsonian deformation and metamorphism, which overprinted east-trending Archean structures and mineral assemblages to different extents. This overprint is particularly strongly developed in the Thompson Nickel Belt (Weber 1990).

The Superior Boundary Zone in Manitoba is subdivided into the Thompson Nickel Belt, Orr Lake Block, Split Lake Block, Assean Lake Crustal Complex, and the Fox River Belt, and includes the terrane at Gull Rapids (Figures 1.1–1.3). In this chapter, the tectonic framework and history of the Superior Boundary Zone is reviewed, including a discussion on the northwestern Superior Province, Trans-Hudson Orogen, and Split Lake Block.

2.2 TECTONIC FRAMEWORK OF THE SUPERIOR BOUNDARY ZONE

The Superior Boundary Zone can be subdivided into 1) Archean middle to lower crustal terranes dominated by Pikwitonei-type granulite and amphibolite facies lithologies (e.g. Pikwitonei Granulite Domain, Split Lake Block, Assean Lake Crustal Complex, parts of Orr Lake Block, and the Gull Rapids area; Figure 1.2); 2) mostly reworked Archean crustal terranes (e.g. Thompson Nickel Belt, parts of Orr Lake Block), which contain Pikwitonei-type crust that was largely overprinted and reworked during Hudsonian orogenesis, as well as juvenile Proterozoic rocks; and 3) Proterozoic rocks north, west, and east of the currently exposed Archean crust that are strongly contaminated and possibly underlain by Archean crust (e.g. Fox River Belt) (Figure 1.2; Weber and Mezger 1990; Böhm et al. 1999, 2000, 2001, 2003c, d). The Superior Boundary Zone is crosscut by major deformation zones, such as the Assean Lake, Aiken River, and Owl River cataclastic-mylonitic deformation zones, and is in fault contact along these major deformation zones with the Pikwitonei Granulite Domain of the Superior Province to the south and the Reindeer Zone of the Trans-Hudson Orogen to the north (Figure 1.2; Bleeker 1990a; Weber 1990; Norquay 1997; Böhm et al. 2000; White et al. 2002). These major deformation zones have traditionally been used to determine the position of the Archean-Proterozoic boundary (the Superior craton margin proper) in northeastern Manitoba (Figure 1.2). However, the determination of the exact Archean-Proterozoic boundary is complicated by a complex and anastomosing network of such deformation zones within and on the edges of the Superior Boundary Zone. For example, the eastern portion of the Assean Lake deformation zone and western portion of the Aiken River deformation zone, which structurally bound the northern portions of the Split Lake and Orr Lake blocks, respectively, have been thought to represent the Superior Province – Trans-Hudson Orogen boundary (e.g. Corkery 1985). However, recent work has shown that Archean rocks exist to the north of these deformation zones, in the Assean Lake Crustal Complex (Figure 1.2; Böhm et al. 2000, 2003c, d; Kuiper et al. 2003, 2004a). These deformation zones therefore do not represent the true Archean-Proterozoic boundary, and the boundary must therefore lie further to the north. Instead, they represent Archean faults that may have

been re-activated during Hudsonian collisional tectonism (Böhm et al. 2000; Kuiper et al. 2004a, b, 2005). For instance, at least part of the movement along the Assean Lake deformation zone occurred after ca. 1.84 Ga, based on the age of a deformed aplite (Kuiper et al. 2005).

Most of the Thompson Nickel Belt, Orr Lake Block, Split Lake Block, Assean Lake Crustal Complex, and southern margin of the Fox River Belt comprise polymetamorphic migmatitic, largely orthogneissic rocks, which were probably mainly derived from Archean Pikwitonei-type granulites through selective retrogression, migmatization, and metamorphic and deformational recrystallization under amphibolite-grade conditions during Neoarchean orogenesis (Bleeker 1990a; Weber 1990; Böhm et al. 1999; Percival et al. 2004, 2005). Other portions of the Superior Boundary Zone, including most of the Fox River belt and the Ospwagan Group of the Thompson Nickel Belt, represent Paleoproterozoic low-grade supracrustal rocks deposited on Archean Superior Province basement at the margin of the continent (Weber and Scoates 1978; Heaman et al. 1986b; Weber 1990; Lindal 1992; Norquay 1997; White et al. 2002). Supracrustal rocks are also found in the Assean Lake Crustal Complex and in the Gull Rapids area. All rocks of the Superior Boundary Zone have been intruded by a series of Neoarchean felsic plutons, and by Paleoproterozoic mafic dykes.

The Pikwitonei Granulite Domain and Split Lake Block have been thought to represent high-grade equivalents of the Superior Province granitoid-greenstone terranes to the southeast (Weber and Scoates 1978; Weber 1990). The Pikwitonei Granulite Domain is structurally bound to the north by the Assean Lake and Aiken River deformation zones of the Superior Boundary Zone, and to the south by the Northern Superior superterrane. The southern boundary is a major metamorphic transition defined by an orthopyroxene isograd that obliquely crosscuts regionally consistent structural trends in the Northern Superior superterrane (Figure 1.2; Hubregtse 1980; Card 1990; Parmenter 2002). This orthopyroxene isograd reflects prograde Neoarchean metamorphism (Weber and Scoates 1978; Hubregtse 1980; Weber 1990).

Previous and current field investigations (e.g. Haugh and Elphick 1968; Corkery 1985; Böhm et al. 2003a, b, d; Bowerman et al. 2004; Downey et al. 2004) and regional magnetic surveys suggest

that Gull Rapids is located near the boundary between two geological terranes: 1) the dominantly Archean intrusive Split Lake Block (Superior Province); and 2) the dominantly Paleoproterozoic metasedimentary (paragneissic) Kisseynew Domain of the Reindeer Zone of the Trans-Hudson Orogen (Figure 1.2; Böhm et al. 2003a). Indeed, there is a noticeable change in the nature of the rock assemblages across the proposed Superior Province boundary near Gull Rapids, from typical Burntwood Group (Kisseynew Domain) Paleoproterozoic metagreywacke in the Stephens Lake area to the east, to a mixed supracrustal assemblage at Gull Rapids to the west that includes metagreywacke (psammite), metamudstone (pelite), amphibolite, iron formation, and minor calc-silicate rocks, to an orthogneissic assemblage further to the west at Gull Rapids that is interpreted as belonging to the Split Lake Block. The supracrustal assemblage at Gull Rapids shares similarities with the Mesoarchean supracrustal assemblage at Assean Lake (Böhm et al. 2000, 2003c, d), located in a similar tectonic position approximately 100 km west along the Superior margin. Such supracrustal rocks are not known from the Split Lake Block (Corkery 1985; Böhm et al. 1999).

2.3 TECTONIC HISTORY OF THE SUPERIOR BOUNDARY ZONE

Studies have shown that tectonism in the northwestern Superior Province occurred during two main orogenic pulses – the Neoarchean Northern Superior and the Paleoproterozoic Trans-Hudson orogenies (Corkery 1985; Bleeker 1990a; Weber 1990; Böhm et al. 1999, 2000; Parmenter 2002; White et al. 1999, 2002; Percival et al. 2004, 2005).

From ca. 3.2 to 2.7 Ga, episodic pulses of volcanism and plutonism, with related sedimentation, produced rocks which were subsequently deformed, metamorphosed, and accreted together during the Northern Superior orogeny to form the northern portion of the composite Superior Province between 2.72 and 2.70 Ga (Card 1990; Thurston et al. 1991; Parmenter 2002; Stott 1997; Percival and Skulski 1998; Skulski et al. 1999, 2000; Percival et al. 2004, 2005). Archean rocks of the Superior Boundary Zone have been deformed and metamorphosed by such Neoarchean orogenesis, and the Pikwitonei Granulite Domain and Split Lake Block were possibly uplifted with respect to the

rest of the northwestern Superior Province as a result of the Northern Superior orogeny (Hubregtse 1980; Green et al. 1985; Card 1990; Böhm et al. 1999, 2000; Parmenter 2002; Percival et al. 2004, 2005).

Based on geological, geochemical, and geochronological studies, as well as extensive LITHOPROBE seismic profiling, the main pulse of the Trans-Hudson Orogen is interpreted to have resulted from the ca. 1.92 to 1.77 Ga continent-continent collision of three Archean cratons, the Superior, Hearne, and Sask cratons, with resultant trapping of juvenile intraoceanic rocks in the Reindeer Zone (Figure 1.1, 1.2; Hoffman 1988, 1990; Lewry and Collerson 1990; Ansdell and Norman 1995; Norquay 1997; White et al. 1999; Machado et al. 1999; Zwanzig 1999, 2005; Corrigan 2004a, b). Most of the Trans-Hudson Orogen comprises thermotectonically reworked Archean continental basement (the 'external zone' of the Trans-Hudson Orogen) and predominantly juvenile Paleoproterozoic supracrustal and plutonic assemblages (the 'internal zone', or 'Reindeer Zone' of the Trans-Hudson Orogen) (Lewry et al. 1990). Rifting at the margin of the Superior and Hearne Provinces at ca. 2.1 Ga is interpreted to represent the start of Hudsonian orogenesis (Stauffer 1984; White et al. 1999; Zwanzig 1999, 2005; Corrigan 2004a, b; H. Zwanzig pers. comm., 2005). The 'Cauchon' mafic dyke swarm in the Superior Boundary Zone has been dated at 2.1 Ga, although it is not known whether or not these dykes formed as a result of the ca. 2.1 Ga rifting (Zwanzig 1999, 2005; Halls and Heaman 2000; Corrigan 2004a, b; L. Heaman, pers. comm., 2005; H. Zwanzig pers. comm., 2005). The main pulse of Hudsonian orogeny at ca. 1.8 Ga was the last tectonic event to affect the Superior Boundary Zone. It overprinted and re-worked Archean and older Proterozoic rocks of the Superior Boundary Zone. Rocks further south, in the Superior Province itself, were not affected to any great extent (Zwanzig 1999, 2005; Corrigan 2004a, b). The Pikwitonei Granulite Domain and Split Lake Block may have been uplifted with respect to the rest of the northwestern Superior Province as a result of the ca. 2.1 Ga rifting event, rather than by Neoarchean orogenesis (Hubregtse 1980; Green et al. 1985; Card 1990; Böhm et al. 1999, 2000; Halls and Heaman 2000; Parmenter 2002; Percival et al. 2004, 2005).

The overthrusting of the Reindeer Zone of the Trans-Hudson Orogen onto the Superior craton during terminal Hudsonian collision (ca. 1.80-1.77 Ga) is interpreted to be the cause of the highly tectonized nature of portions of the Superior Boundary Zone (e.g. Thompson Nickel Belt; Lindal 1992). In fact, Hudsonian thermotectonic overprinting affected the entire Superior Boundary Zone, but with some crustal blocks being affected in different ways to different degrees (for example, the Thompson Nickel Belt has been far more re-worked than the Split Lake Block, and most structures within the Split Lake Block are Archean in age). Other crustal blocks of the Superior Boundary Zone are Proterozoic and juvenile. The Hudsonian metamorphic-metasomatic overprint extended down into the Pikwitonei Granulite Domain, much further than the structural overprint (Weber 1990). In agreement with this, at Gull Rapids and in the Split Lake Block, the deformational overprint of Hudsonian tectonism on Archean rocks is much weaker than the metamorphic overprint.

2.3.1 The Split Lake Block

The Split Lake Block forms a fault-bounded, boudin-shaped, partly retrogressed and reworked granulite-grade segment of the Superior Boundary Zone (Figure 1.2; Böhm et al. 1999, 2000; Kuiper et al. 2003, 2004a, b; Hartlaub et al. 2003, 2004). It is interpreted to represent a portion of the Superior craton that was deformed and metamorphosed by a late Archean tectono-metamorphic event and further modified during terminal Hudsonian collision (Lindal 1992; Kuiper et al. 2003, 2004a, b). However, unlike other portions of the Superior Boundary Zone, the effects of Hudsonian tectonism on the Split Lake Block are relatively minor, thus allowing for the establishment of firm temporal constraints on the Archean structural and metamorphic history of the Superior Boundary Zone (Böhm et al. 1999, 2000).

The Pikwitonei Granulite Domain to the south is interpreted to have a common crustal history and petrogenesis with the Split Lake Block (Heaman et al. 1986b; Mezger et al. 1990). Like the Pikwitonei domain, the Split Lake Block is largely orthogneissic and comprises enderbite, opdalite, and charnokite (meta-igneous rocks of tonalitic to granodioritic composition), with a relatively minor

amount of supracrustal rocks. These rocks include traces of banded iron formation, pillow basalt, and paragneiss (Weber and Scoates 1978; Hubregtse 1980; Weber and Mezger 1990; Weber 1990; Böhm et al. 1999). The rocks of the Pikwitonei and Split Lake Block are thought to represent the high-grade equivalents (i.e. a deeper crustal section) of plutonic and supracrustal rocks exposed in the Northern Superior superterrane, Oxford-Stull Lake terrane, Munro Lake terrane, Island Lake terrane, and North Caribou terrane (Weber and Scoates 1978; Hubregtse 1980; Card 1990; Percival et al. 2004, 2005).

Based on field relationships, petrography, and U-Pb and Pb-Pb geochronology, there is an indication of at least three high-grade Archean and one medium-grade Proterozoic deformational and/or metamorphic events in the Pikwitonei and Split Lake domains. There is metamorphic zircon growth at 1) ca. 2705 Ma; 2) 2695–2685 Ma; 3) 2640–2620 Ma, and 4) ca. 1800 Ma (Hubregtse 1980; Corkery 1985; Heaman et al. 1986a, b; Mezger et al. 1986, 1990; Weber and Mezger 1990; Böhm et al. 1999, 2000; Halls and Heaman 2000). During the first metamorphic event (2705 Ma; M1a of Corkery 1985), amphibolite to hornblende-granulite facies conditions were attained; during the second event (2695–2685 Ma; M1b of Corkery 1985) granulite facies peak metamorphic conditions were attained; and the third event (2640–2620 Ma; M2 of Corkery 1985) reached upper amphibolite facies conditions throughout the Pikwitonei Granulite Domain and pervasively overprinted most of the older assemblages. The 2695-2685 Ma and 2640–2620 Ma metamorphic ages, which represent peak granulite and upper amphibolite facies conditions, respectively, can be correlated in the field with two major deformational events (D1 and D2 of Hubregtse 1980). The fourth metamorphic event (ca. 1800 Ma; M3 of Corkery 1985) reached greenschist facies conditions interpreted to be linked to Paleoproterozoic terminal collision and the emplacement of Paleoproterozoic intrusive bodies (e.g. the 1883 Molson mafic dyke swarm; Heaman et al. 1986b; Heaman and Corkery 1996; and the 1825 Ma Fox Lake granite; Böhm et al. 1999).

The Split Lake Block is structurally bound by two discrete linear belts of cataclastic-mylonitic rocks: the Aiken River deformation zone to the south, and the Assean Lake deformation zone to the north (Figure 1.2). These and other deformation zones in the area (e.g. Owl River shear

zone) display distinctive linear magnetic low trends on the regional aeromagnetic map (Böhm et al. 2000). The Assean Lake and Aiken River deformation zones form a part of a cryptic suture separating typical Superior Province Archean crust from ancient (pre-3.5 Ga) Archean crustal material of the Assean Lake Crustal Complex (Böhm et al. 1999, 2000; Kuiper et al. 2003, 2004a, b), rather than forming the Archean-Proterozoic boundary proper. The original kinematics along the Assean Lake and Aiken River deformation zones are difficult to unravel due to reactivation during the Paleoproterozoic Hudsonian orogeny (Bleeker 1990a; Böhm et al. 1999, 2000). Recent work by Kuiper (2003, 2004a, b) has shown that the Split Lake Block has moved up relative to the Pikwitonei domain to the south and the Assean Lake Crustal Complex to the north. The timing of this uplift is in part the focus of this study.

Chapter 3

LOCAL GEOLOGICAL SETTING OF THE GULL RAPIDS AREA

3.1 INTRODUCTION

The Gull Rapids area is host to a spectacularly exposed assemblage of multiply deformed Archean supracrustal and orthogneissic rocks (Figure 1.3). Mapping at Gull Rapids has identified two main crustal assemblages: 1) an Archean mid- to upper-amphibolite facies supracrustal assemblage consisting of interlayered amphibolite (largely mafic metavolcanics) and Fe-rich psammite–pelite (meta-greywacke/meta-arkose and meta-mudstone) sequences, with interlayered banded iron formation and mafic conglomerate, in contact with 2) Archean granulite facies granodiorites and derived gneisses. These orthogneisses are of possible Split Lake Block origin (Böhm et al. 2003a). The main lithological assemblages generally strike northwest to north, subparallel to the presumed Archean-Proterozoic boundary to the east and the general strike of Archean lithologies in the Split Lake Block to the west (Böhm et al. 1999, 2003a; Bowerman et al. 2004; Downey et al. 2004). Both crustal packages are heavily injected by several phases of mostly leucocratic granitoid dykes, sills, and dykelets. Structural relationships and compositions of the main injection phases suggest that at least some phases may be correlated across the orthogneiss – supracrustal contact. All the above lithologies are cut by abundant generally undeformed mafic dykes that form part of a major, generally east-west trending swarm.

3.2 ARCHEAN SUPRACRUSTAL ROCKS

Mapping at Gull Rapids has identified an Archean high-grade supracrustal assemblage dominated by mafic, largely metavolcanic rocks (amphibolite) and iron-rich metasedimentary rocks (meta-greywacke, meta-arkose, meta-mudstone) (Böhm et al. 2003a, b; Bowerman et al. 2004; Downey et al. 2004). The rocks within both of these units have been subject to multiple stages of

deformation, in the form of foliation and lineation development, boudinage, folding, and shearing. Bedding and foliation within the supracrustals is subparallel and generally strikes north-northwest, and parallels unit boundaries. A mineral and stretching lineation is common and subparallel throughout the supracrustals. Folding and shearing within the supracrustal package has created a series of alternating packages of amphibolite and metasedimentary rocks, ranging in apparent thickness from 70 to 1000 metres for the amphibolite, and from 600 to 1500 metres for the metasedimentary rocks (Figure 1.3). Contacts between amphibolite and metasedimentary packages are not exposed and could therefore not be studied in detail. Both supracrustal assemblages were metamorphosed to mid- to upper-amphibolite facies, and were altered during retrograde greenschist facies metamorphism.

3.2.1 Amphibolitic Rocks

The map area contains a substantial amount of amphibolite, the majority of which is fine- to medium-grained and has a distinct compositional banding that is marked by black and green striped units as well as abundant crosscutting felsic injection and pods of partial melt (Figure 3.1a, b). The fine- to medium-grained amphibolite contains dominantly hornblende, plagioclase, and epidote, which exist in alternating hornblende-rich, hornblende-poor, and epidote-rich (calc-silicate) bands throughout (Figure 3.1a, b). Based on composition and texture (although all textures are recrystallized due to metamorphism), the fine- to medium-grained amphibolite is interpreted to represent volcanics of dominantly basaltic composition (Böhm et al. 2003a; Bowerman et al. 2004). More massive, coarse-grained amphibolite interpreted as metagabbro (Böhm et al. 2003a; Bowerman et al. 2004) contains dominantly hornblende and plagioclase, and lacks the alternating hornblende- and epidote-rich bands as seen in the fine- to medium-grained amphibolite (Figure 3.1c, d). Packages of coarse-grained amphibolite are subparallel to packages of fine- to medium-grained amphibolite. Basalt with gabbro dykes and sills is a common association.

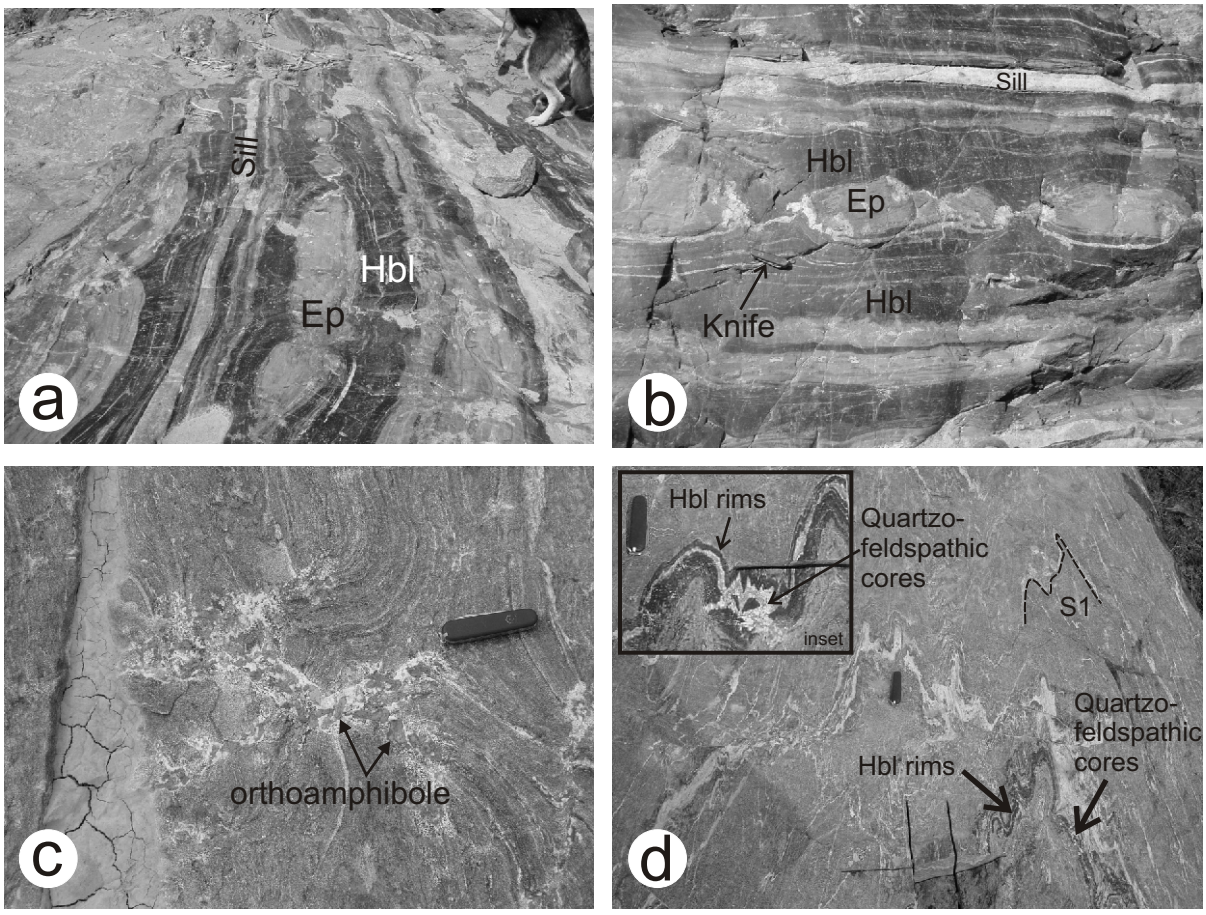

Figure 3.1. Amphibolitic rocks at Gull Rapids. a), b) Fine- to medium-grained layered amphibolite. Alternating layers are hornblende- (dark layers) and epidote- (light layers) rich bands. Note foliation-subparallel granodiorite sills and boudinage in epidote-rich layers. Hbl = hornblende-rich band; Ep = epidote-rich band. c) Large orthoamphibole grains in granodioritic pod of partial melt in coarse-grained amphibolite. d) Coarse-grained amphibolite with folded foliation-subparallel injection dykelets and sills. Note partial melting at dykelet and sill margins, and lack of layering in the amphibolite. Inset shows melt segregation: hornblende rims and quartzofeldspathic cores.

Overall, the amphibolite ranges in composition from ultramafic to mafic (44–52 wt. % SiO2 and 4.2–8.9 wt. % MgO), and plots within the tholeiitic basalt field on a volcanic alkali-FeO-MgO diagram, similar to mafic granulite from the adjacent Split Lake Block (Bowerman et al. 2004). Both types of amphibolite have the general mineral assemblage of hornblende + plagioclase ± epidote ± chlorite ± quartz ± biotite ± muscovite (or sericite) ± pyroxene ± carbonate ± sulphides.

The amphibolite initially reached metamorphic conditions of mid-amphibolite facies, as characterized by the presence of hornblende, plagioclase, and epidote. Hornblende grains are subhedral to euhedral, and define the S1 foliation in the amphibolite: they do not overprint it. There are no overgrowths of hornblende on other hornblende grains, but in a few localities, hornblende overgrows older quartz and feldspar grains. The abundance of subhedral to euhedral hornblende in the rock, the overgrowths of quartz and feldspar by hornblende, and the interpretation that the amphibolite protolith is basalt and gabbro (which generally lack hornblende), all suggests that the hornblende in the rock grew during mid-amphibolite facies metamorphism. This metamorphic event at Gull Rapids can be correlated to the regional M1a event described by Corkery (1985). Crosscutting granitoid dykes, sills, and pods of partial melt within the amphibolite assemblage contain large euhedral orthoamphibole, indicative of peak metamorphic conditions of upper-amphibolite grade (Figure 3.1c). Orthoamphibole is not observed in the amphibolite itself. This peak metamorphic event can be roughly correlated to the M1b event of Corkery (1985): the event at Gull Rapids is not as high grade as the regional M1b event. Locally, clinoamphibole are pseudomorphing from orthoamphibole, suggesting retrogression to mid-amphibolite facies metamorphism. This metamorphism can be correlated to the M2 metamorphic event of Corkery (1985). Widespread and pervasive retrograde greenschist facies metamorphic conditions were eventually reached throughout the amphibolite assemblage, as indicated by the alteration of hornblende and plagioclase to chlorite and muscovite (or sericite). This greenschist facies event can be correlated to the M3 event of Corkery (1985).

The layered amphibolite has an εNd value of +1.0 (Bowerman et al. 2004). The positive εNd value indicates a juvenile-mantle origin with only small amounts of crustal contamination. It is now

suggested that the earliest unit exposed at Gull Rapids is the amphibolite unit that erupted through thin, likely mafic crust to produce tholeiitic basaltic magma (Bowerman et al. 2004). The interpretation that the amphibolite is the oldest unit at Gull Rapids is based on the fact that amphibolitic rafts of similar composition to the main amphibolite assemblage (Bowerman et al. 2004) occur in the orthogneiss. This indicates that the basalt (amphibolite) predates the orthogneiss, which has an oldest rock crystallization age of 3.18 Ga (L-tectonite; Böhm et al. 2003a). Unfortunately, a proper age date of the mafic volcanic assemblage cannot be produced (C. Böhm, pers. comm., 2005).

3.2.2 Metasedimentary Rocks

A significant portion of the map area is dominated by thick packages of metasedimentary rocks that are highly injected and crosscut by felsic material (Figure 3.2). Distinct pods of partial melt are not seen within the metasediments as they are within the amphibolites. These metasedimentary packages are largely composed of meta-greywacke (psammite) and meta-mudstone (pelite) (Figure 3.2a, b), with minor amounts of arkosic sediments (Figure 3.2c), silicate-, oxide-, and sulphide-facies banded iron formation (Figure 3.2d, e), and polymictic metaconglomerate (Figure 3.2f). They range in composition from mafic to felsic (49–70 wt. % SiO_2), and are generally Fe-rich and Al-poor (Böhm et al. 2003a; Bowerman et al. 2004). These metasediments have the mineral assemblages of quartz + biotite + plagioclase + K-feldspar ± garnet ± muscovite (or sericite) ± chlorite ± cordierite ± Fe-amphibole ± graphite ± epidote ± carbonate ± sulphides. It has been suggested that the psammite-pelite sequence represents a turbiditic sedimentary environment (e.g. Corkery 1985). It is common for the metasediments to display distinct mineralogical banding that is most likely the product of primary compositional layering (Figure 3.2a, b). The metasediments are typically medium grey and well layered to almost massive, and locally preserve graded bedding. Rare beds of arkosic material that preserve primary bedding (parallel to foliation; Figure 3.2c), as well as thin (<20 cm thick) lenses of calc-silicate material (epidote + carbonate), are found interbedded within the psammite-pelite sequences.

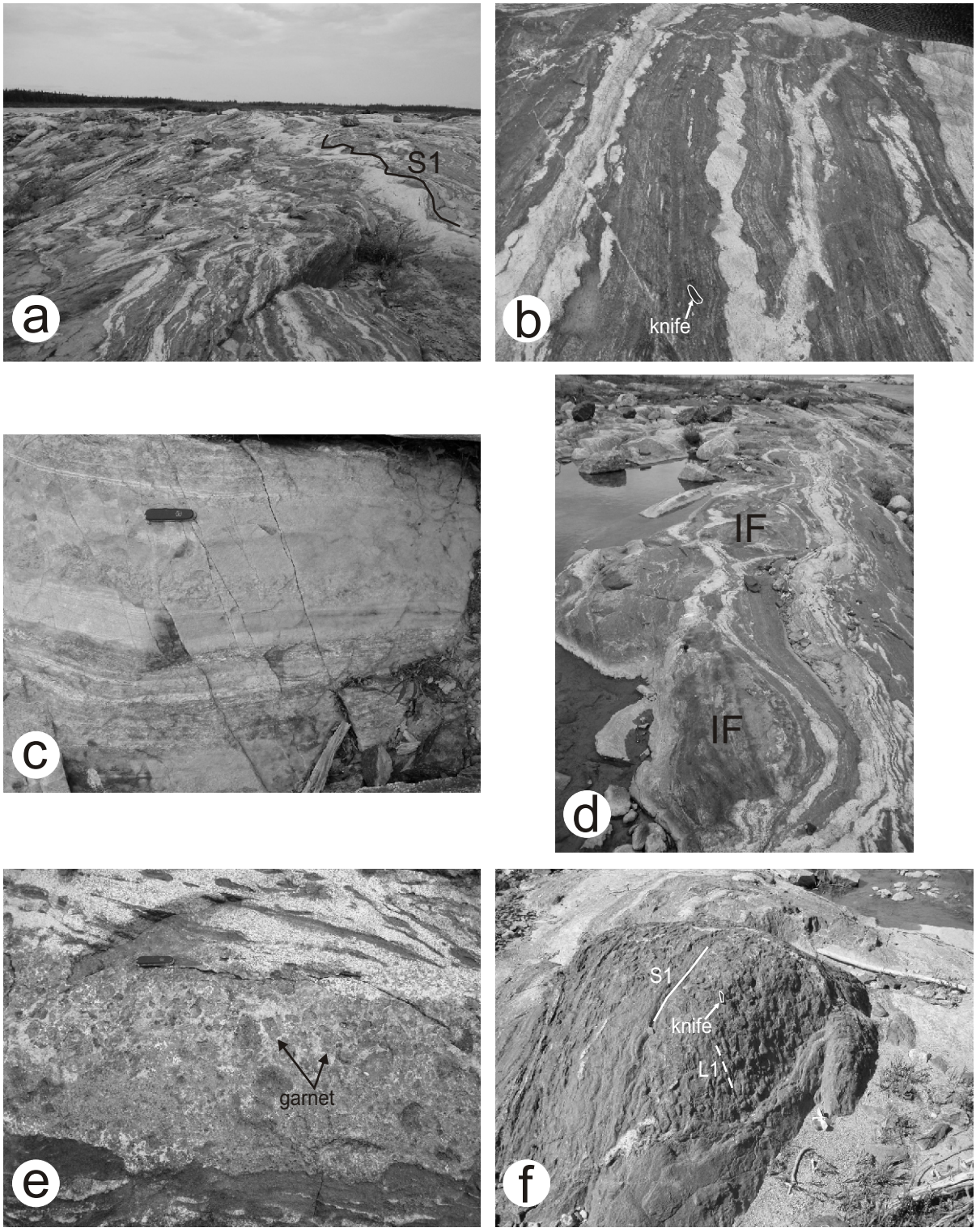

Figure 3.2. Metasedimentary rocks at Gull Rapids. a) Highly injected metagreywacke sequence. Injection dykes, dykelets, and sills are subparallel to the foliation in the metasediments. Foliation dips towards left side of photo. b) Psammite-pelite sequence with boudinage of foliation-subparallel injection. c) Primary bedding in felsic metasedimentary rocks. d) Iron formation (IF) boudins. e) Garnetite layer in iron formation, parallel to foliation. f) Mafic-ultramafic conglomerate boudin. Boudin is parallel to foliation, and elongated pyroxenite pebbles define lineation.

The metasediments reached peak metamorphic conditions of mid- to upper-amphibolite facies, as characterized by the presence of biotite, garnet, and cordierite. Many biotite grains are subhedral to euhedral, suggesting that they are metamorphic and not detrital. Biotite defines the S1 foliation in the metasediments. This amphibolite facies metamorphic event can be correlated to the regional M1 event described by Corkery (1985). Crosscutting felsic injection within the metasediments does not contain orthoamphibole as it does within the amphibolite sequence. In one locality within the psammite-pelite sequence, there may exist orthopyroxene, which would suggest that the metasediments locally reached peak metamorphic conditions of granulite facies. Subsequent retrograde greenschist facies metamorphic conditions, as characterized by the alteration of garnet to chlorite, and feldspars to muscovite (or sericite), were reached. This prograde mid- to upper-amphibolite and retrograde greenschist facies metamorphism is widespread and pervasive throughout the sequence, as it is in the amphibolite sequence.

Iron formation with centimetre-scale bands of oxide, sulphide and silicate facies (quartz/chert ± magnetite ± hematite ± garnet ± biotite ± amphibole ± sericite ± sulphides) usually form boudins along discontinuous layers within the metasediments (Figure 3.2d). Exposures of iron formation are less than 2 metres wide and no more than 4 metres long. These boudins can be traced along foliation. In a few localities, garnet-rich layers of iron formation (garnetite) were found (Figure 3.2e). Ultramafic to mafic polymictic metaconglomerate is present as rare boudins within the metasediments (Figure 3.2f). A single discontinuous layer of five boudins can be traced in one locale while single boudins occur elsewhere. The conglomerate is clast-supported and features sub-angular, well-sorted meta-pyroxenite with minor meta-hornblendite within a mafic (biotite-rich) matrix. A lack of markers renders it difficult to better define the internal geometry of the metasedimentary assemblage.

Detrital zircon grains indicate that sediment sources range in age from ca. 2.7 to ≥3.3 Ga (Bowerman et al. 2004). The majority of grains are between 2.7 and 2.8 Ga, which agrees well with the U-Pb ages obtained for rocks in the nearby Split Lake Block. The youngest detritus is considered a maximum age constraint for the sedimentary rocks, which means that the metasedimentary rocks

exposed at Gull Rapids are younger than ca. 2.70 Ga (Bowerman et al. 2004). The metasediments are crosscut by felsic dykes, which are 2.68 Ga in age (see Chapter 5), thereby constraining the minimum age of the metasediments. These constraints clearly show that the metasediments in the Gull Rapids map area are Neoarchean in age (2.70 – 2.68 Ga), and therefore do not form part of the Burntwood Group as proposed by Corkery (1985). The M1a metamorphic event of Corkery (1985) has been dated at 2705 Ma, and the M1b event at 2695–2685 Ma (Böhm et al. 1999). Since the metasediments were deposited between 2700 and 2680 Ma, the amphibolite facies event that affected the metasediments must be the M1b event.

The mafic nature of these metasedimentary rocks may indicate a mafic igneous protolith as a source of detritus. A trace-element pattern comparison between the compositions of the metasedimentary rocks and the Gull Rapids amphibolite, the Gull Rapids orthogneiss, and the Split Lake Block orthogneiss supports the hypothesis that the Gull Rapids and Split Lake orthogneiss and Gull Rapids amphibolite were the sources of detritus for the Gull Rapids metasedimentary rocks (Bowerman et al. 2004). This implies that an unconformity exists between the Gull Rapids orthogneiss/amphibolite and the metasediments. Taking into account the interpretation that these metasedimentary rocks are turbiditic (e.g. Corkery 1985; Böhm et al. 2003a), it is most likely that the metasediments were deposited on top of a basement of orthogneiss and amphibolite, at a continental margin.

3.3 ARCHEAN ORTHOGNEISSIC ROCKS

The Archean supracrustal assemblage at Gull Rapids is in contact with an Archean high-grade (granulite facies) orthogneissic assemblage dominated by 3180–2850 Ma (rock crystallization ages) granitoid intrusive rocks, of dominantly granodiorite composition, and derived gneisses (Figure 3.3; Böhm et al. 2003a, b; Bowerman et al. 2004; Downey et al. 2004). The orthogneiss has a uniform composition, although locally the composition of gneissic layers ranges from tonalitic to granodioritic to granitic. These rocks have the general mineral assemblages of plagioclase + K-feldspar + quartz +

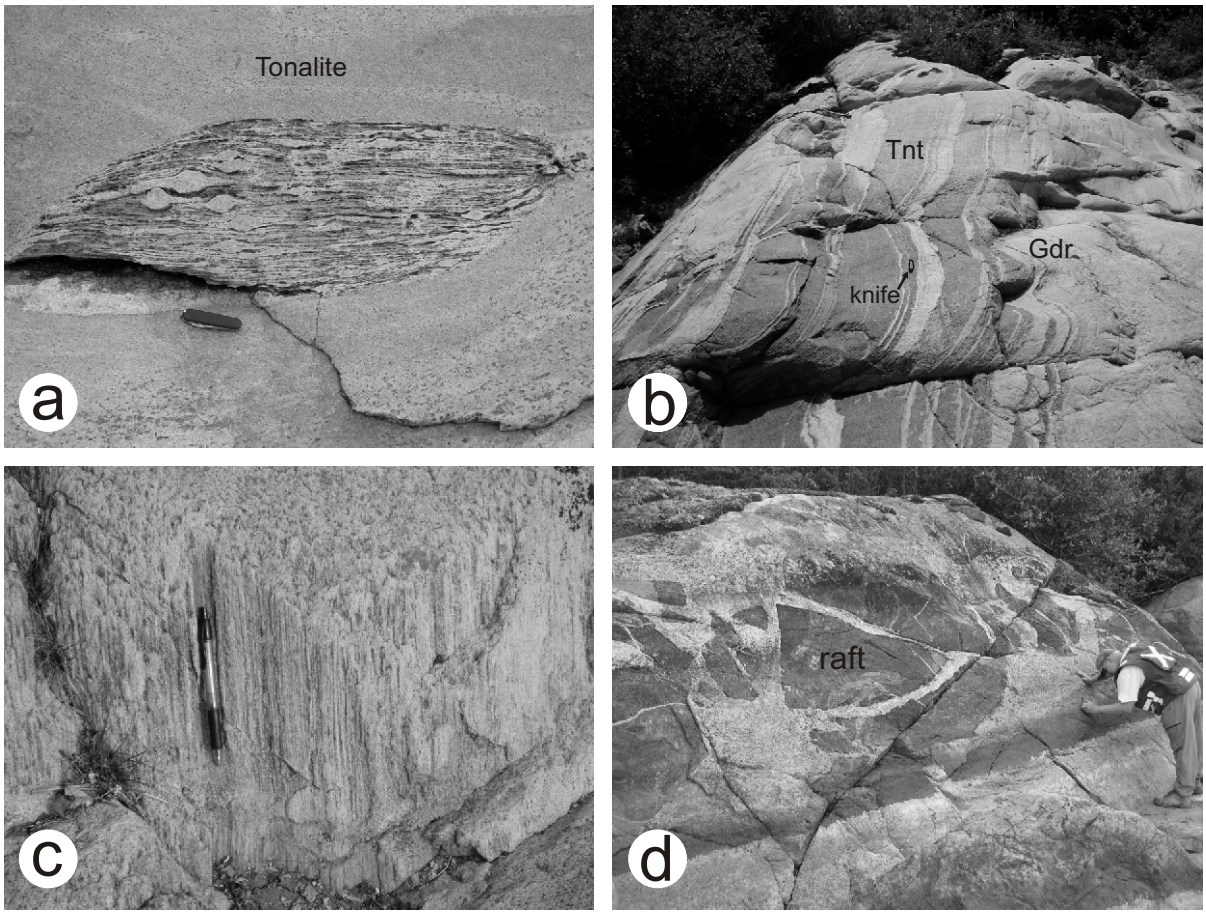

Figure 3.3. Orthogneissic rocks at Gull Rapids. a) Augen gneiss with large K-feldspar augen surrounded by tonalitic injection. b) Straight-layered gneiss. Tnt = tonalite(dark) layer; Gdr = granodiorite (light) layer. Knife in centre of photo for scale. c) L-tectonite. Pen is parallel to lineation. Note stretched rods of feldspar. d) Amphibolite rafts in orthogneiss. Rock face seen is foliation plane; trains of amphibolite rafts are parallel to the foliation. Foliation within amphibolite rafts is not always parallel to that in the host rock, suggesting an older pre-gneissosity foliation development.

biotite ± hornblende ± garnet ± chlorite ± muscovite. Structural and textural rather than compositional changes provide distinctive features that allow subdivision of the assemblage along generally north-trending zones, which parallel the general trend of contacts within the supracrustal assemblage, as well as the local foliation in the Gull Rapids area (Böhm et al. 2003b). These zones comprise 1) augen gneiss (Figure 3.3a); 2) straight layered and banded orthogneiss (Figure 3.3b); and 3) strongly rodded L-tectonite (Figure 3.3c). These boundaries are not sharp; a wide transition zone usually borders them. The orthogneissic rocks of these units have been subject to foliation development and ductile-brittle shearing.

These rocks reached peak metamorphic conditions of granulite facies, as indicated by the local presence of orthopyroxene. Conditions of amphibolite facies were later reached, as characterized by the presence of hornblende (although some of the hornblende is most likely primary igneous). Even later, retrograde greenschist facies conditions were attained, as characterized by the alteration of quartz, feldspar, and mafic minerals to fine-grained chlorite and muscovite (or sericite).

Rafts of amphibolite are common in the orthogneiss assemblage and occur as discontinuous trains or layers of angular to rounded, partially resorbed xenoliths that are generally parallel to local foliations/gneissosity and generally have an older foliation within themselves that is not always parallel to that in the host rock (Figure 3.3d). Compositional banding is rare and unlike the distinct lamination in the main amphibolite sequence.

The orthogneiss at Gull Rapids texturally and compositionally resembles that of the adjacent Split Lake Block (Bowerman et al. 2004). Recent U-Pb zircon and Nd model studies on orthogneiss from Gull Rapids support the interpretation that the Gull Rapids and Split Lake Block orthogneiss are similar to each other (Böhm et al., 1999, 2003a; Bowerman et al. 2004).

3.3.1 Augen Gneiss

Augen granodioritic gneiss is predominant in an approximately 400 metre wide zone (at its maximum thickness) that parallels the Gull Rapids local foliation and unit boundaries, and is flanked

by zones of straight-layered orthogneiss (Figure 1.3). In this augen gneiss zone, feldspar augen make up approximately 20-30% of the rock, whereas in other zones of Gull Rapids orthogneiss, augen are non-existent or rare. The margins of the augen gneiss zone are gradational: away from the margins, fewer and fewer augen are found in the bordering straight-layered gneiss, and these marginal augen are poorly developed and preserved. The augen gneiss is dominated by subhedral, symmetrical, flattened and aligned (parallel to local S1 foliations) and stretched (subparallel to local L2 lineations), 1-2 cm wide K-feldspar augen set in a foliated matrix (Figure 3.3a). The foliation is defined by elongated biotite and hornblende, and by lenticular aggregates of recrystallized quartz and feldspar. These augen commonly show internal plastic deformation (deformation lamellae in feldspars, lattice misorientation and formation of subgrains) as well as marginal recrystallization (formation of quartz and feldspar subgrains). Microcline twinning is common, as are quartz and plagioclase inclusions within large K-feldspar augen. In the matrix, the foliation is always deflected around the augen, suggesting augen growth before, or during the deformation responsible for the gneissic foliation of the rock, with foliation-creating deformation possibly continuing past augen growth.

It has been debated as to whether or not K-feldspar augen in felsic gneisses and mylonites are phenocrystic or porphyroblastic, i.e. did they develop before, during, or after deformation (Vernon 1986, 1990; Passchier et al. 1990). Vernon (1990) and Passchier et al. (1990) suggest that, although positive identification cannot always be made, most K-feldspar megacrysts and augen have a porphyroclastic (phenocrystic) origin rather than a porphyroblastic one. The augen probably developed from coarse porphyritic granitoid rocks in which the grain size was gradually reduced during dynamic recrystallization of quartz and feldspar. Deformation of early-formed porphyroblasts cannot be excluded as a possible interpretation, but a number of common features indicate a porphyroclastic origin, such as plagioclase and quartz inclusions in K-feldspar augen, zoning, simple and microcline twinning, myrmekite replacement along internal fractures or in high-strain sites, deflection of foliation around pre-existing or syn-tectonic phenocrysts, and variable internal deformation and recrystallization. It is evident that the augen in the Gull Rapids augen gneiss do

follow some of the criteria listed above: there is evidence for plastic deformation and dynamic recrystallization, twinning, some inclusions of quartz within large K-feldspar grains, and deflection of the matrix foliation around the augen. High-strain ductile deformation may be responsible for the formation of the foliation and recrystallization within the matrix as well as the plastic deformation and recrystallization within the K-feldspar augen. The reason for the existence and location of such augen gneiss zones is currently poorly understood, because of poor constraints on the boundary conditions of such zones at Gull Rapids.

A sample of augen gneiss from the south shore of Gull Rapids was dated using the LA–ICP-MS and ID–TIMS U-Pb techniques. The LA–ICP-MS data show that a majority of the magmatic zircons in the sample yield an age near 2.85 Ga (Bowerman et al. 2004). This age is confirmed by an ID-TIMS concordant age of 2.86 Ga (Böhm et al. 2003a; Bowerman et al. 2004), which indicates that the augen gneiss has a Neoarchean crystallization age.

3.3.2 Straight-Layered Gneiss

Compositionally banded granitoid gneiss is predominant in two north-trending zones (700 metres wide at the maximum thickness) that parallel the local foliation and unit boundaries (Figure 1.3; 3.3b). Contacts between flanking zones of L-tectonite and augen granitoid gneisses are gradual: augen are seen in the straight-layered gneiss locally near the contacts with the augen gneiss zone, and the L-tectonite grades into an S>L tectonite in the straight-layered gneiss. This compositionally banded gneiss has very straight layers, which range in composition from tonalite to granodiorite to granite. These layers define the gneissosity. The straight-layered gneiss is mineralogically fairly homogenous, with the assemblage quartz + feldspar + biotite + hornblende ± chlorite ± muscovite. Tonalite layers are generally more hornblende-rich, giving them an amphibolitic appearance. An ID-TIMS U-Pb zircon age of a sample of layered orthogneiss yielded ($^{207}Pb/^{206}Pb$) crystallization ages between 3.03 and 3.14 Ga (Böhm et al. 2003a; Bowerman et al. 2004).

3.3.3 L-Tectonite

A strongly rodded L-tectonite orthogneiss is predominant in an approximately 600 metre wide zone (at its maximum thickness) that again parallels the local foliation and unit boundaries (Figure 1.3; 3.3c). The L-tectonite grades into an S>L tectonite (straight-layered gneiss) over 30 metres. These gneisses are chemically similar to other Gull Rapids orthogneisses (Bowerman et al. 2004), and have the same mineral assemblages. The lineation is defined by strongly stretched quartz and feldspars (grains are stretched up to 20 cm, or 20 times the original length). Where a lineation is seen within the L-tectonite, no foliation is seen. Due to a lack of knowledge of the boundary conditions on the L-tectonite (e.g. lack of outcrop to the west, south, and north), little can be said on its origin or existence in a region where lineations are generally weak to non-existent and strong foliations prominent. A sample of L-tectonite orthogneiss yielded an ID-TIMS U-Pb zircon crystallization age of 3.18 Ga (Böhm et al. 2003a; Bowerman et al. 2004).

3.4 ARCHEAN GRANITOID ROCKS

Leucocratic felsic injections are common throughout the map area and crosscut supracrustals and orthogneiss (Figure 3.4). There appear to be several phases of injection throughout the map area (e.g. tonalite, granodiorite-granite, and pegmatitic granite). The separation into individual phases must be done on phase-crosscutting relationships alone, and is key to unravelling the crosscutting relationships with structures, and thus the timing of deformation (see Chapter 5). The dominant composition of felsic injections is granodioritic to granitic (Figure 3.4a–d), similar to the compositions of the older Gull Rapids orthogneisses. These granodioritic to granitic rocks generally have the mineral assemblages of plagioclase + quartz + K-feldspar + biotite ± hornblende ± garnet. The presence of biotite, hornblende, and local orthoamphibole and clinoamphibole (see section 3.1) suggest prograde mid-amphibolite facies, peak upper-amphibolite facies, and retrograde mid-amphibolite facies metamorphism. Aggregates of biotite, garnet, and hornblende are retrogressed to

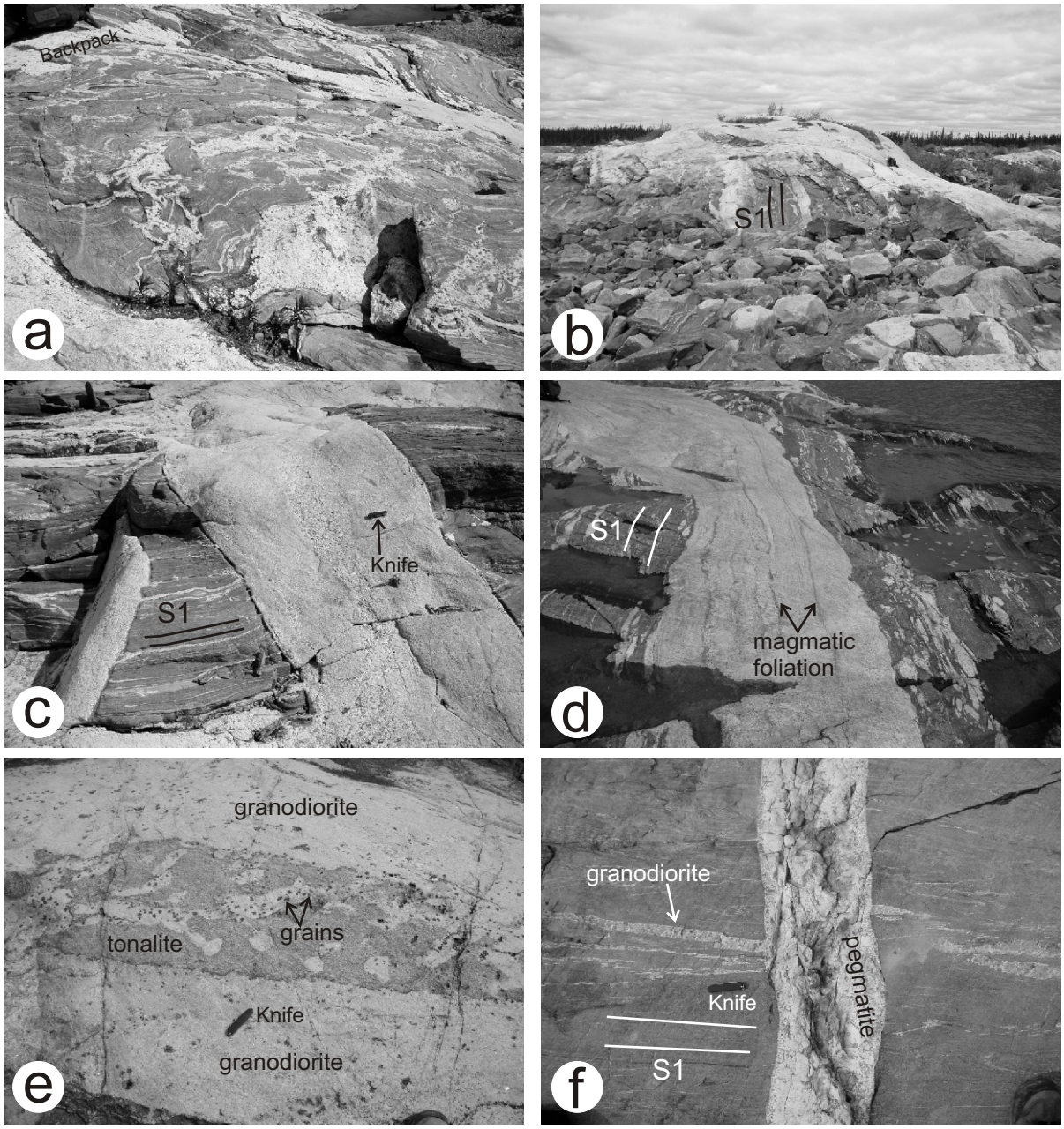

Figure 3.4. Granitoid rocks at Gull Rapids. a) Pods of partial melt in amphibolite. Backpack in top left corner for scale. b) Granitoid dyke covering metasedimentary rocks. Sills branch off from the dyke and are subparallel to the foliation in the metasediments. c) Granitoid dyke cutting amphibolite, with dykelets extending out along the foliation. d) Magmatic foliation in large granitoid dyke. Note light quartzofeldspathic-rich bands and dark biotite- and hornblende-rich bands. Granitoid dyke is approximately 5 metres wide. e) Large orthoamphibole or orthopyroxene grains in granodioritic (light) injection, suggesting upper-amphibolite or granulite facies metamorphism. Note lack of orthoamphibole or orthopyroxene in tonalitic (dark) injection. f) Straight-walled pegmatite dyke crosscutting older foliation-subparallel granodiorite dykes and sills in amphibolite.

mainly chlorite and muscovite (or sericite), and give a spotted to clotted appearance in places. Locally, felsic injections contain nebulitic biotite trails and xenoliths of host rock.

Grey tonalitic injection is also found in the map area, and crosscuts both the metasediments and orthogneiss. The tonalite is fine-grained and contains dominantly plagioclase, quartz, and less than 5% biotite ± hornblende. These tonalitic injections are generally less than 5 metres wide, weakly foliated to massive, and are crosscut by the granodioritic to granitic injection phase (described above). The tonalitic phase does not contain orthoamphibole (Figure 3.4e), but does contain minerals characteristic of mid-amphibolite facies metamorphism (biotite, hornblende). Retrograde greenschist metamorphism was attained in the tonalitic phase, as characterized by the alteration of quartz, feldspar, and mafic minerals to fine-grained chlorite and muscovite (or sericite).

A late pegmatitic phase crosscuts all of the above lithologies including the finer-grained granitoid injections (Figure 3.4f). The pegmatite contains dominantly plagioclase and quartz, with less than 5% biotite ± hornblende. Pegmatite dykes range up to 1.5 metres in width and locally feature large (up to 20 centimetres long) feldspar phenocrysts along with large grains of dark grey-blue quartz. Zones of graphic texture are also found in some of these dykes. These pegmatites do not appear to be the product of partial melting of their host rocks because dyke margins are usually very abrupt with little mingling with the country rock. A small outcrop of anorthosite is also found in the map area. It is undeformed and is probably a localized separate phase of the commonly granodioritic to granitic bodies that cover much of the map area. Mid-amphibolite prograde and greenschist retrograde metamorphism is evident in this phase.

Most of the granitoid samples from Gull Rapids are compositionally similar to the orthogneisses at Gull Rapids and from the Split Lake Block (Bowerman et al. 2004). A number of granitoid samples, including pegmatite, have yielded U-Pb zircon crystallization ages of ca. 2.68–2.61 Ga (see Chapter 5).

3.5 PALEOPROTEROZOIC MAFIC DYKES

Mafic dykes of varying width, grain size, and orientations occur throughout the map area and form part of a generally east-trending major dyke swarm, which can be traced for more than 50 kilometres along the Nelson River to the west (Figure 3.5; Böhm et al. 2003a). These dykes represent the youngest lithological unit in the Gull Rapids area, and for the most part are undeformed and unmetamorphosed. They crosscut all structures, except for the youngest generation of brittle-ductile deformation (Figure 3.5a). Metamorphism in these dykes is limited to greenschist facies, as characterized by the presence of chlorite. This greenschist facies metamorphism is prograde in these dykes, whereas in the rest of the map area greenschist facies metamorphism is retrograde. Grain size within these dykes ranges from aphanitic (diabase; pyroxene + plagioclase ± olivine; Figure 3.5b) to coarse-grained (gabbroic; pyroxene + plagioclase ± hornblende; Figure 3.5c). Gabbroic dykes tend to contain pegmatitic gabbro segregations in their core, and in larger bodies develop chilled margins. Aphanitic diabase dykes intrude gabbroic dykes in places (Figure 3.5d). Coarse-grained pods of gabbroic material within these dykes have crystallization ages of 2102 ± 2 Ma (from a Gull Rapids mafic dyke; L. Heaman, unpublished data) and 2073 ± 2 Ma (from a mafic dyke a few kilometres upstream of Gull Rapids; L. Heaman, unpublished data). It is noteworthy that these east-trending mafic dykes provide a minimum age constraint not only for the protoliths but also for granulite and amphibolite facies metamorphism and deformation. In other words, the supracrustal rocks at Gull Rapids cannot be coeval with Paleoproterozoic supracrustal rocks of the nearby Trans-Hudson Orogen or those in the Thompson Nickel Belt (Ospwagan Group; e.g. Bleeker, 1990a, b). This observation is consistent with a preliminary Nd model age of ~ 3.5 Ga for a sample of Gull Rapids metagreywacke that lies in stark contrast to a ~ 1.95 Ga Nd model age obtained for a Burntwood River Group greywacke sample from northwest Stephens Lake (Böhm et al. 2003a).

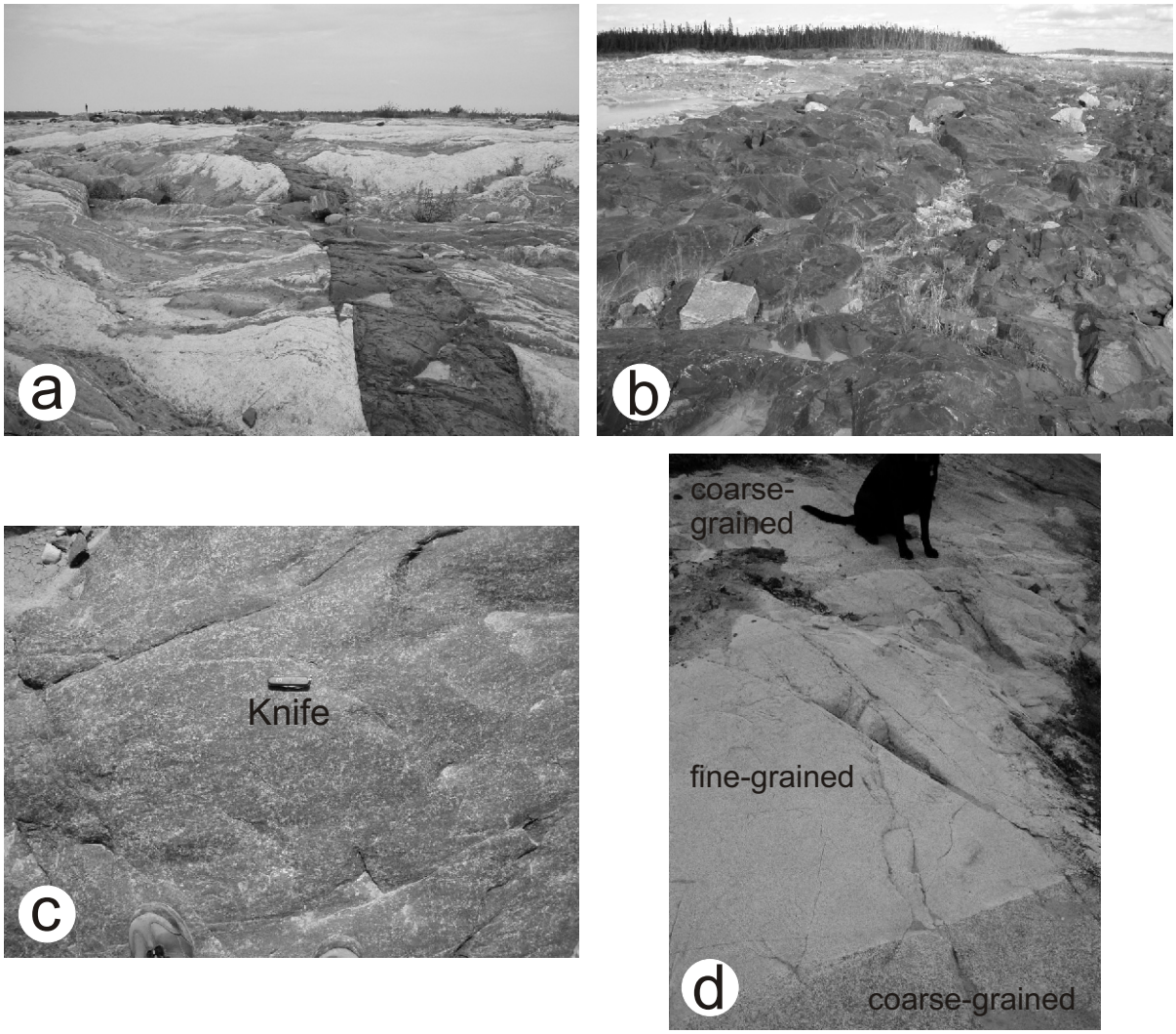

Figure 3.5. Paleoproterozoic mafic dykes at Gull Rapids. a) Fine-grained 1 metre-wide mafic dyke crosscutting metasedimentary and granitoid rocks. b) Fine-grained mafic dyke (diabase), with soapstone-type weathering appearance. c) Coarse-grained mafic dyke (gabbro). d) Fine-grained mafic dyke crosscutting a coarse-grained mafic dyke. Black Labrador dog in d) for scale.

3.6 SUMMARY

In detail, there are five main rock assemblages at Gull Rapids: 1) orthogneiss between ca. 3180 Ma (L-tectonite) and 2850 Ma (augen gneiss); 2) mafic metavolcanic (amphibolitic) rocks (pre-3180 Ma); 3) metasedimentary rocks (2700–2680 Ma); 4) granitic dyke-like intrusions (ca. 2680–2610 Ma); and 5) mafic dykes (ca. 2100 Ma) (Figure 1.3). The relationship between the supracrustal assemblage and the orthogneiss assemblage is unclear due to a lack of exposure at the contact. However, the geochronological evidence presented in the above sections suggests that a large granodioritic body intruded a volcanic assemblage, followed by deposition of a sedimentary package on the granodiorite-volcanic sequence. Since the early granodiorites intruded into a portion of the now existing supracrustal assemblage, an allochthonous origin for the supracrustal assemblage can be ruled out. The intrusion and deposition of the granodiorite-volcanic-sedimentary assemblage was followed by the intrusion of a late granitic body throughout the assemblage, and then by a Paleoproterozoic mafic dyke swarm. All of the above rocks were metamorphosed during a number of events: M1a mid-amphibolite, M1b upper-amphibolite, M2 mid-amphibolite, and M3 greenschist. These metamorphic events correlate consistently with the regional metamorphism described by Corkery (1985). These rocks have also been deformed, and this is discussed in the following chapter (Chapter 4).

Chapter 4

STRUCTURAL GEOLOGY

4.1 INTRODUCTION

Investigations of overprinting relationships and orientations and styles of structure have revealed at least five generations of deformation at Gull Rapids. The five generations of structures are hereby termed G1 to G5, and the associated foliations, lineations, and folds, where present, are termed S1 to S5, L1 to L5 and F1 to F5, respectively. More than one generation of structure (G) may appear within a single progressive deformation event (D), so the term ‘generation of structure’, rather than ‘deformation event’, is used to describe the structural geology of the multiply deformed Archean terrane at Gull Rapids. In the map area, G1 to G3 are represented entirely by ductile structures (foliations, lineations, and folds, with related shearing), whereas G4 and G5 are represented by both ductile and brittle shearing.

4.2 DUCTILE STRUCTURES OF THE GULL RAPIDS AREA

4.2.1 G1 Structures

The G1 generation of structures has been recognized in all rock types with the exception of late mafic dykes. Folds (F1) and a foliation (S1) were developed throughout the supracrustal rocks, whereas a gneissosity (S1) was developed in the orthogneiss. G1 is characterized by a strong regional S1 foliation that strikes approximately 340–040°, dips 40–50°E, and is approximately subparallel throughout the entire map area (Figure 4.1), but varies somewhat in orientation due to later folding and faulting (Figure 4.2). Throughout the supracrustal rocks, S1 foliation is commonly folded by F2 at the micro-, meso-, and macro-scale. In metasedimentary rocks, S1 is a moderate to strong schistosity that is represented by the elongation and alignment of mica grains and aggregates (Figure 3.2a–c, 4.3a). The entire sequence is highly injected by felsic material that crosscuts or is subparallel

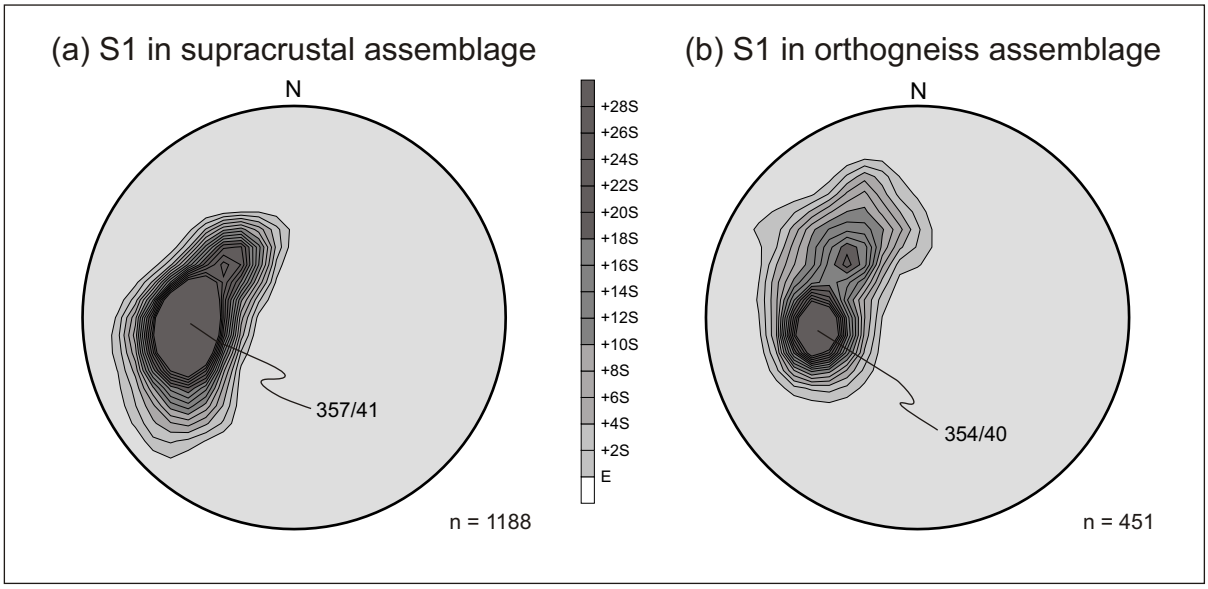

Figure 4.1. a) Equal-area lower-hemisphere projection of S1 foliation from the Gull Rapids supracrustal assemblage. Average strike/dip is 357/41E. b) Equal-area lower-hemisphere projection of S1 foliation from the Gull Rapids orthogneiss assemblage. Average strike/dip is 354/40E.

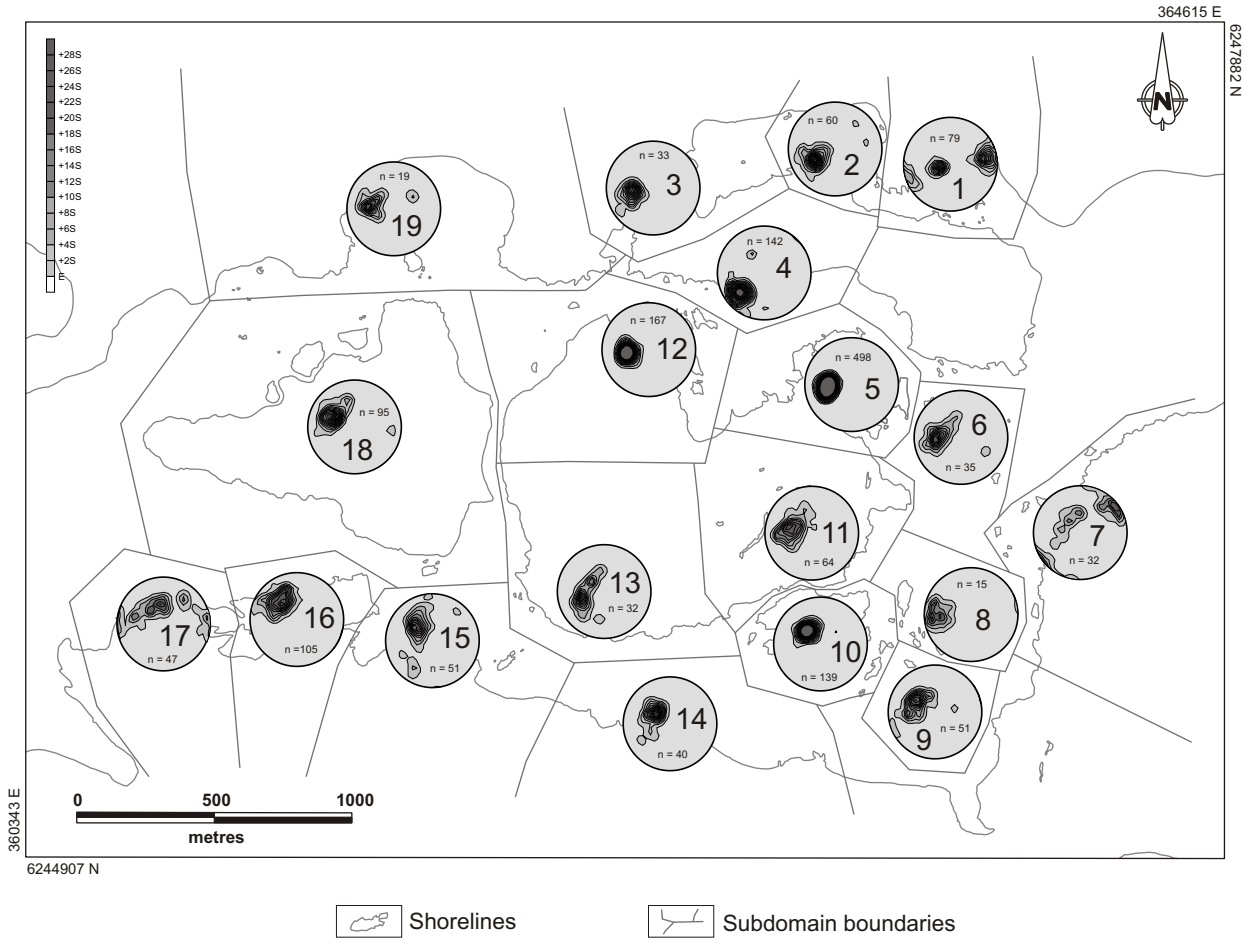

Figure 4.2. Equal-area lower-hemisphere projections of poles to S1 foliation from 19 geological subdomains throughout the Gull Rapids map area. Note general subparallelism of foliation, as well as some folding of the foliation by F2 (e.g., plots 1, 6, and 7 in the metasedimentary rocks), and by shearing (plots 15 and 17 in the granodiorite gneisses). In the easternmost portion of the map area, possible major F2 sheath fold axial planes can be traced from north to south along strike in the amphibolite (plot 1 and plot 7).

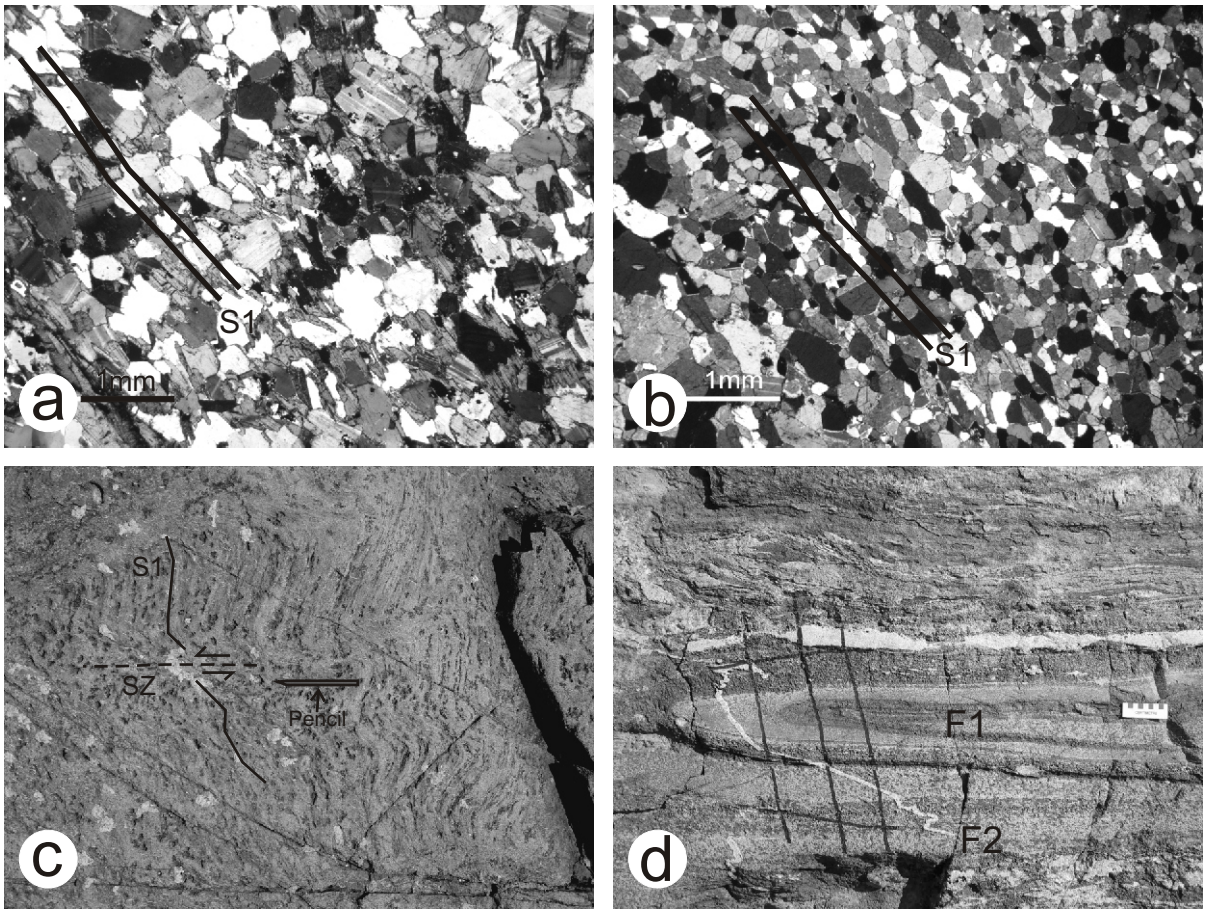

Figure 4.3. G1 structures. a) Photomicrograph of S1 foliation in metasedimentary rocks, with aligned and elongated biotite and aggregates of quartz and feldspar defining the foliation. Crossed polars. b) Photomicrograph of S1 foliation in amphibolitic rocks, with aligned hornblende defining the foliation. Crossed polars. c) Typical S1 gneissosity in orthogneiss. Note the weak foliation and local shearing and folding. Pencil (15 cm long) for scale. d) F1 isoclinal fold in metasedimentary rocks, cut by F2-folded granitic injection dykelet. Black marker lines represent samples taken. See text for discussion.

to the main plane of foliation (Figure 3.2a, b). In the metavolcanic rocks (amphibolite), S1 is a moderate to strong gneissosity that is best represented by the compositional banding of more competent iron-, sulphide- and epidote-rich bands and less competent hornblende-rich bands. Hornblende and lenticular aggregates of epidote and quartzofeldspathic material define the foliation (Figure 3.1a–c, 4.3b). This gneissosity is also defined by laterally continuous felsic dykes, dykelets, sills, and pods of partial melt material. The presence of foliation-subparallel granitoid dykes, dykelets, and sills throughout the supracrustal assemblages give the rocks a migmatitic appearance (Figure 3.1a–c, 3.2a–c). Where bedding, S0, can be recognized in the metasedimentary rocks, it parallels S1 (except at F1 fold closures). The distinction between S0 and S1 is typically difficult to make clearly in outcrop because of the deformational overprint on the primary layering.

In the orthogneiss, S1 is a weak to strong gneissosity. It is strongest and best represented by the compositional banding of tonalite, granite, and granodiorite in the straight-layered gneiss, and by the alignment of flattened augen in augen gneiss. In other portions of the orthogneiss that are not augen-rich or compositionally banded, a gneissosity is present but weak, and is represented by the alignment of mafic grains (biotite and hornblende) and by quartz-feldspar aggregates (Figure 4.3c). It is not known whether the foliation development within the older orthogneissic rocks is contemporaneous with the foliation development within the younger supracrustal rocks or if it represents an older deformation event, as foliation throughout the Gull Rapids supracrustal and orthogneissic assemblages are approximately parallel (Figure 4.1). Locally within the orthogneiss, late-stage, foliation-subparallel granitoid intrusion is present, similar to the granitoid material that intruded the supracrustals. Amphibolite rafts in the orthogneiss have a foliation that is not always parallel to the host rock foliation, suggesting the presence of some early pre-G1 fabric.

Late granitoid phases (dykes, dykelets, sills, and pods of partial melt) preserve a weak foliation defined by elongated biotite and hornblende grains. Late phase pegmatite does not preserve a foliation. Some of the larger crosscutting bodies have a strong magmatic foliation defined by alternating bands of felsic and mafic material. This foliation commonly parallels dyke margins rather

than being parallel to the local tectonic foliation in the surrounding host rocks, suggesting a magmatic origin (Figure 3.4d). For example, at one locality, there is a granitic dyke that has a strong magmatic foliation, however, hornblende laths within this dyke are randomly oriented, indicating a lack of a tectonic foliation. Distinguishing between magmatic and tectonic foliations in other localities can be difficult at times.

Within the map area, there are three generations of folding, F1 to F3, with the most predominant generation being F2. Folding is only evident in supracrustal rocks and crosscutting granitoid phases. Evidence for F1 folding is sparse. Where seen, the F1 generation is a shallowly plunging and upright, isoclinal style of folding, with an axial surface striking approximately north-south (Figure 4.3d). F1 is best developed in the metasedimentary rocks where bedding is seen.

4.2.2 G2 Structures

The G2 generation is the best developed structural event in the map area, and has been recognized in all rock types with the exception of late mafic dykes. Folds (F2), a stretching lineation (L2), and a local F2-axial planar foliation (S2) were developed throughout the supracrustals, whereas a stretching lineation (L2) was developed in the orthogneiss. In the supracrustals, G2 is characterized by F2 folds that plunge moderately (20–40°), are of tight to isoclinal style, and fold S1 and S1-subparallel granitoid dykes, dykelets, and sills (Figure 4.4). F2 folds are less isoclinal than F1 folds. F2 folds plunge southeast (135–155°) throughout most of the map area, except in amphibolite in the northeastern portion of the map area, where they plunge northwest (335–350°; Figure 4.4). Outcrop-scale F2 folding of S1 foliation planes can be observed in some localities within the supracrustal rocks (Figure 4.4). Minor M-, U-, S- and Z-shaped, tight to isoclinal F2 folds (cm- to m-scale) of S1 foliation planes, and ptygmatic folds of foliation-subparallel granitic injection are most common throughout the supracrustal rocks (Figure 4.5a–d, 4.6a, b). Minor U-shaped folds are more common than S- and Z-shaped folds (e.g. Figure 4.5c, d and 4.6a, b, respectively). Locally, these minor folds are more open (Figure 4.6c, d). Stereographic projections of F2 fold axes and S1 foliation planes from

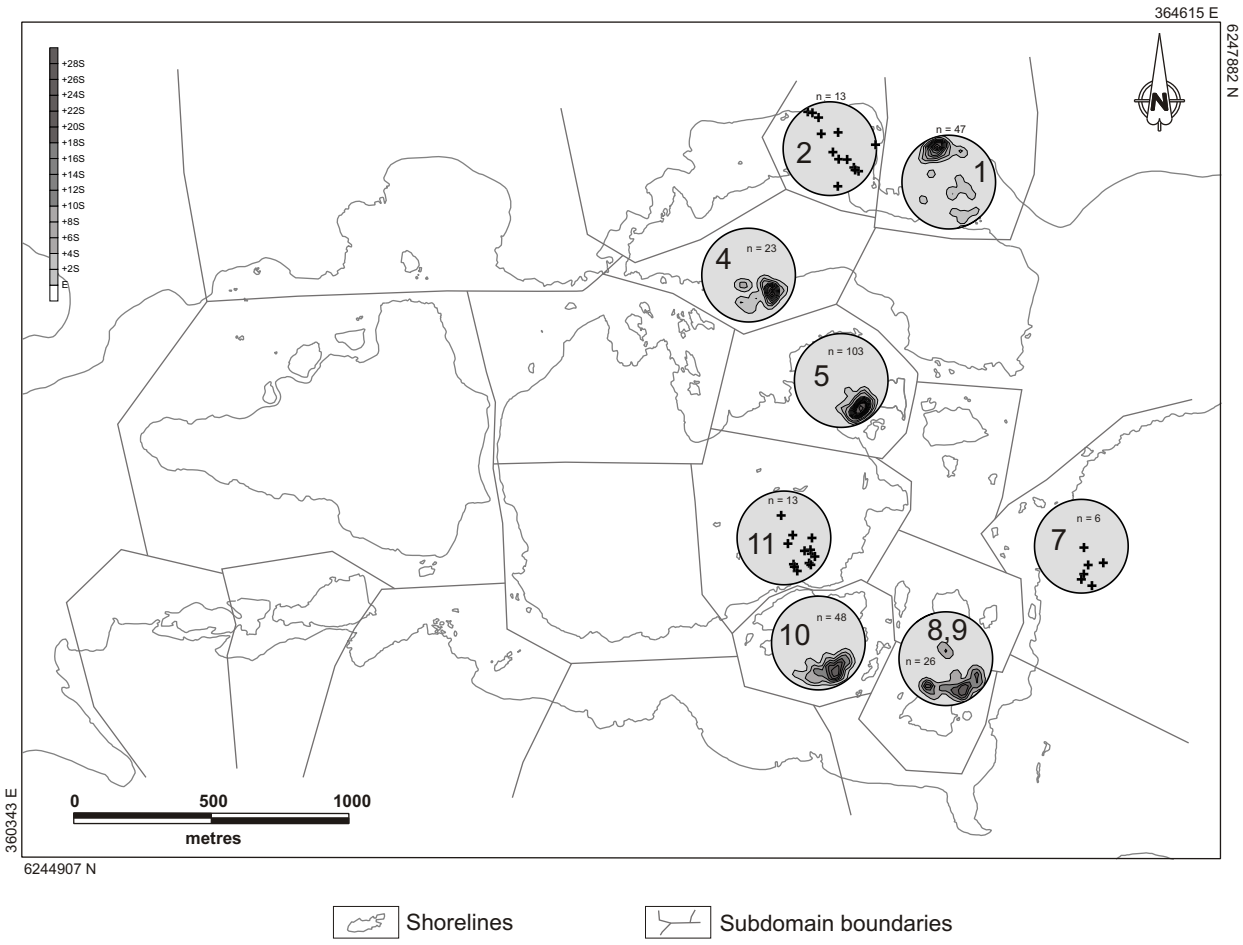

Figure 4.4. Equal-area lower-hemisphere projections of F2 minor (S-, Z-, U, and M-style) fold axis measurements from nine geological subdomains in the supracrustal assemblage of the Gull Rapids map area. Subdomain numbers refer to those presented in Figure 4.2. Folding in the granodiorite gneiss (western part of map area) has not been observed. Plots 2, 7 and 11 are poorly constrained because of a lack of measurable fold axes; however, plots 1, 4, 5, 8, 9, and 10 are much better constrained and show that the F2 minor fold axes generally are southeast-trending, moderately plunging, tight to isoclinal folds. In plots 1 and 2, the fold axes plunge southeast (primarily S-folds) and northwest (primarily Z-folds). The F2 minor fold axes are parallel to L2 stretching lineations. See text for discussion.

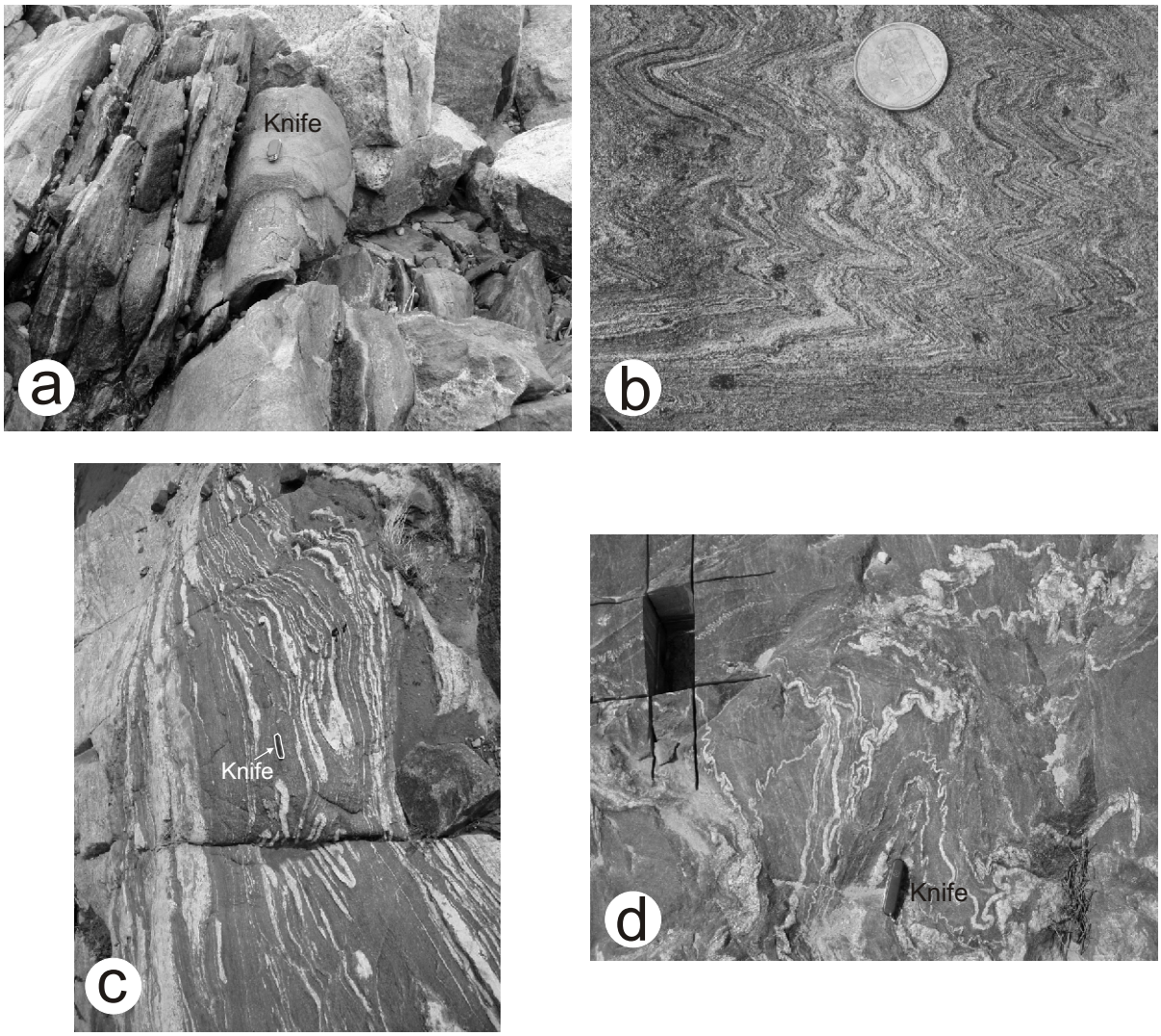

Figure 4.5. F2 folding. a) Meso-scale, upright, tight to isoclinal fold of S1 in layered amphibolite. b) Micro-scale, tight, minor folds of S1 in layered amphibolite. c) Minor, tight to isoclinal ptygmatic M-folds of S1-subparallel granitic injection dykelets and sills in metasedimentary rocks. Knife in centre of photo for scale. d) Highly folded area, showing ptygmatic folding of granitic injection dykelets. Rock cut in upper left hand of photo is a sampling site.

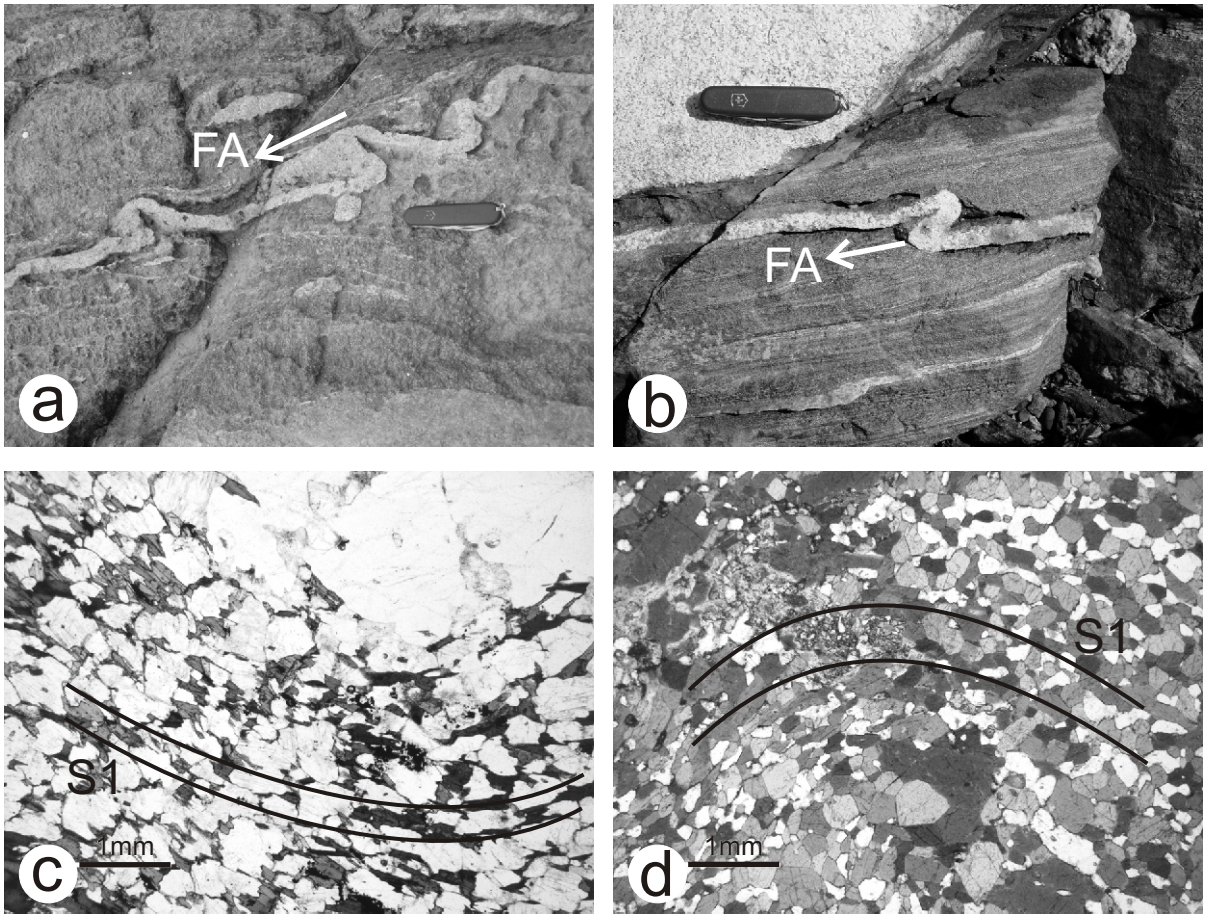

Figure 4.6. F2 folding. a) Well exposed minor tight S-fold of S1-subparallel granitic injection sill in metasedimentary rocks. Fold axis plunges to the southeast. b) Well exposed minor tight Z-fold of S1-subparallel granitic injection sill in amphibolite. Fold axis plunges to the northwest. c) Photomicrograph of folded metasedimentary rocks, showing a more open (tight to open) fold hinge. Note curvature of elongated biotite (S1) around hinge. Also note lack of axial planar cleavage and primary bedding planes. Plane polarized light. d) Photomicrograph of folded amphibolite, showing a more open (tight to open) fold hinge. Note curvature of elongated hornblende (S1) around hinge. Also note lack of axial planar cleavage. Plane polarized light.

certain subdomains throughout the supracrustal assemblage show that the observed minor F2 folding is of the same generation as the major F2 folding (Figure 4.7a–d). Distinguishing between F1 and F2 folds, as well as S1 and S2 foliation, is often difficult due to the strong overprint of G2. This has resulted in the parallelism of F1 and F2 fold axial planes and axes, as well as S1 and S2 foliations. Therefore, discerning F1 folds from F2 folds is easiest when crosscutting dykes or dykelets exist. In one locality, a small, F2-folded granitic dykelet is seen to crosscut an isoclinal F1 fold in metasedimentary rocks (Figure 4.3d). Folding was not observed anywhere in the orthogneiss, other than metre- to centimetre-scale shear-related folding of S1.

A second foliation (S2), axial planar to F2, is rare (Figure 4.8a). Where seen, this axial planar S2 is subparallel to S1, except at F2 fold hinges. The S1 foliation may actually be transposed into S2 locally within the supracrustal rocks, thus meaning that the strong fabric seen in these areas is actually a composite of S2 and S1. The best evidence for transposition comes from the existence of widespread tight to isoclinal F2 folds of S1 foliation planes, which leave most axial planes parallel to the foliation, and most foliation planes dipping in a constant direction. Detachment of fold hinges is also relatively common. This evidence is best observed in layered amphibolite, where the gneissosity is strongest, and where there is a significant amount of folding. However, because of the tight to isoclinal nature of the folding, S2 foliation planes become parallel to S1, and it is therefore difficult to distinguish a first foliation from a second transposition foliation in these highly folded areas, or in any folded area in the supracrustal assemblage for that matter. Also, F2 folding and the development of an S2 transposition foliation may overprint any original S1 fabric. Therefore, it is uncertain that there is an actual transposition of S1 to S2 everywhere in the supracrustal rocks. Regardless, this tight to isoclinal style of folding in not seen everywhere in the supracrustals, and therefore the main foliation remains interpreted as S1.

One generation of lineation, L2, is observed in rocks of the Gull Rapids area. It is a stretching lineation that generally lies on S1 foliation planes. Both host rock (either orthogneiss or supracrustal) and dykes (granitoid dykes only) are stretched (Figure 4.8b, c). L2 is a moderate to strong,

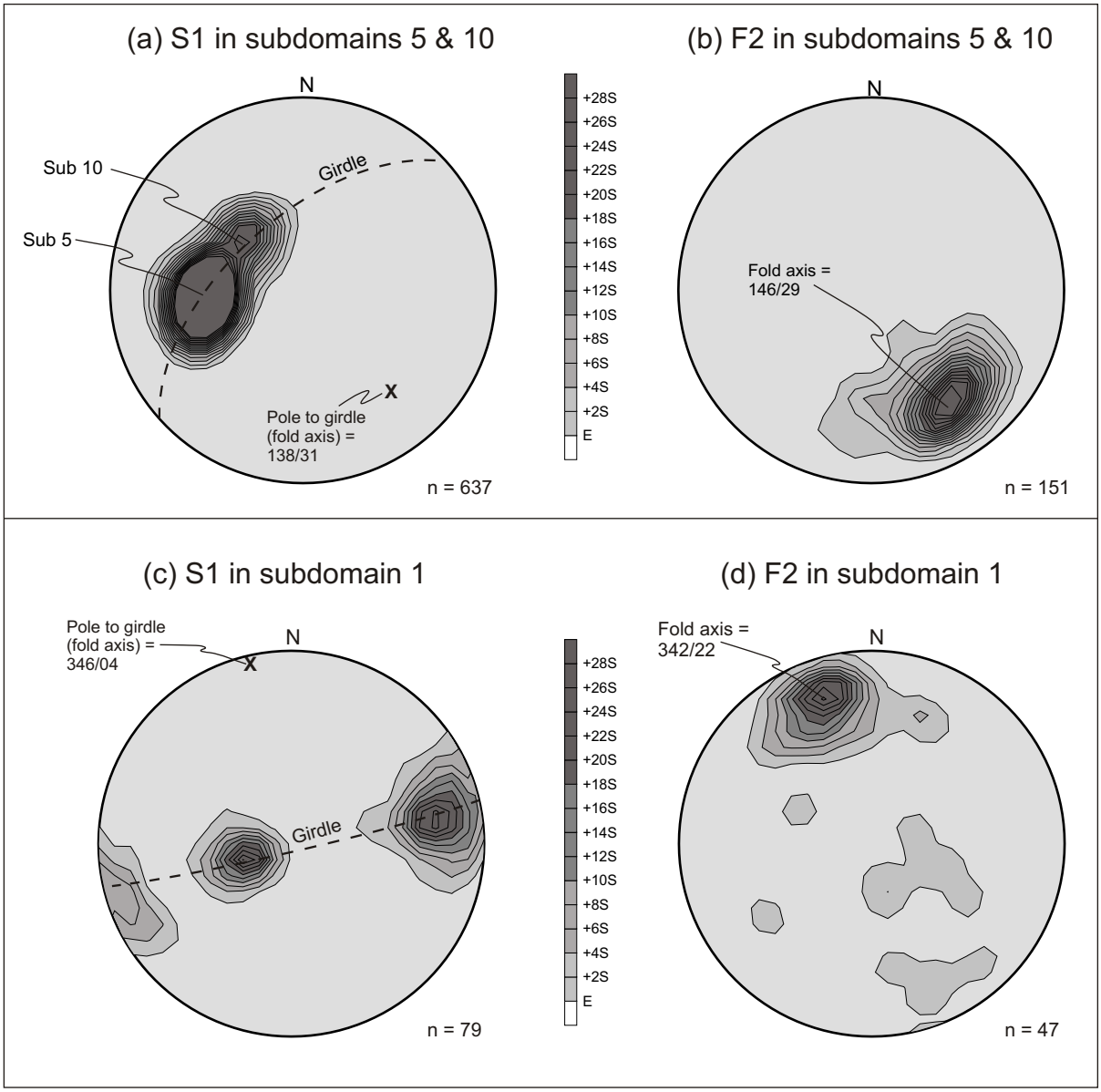

Figure 4.7. A, B. Equal-area lower-hemisphere projections of a) poles to S1 foliation and b) F2 minor fold axes from two geological subdomains (Sub 5 and 10) within metasedimentary rocks. Subdomains 5 and 10 were chosen because together they display variation of the foliation due to folding, whereas individually they do not display such variation in the foliation. Measured F2 minor fold axes (trend and plunge of approximately 146/29) were found to be subparallel to the calculated major F2 fold axis (trend and plunge of approximately 138/31), indicating that the minor and major folding are of the same generation in these metasedimentary subdomains.

C, D. Equal-area lower-hemisphere projections of c) poles to S1 foliation and d) F2 minor fold axes from one geological subdomain (Sub 1) within amphibolite. Measured F2 minor fold axes (trend and plunge of approximately 342/22) were found to be subparallel to the calculated major F2 fold axis (trend and plunge of approximately 346/04), indicating that the minor and major folding are of the same generation in this amphibolite subdomain.

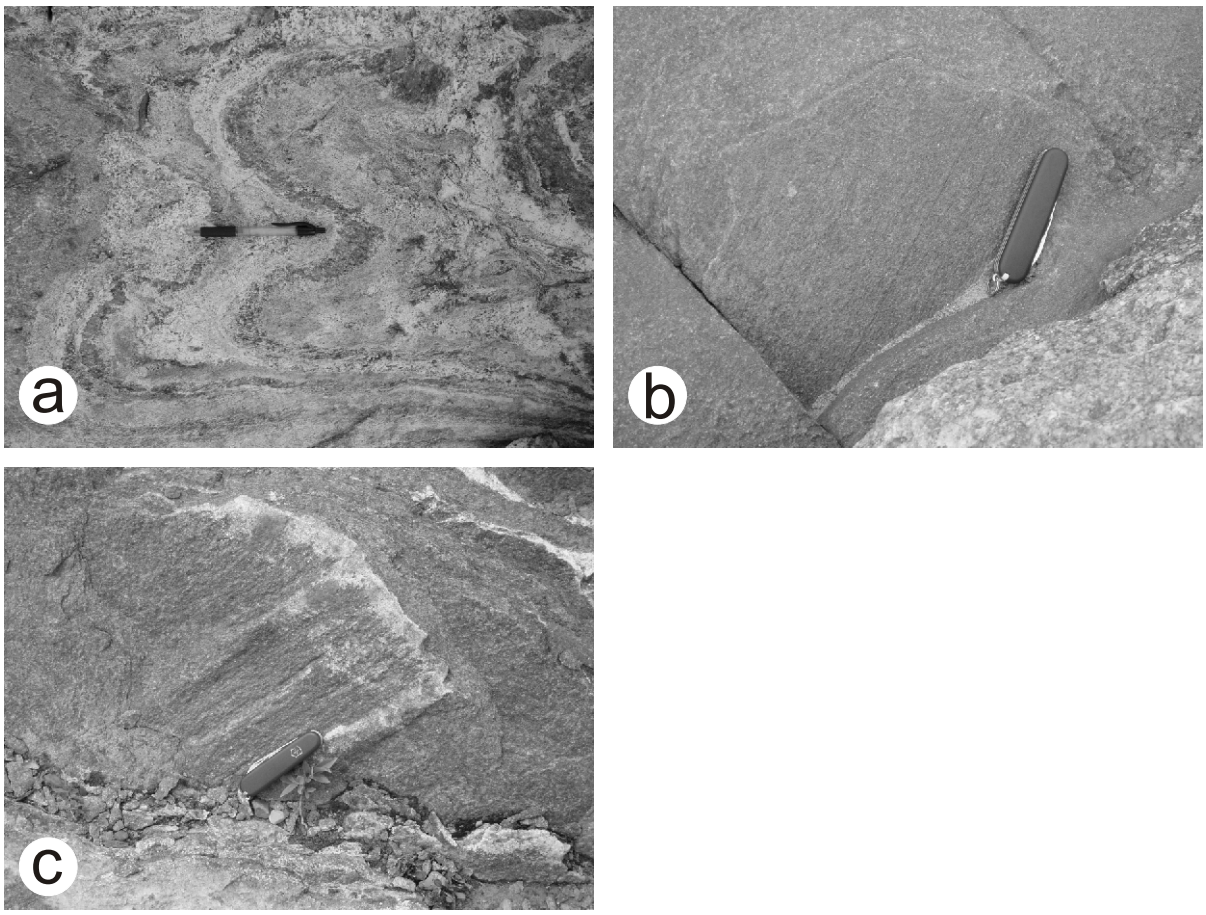

Figure 4.8. G2 structures. a) F2-axial planar foliation (S2) in metasedimentary rocks. Pen for scale, and is parallel to S2. b) L2 stretching lineation in metasedimentary rocks. L2 lies on an S1 foliation plane. c) L2 stretching lineation in a granitic sill that parallels the S1 foliation in metasedimentary rocks. Note that both the host metasediment and intruding granite are stretched. Lineation in b) and c) plunges moderately to the southeast, parallel to most F2 fold axes. Knife in b) and c) is parallel to the lineation.

moderately to shallowly plunging lineation which trends approximately south in the orthogneiss and southeast in the supracrustal rocks (Figure 4.9, 4.10a). In the supracrustal rocks, L2 is characterized by the preferred orientation of stretched biotite, hornblende, and rodded aggregates of quartzofeldspathic material, as well as stretched pyroxenite pebbles in the metaconglomerate. In the orthogneiss it is characterized by stretched quartz, feldspar, and K-feldspar augen. This lineation is deemed to be of the second generation of structure because everywhere in the map area it is parallel to F2 fold axes (Figure 4.10b), and to boudin neck axes. An L1 lineation has not been identified. This L2 lineation may represent the intersection between two foliations, however, this second foliation is rarely distinguished in the field.

The fold system at Gull Rapids is doubly plunging, with most S-folds plunging southeast and many (but not all) Z-folds plunging northwest (Figure 4.11a, b). U-shaped folds are the most abundant and plunge in both directions (Figure 4.11c). Northwest-plunging U-folds may just be Z-folds for which the asymmetry is not seen (i.e. one limb of a Z-fold). The southeast-plunging folds (both S- and Z-shaped) are developed in the southern and western portion of the supracrustals, whereas the northwest-plunging folds (nearly all Z-shaped) are developed in the northeastern portion. The presence and abundance of S- and Z-folds in the supracrustal assemblages suggests sheath folding and shearing on the supracrustal assemblage-scale. The stretching lineation, L2, which is parallel to most fold axes (Figure 4.10b), is also parallel to the long axes of the sheath folds, and S1 foliation planes are parallel to shear surfaces. This L2 lineation therefore represents an approximate shearing direction. Since L2 plunges southeast and is parallel to the long axis of the sheath fold and to the direction of shear, the northwest-plunging Z-folds cannot represent an axis of a fully developed sheath fold, and therefore represent drag folds. The presence of northwest-plunging Z-folds along this shear zone indicates a southwest-side-up and dextral sense of shear (Figure 4.12). Upon further rotation (further southwest-side-up and dextral shearing/development of sheath fold), the northwest-plunging Z-fold axes will rotate through horizontal towards the southeast (becoming S-folds), or will rotate through vertical towards the southeast (remaining as Z-folds) (Figure 4.13). This is evidenced

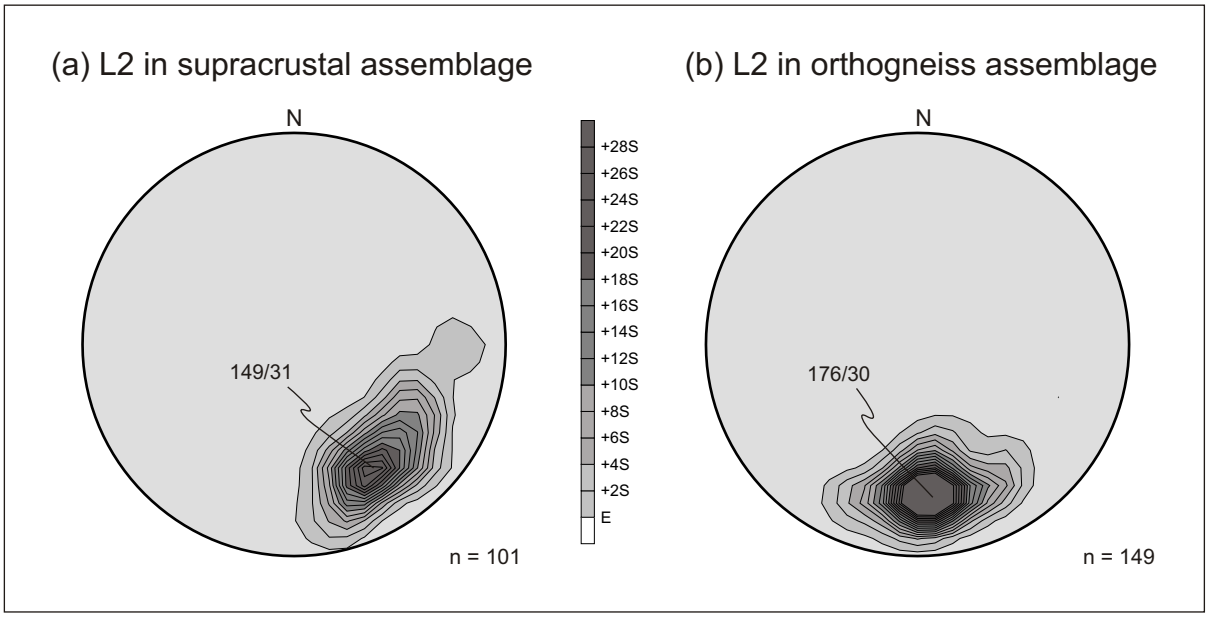

Figure 4.9. a) Equal-area lower-hemisphere projection of L2 lineation from the Gull Rapids supracrustal assemblage. Average trend/plunge is 149/31. b) Equal-area lower hemisphere projection of L2 lineation from the Gull Rapids orthogneiss assemblage. Average trend/plunge is 176/30.

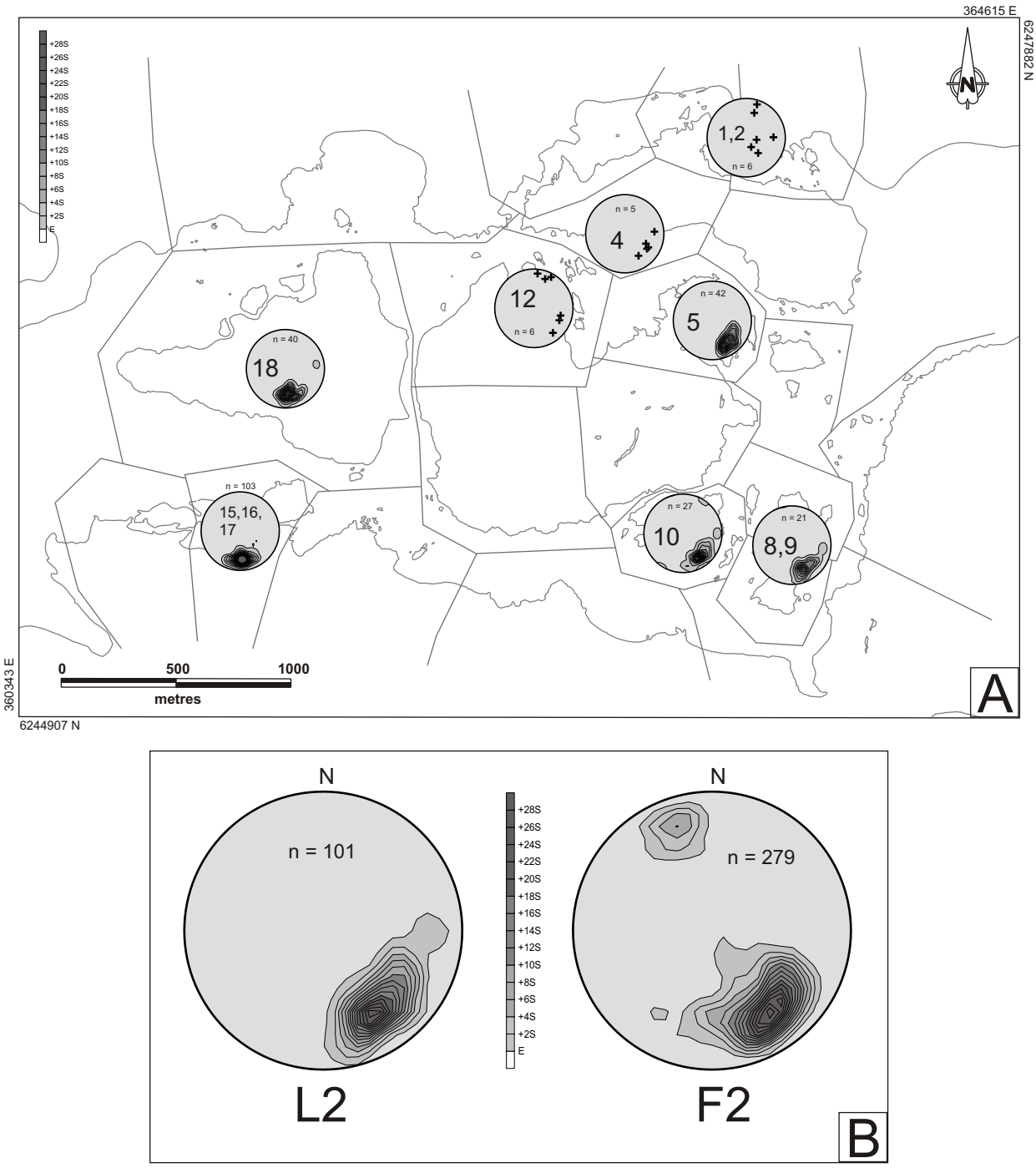

Figure 4.10. A. Equal-area lower-hemisphere projections of L2 lineation from twelve geological subdomains throughout the Gull Rapids map area. Subdomain numbers refer to those presented in Figure 4.2. Note the general subparallelism of lineation throughout the map area; however, in the granodiorite gneiss (plots 15-18), the lineations plunge moderately shallowly to the south, whereas in the metasedimentary rocks (plots 4, 5, 8, 9, and 10), they plunge moderately shallowly to the southeast. B. Equal-area lower-hemisphere projections of all L2 and F2 measurements from the Gull Rapids supracrustal assemblage. Note that the main concentrations are subparallel, suggesting that L2 and F2 are kinematically related.

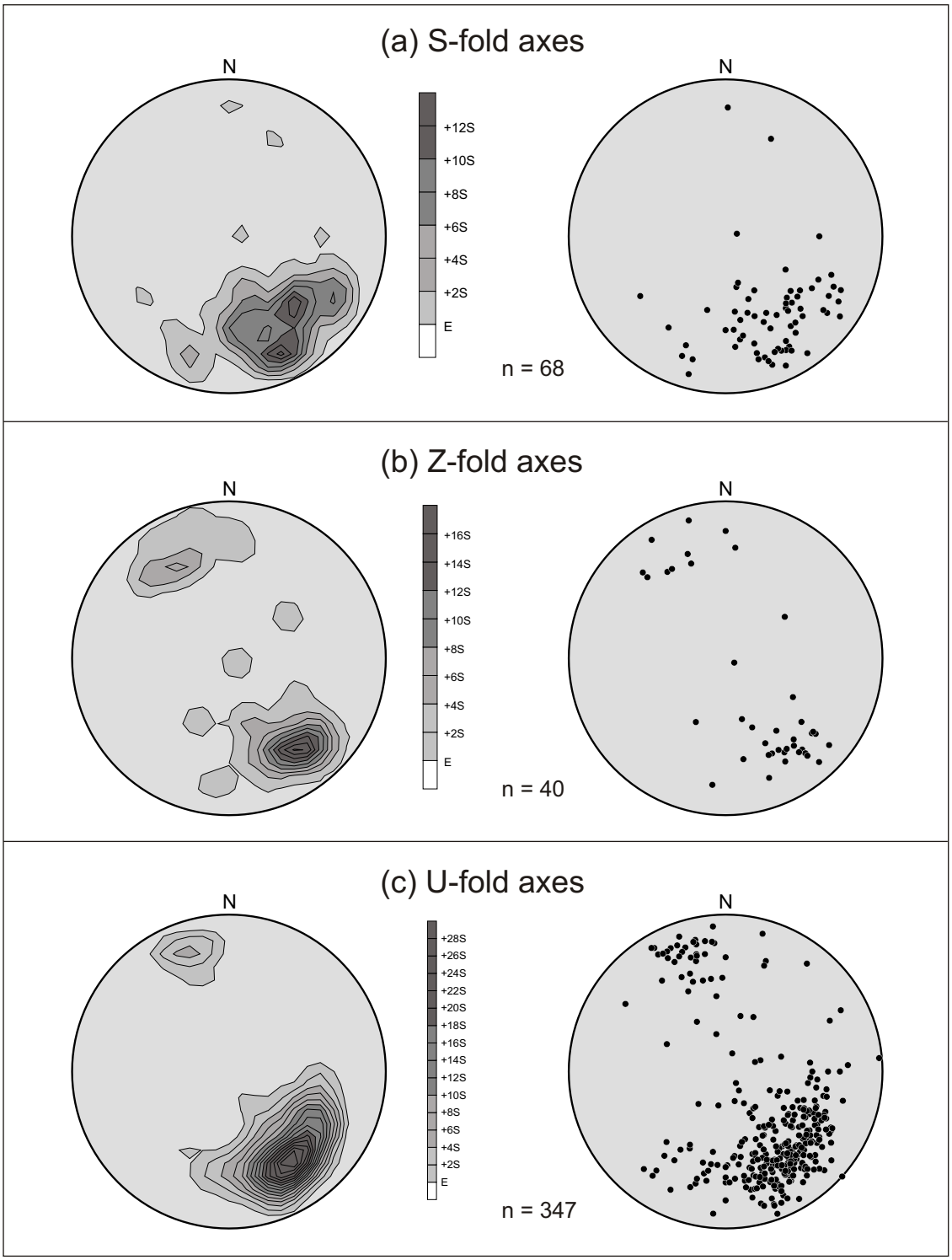

Figure 4.11. Equal-area lower-hemisphere projections of F2 minor fold axis measurements from all supracrustal subdomains. Stereonets on the left side of the diagram show measurement concentrations, those on the right side show data points of same projection. a) All S-fold axes. Note that all measurements are plunging southeast. b) All Z-fold axes. Note that there are roughly equal amounts of axes plunging southeast and northwest. This means that all Z-folds and no S-folds plunge northwest. c) All U-fold axes. Note that these plunge in both directions. U-folds may be Z- or S-folds where the asymmetry is not seen.

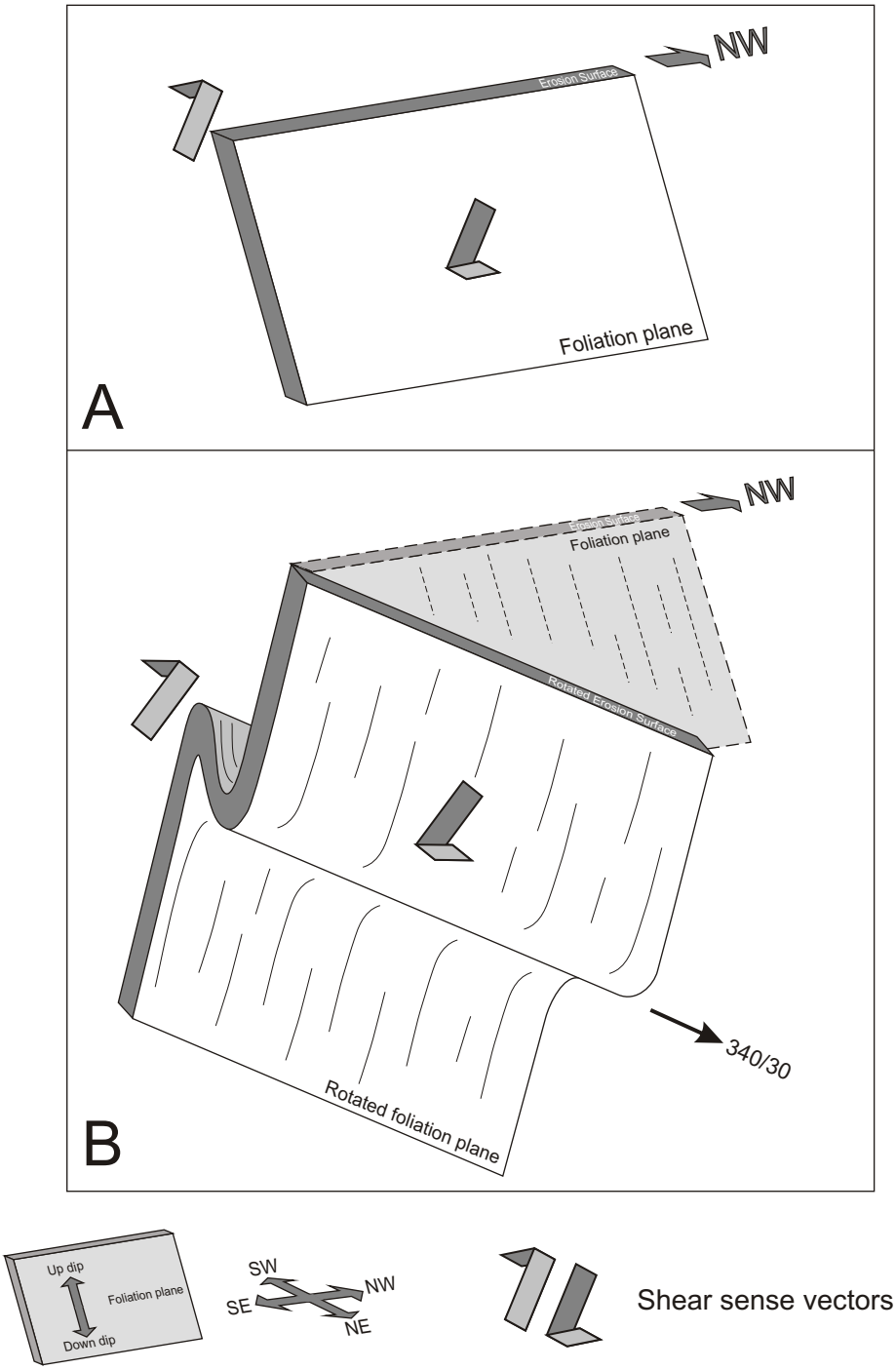

Figure 4.12. Schematic diagram showing the onset of F2 folding in the northeastern portion of the supracrustal assemblage at Gull Rapids. F2 folding in the supracrustals is due to shearing. A. S1 foliation planes before shearing and related folding. B. Southwest-side-up, dextral shearing leads to the development of northwest-plunging tight to isoclinal Z-folds. F2-axial planar foliations (S2) are locally present at Gull Rapids, and are subparallel to S1 due to the tight to isoclinal nature of the shear-related folds. These Z-folds are interpreted to be drag folds in the Gull Rapids supracrustal assemblage.

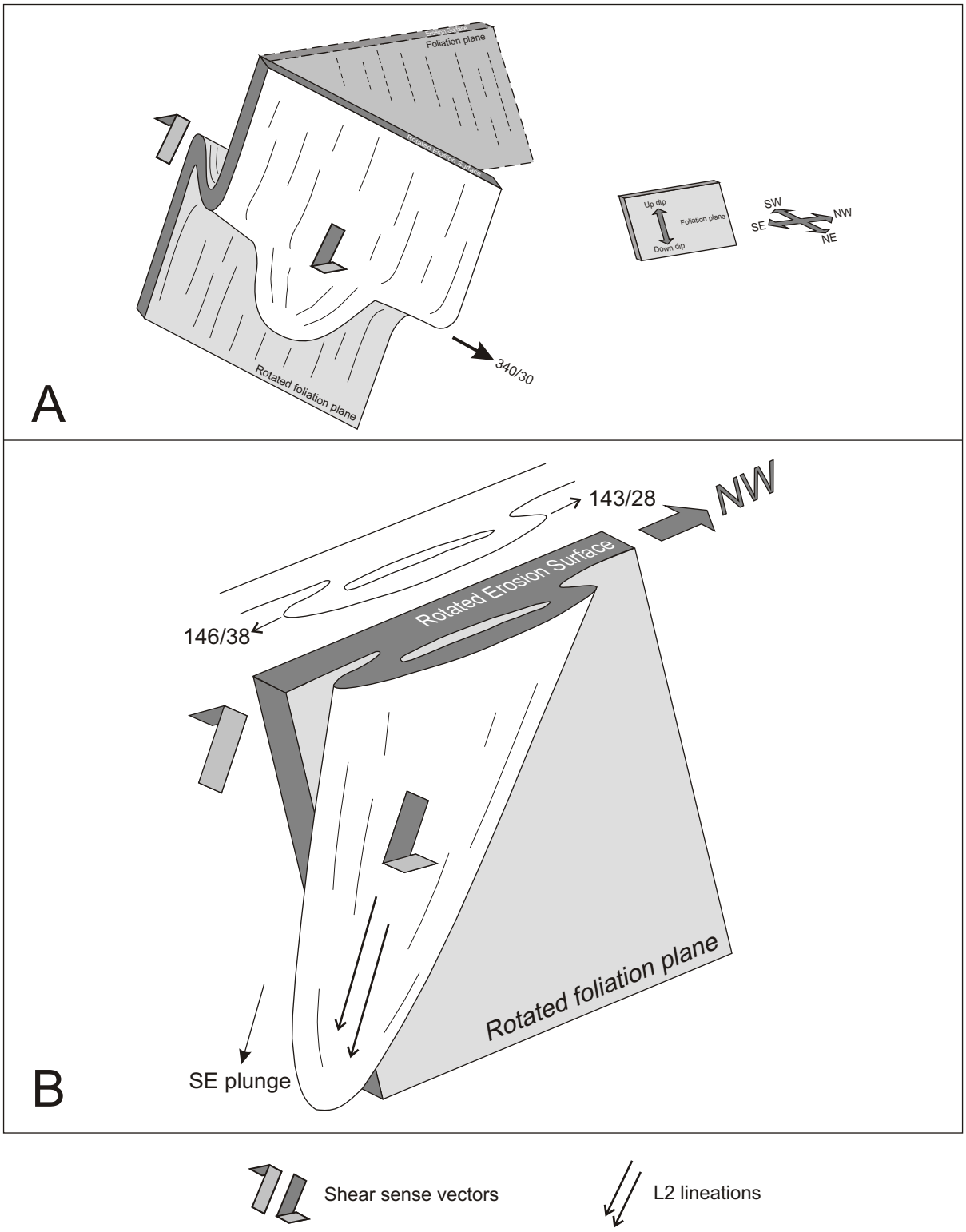

Figure 4.13. Schematic diagram showing the progressive phases of sheath fold development (F2) in the supracrustal assemblage at Gull Rapids. A. Onset of sheath fold development, northeast-side-down and dextral shear. B. Continued development of sheath fold with northeast-side-down (southwest-side-up) and dextral movement. This leads to the development of a tight to isoclinal sheath fold, with L2 lineations subparallel to the long axis of the sheath fold, and with Z- and S-folds both plunging southeast.

by the abundant amount of southeast-plunging S- and Z-folds, which are equally developed throughout the southern and western portions of the sequence. These fold axes are parallel to L2, suggesting proper sheath fold development in this portion of the large sheath fold system, and again suggest southwest-side-up (northeast-side-down) and dextral movement along this shear zone (Figure 4.13). It is quite common in shear zones that such drag folds (i.e. the northwest-plunging Z-folds) develop into sheath folds during progressive deformation (i.e. the southeast-plunging S- and Z-folds; Mawer and Williams 1991; Jiang and Williams 1999). Minor sheath folds (cm-scale) throughout the sequence (with S- and Z-axes) are rare and do not show any measurable fold axes, and therefore cannot give a sense of shear or a sense of sheath fold closure (Figure 4.14a, b). These minor sheath folds are however most likely representative of the larger scale sheath fold system. Minor S- or Z-folds are much more common than minor sheath folds. These abundant minor S- and Z-folds probably represent only one axis of such minor sheath folds, for which the other axis is not observed in outcrop. In other words, the sheath fold system at Gull Rapids is most likely composed of many of these centimetre-scale sheath folds (Figure 4.14a, b). The folding at Gull Rapids is therefore interpreted to be part of a large, tight to isoclinal sheath fold system that developed as a result of large-scale shearing.

The strong deformation that is observed throughout the Gull Rapids supracrustal assemblage, in combination with the abundance of isoclinal folds and ptygmatic folds (which form as a result of shear-related buckling rather than bending fold mechanisms; Williams and Jiang 2001; P. Williams pers. comm., 2004), local drag folds, and of a sheath fold system, all provide evidence that the Gull Rapids supracrustal assemblage is indeed a part of a large (~ 2 km wide) shear zone.

Boudinage is limited to the supracrustal portion of the map area and deforms the S1 foliation, but boudins remain parallel to this foliation (Figure 3.1b, c, 3.2b, 4.15). Boudinage is best seen in the layered amphibolite, where the competency contrast between compositional layers is highest, and where competent iron-, sulphide-, and epidote-rich layers contrast against less competent hornblende-rich layers. In most cases within the layered amphibolite, the competency contrast is such that

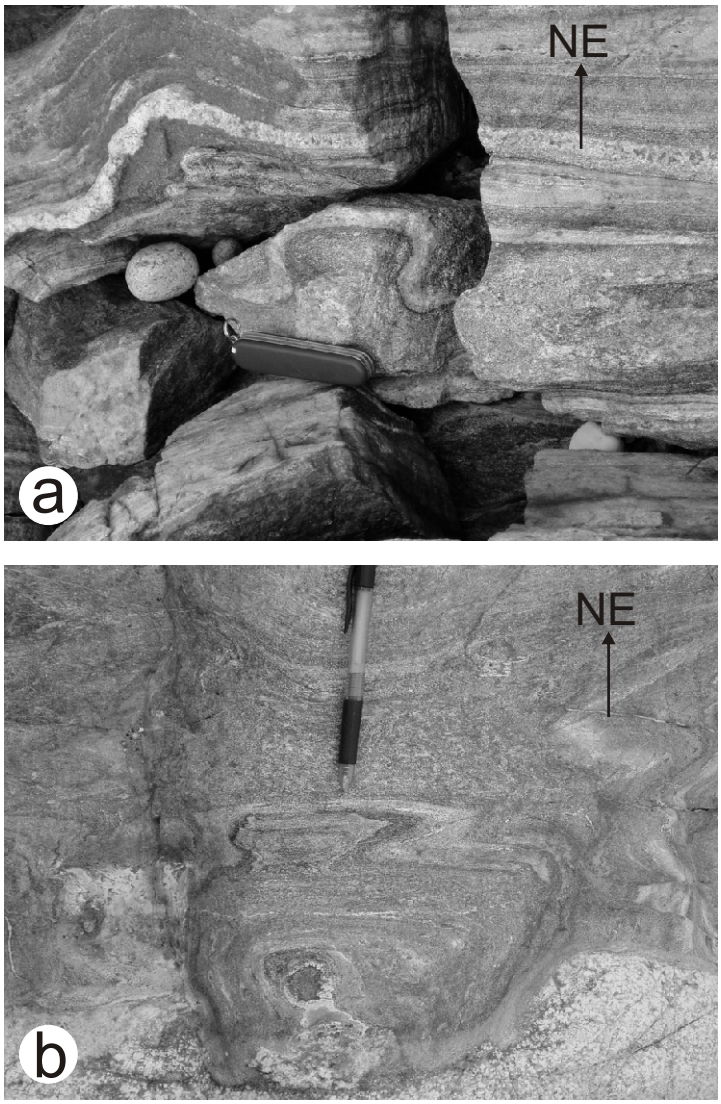

Figure 4.14. Minor (centimetre-scale) sheath folds in the amphibolite. See text for discussion.

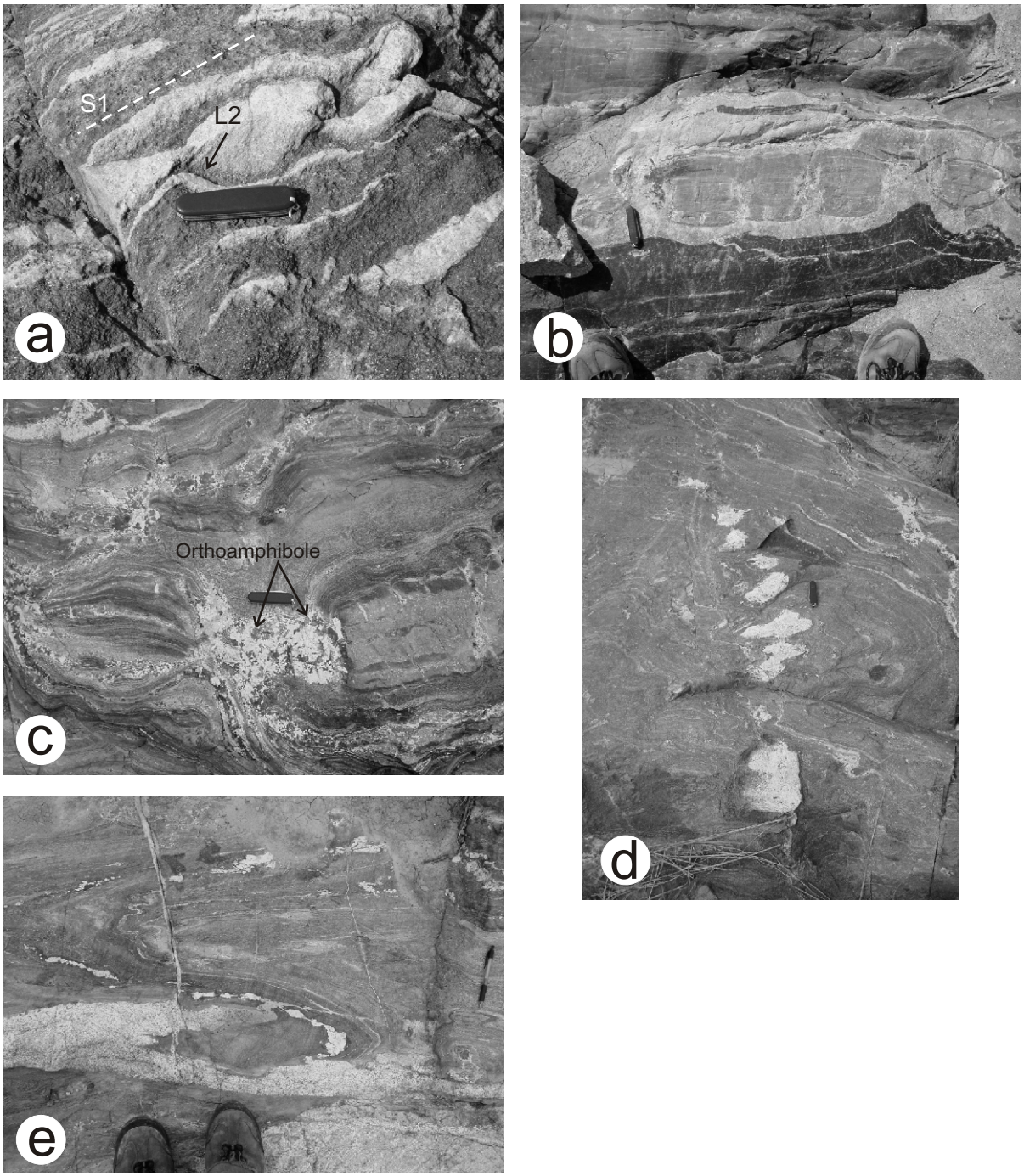

Figure 4.15. Boudinage in the supracrustal assemblage. a) Granitic injection boudin in metasedimentary rocks, showing boudin neck axis, which is parallel to L2 (SE plunge). b) Rectangular-style boudin of calc-silicate layer in layered amphibolite. c) Orthoamphibole-rich granitic injection into boudin neck in amphibolite; injection and amphibolite grade metamorphism are coeval with boudinage. d) Granodioritic boudins folded by F2. e) Apparently-folded boudins of a granitic dykelet. The boudinage is probably related to the folding, rather than the boudins being folded.

moderate pinch-and-swell structures are observed. Boudin neck axes are subparallel to L2 lineations (Figure 4.15a). Locally, the boudins are less necked because the competency contrast is higher. This leads to the formation of rectangular-style boudins (Figure 4.15b). In the metasedimentary rocks, iron formations, subparallel to bedding and S1, are much more competent than the metagreywacke and metapelite layers. This competency contrast leads to pervasive boudinage of the iron formation and, to a lesser extent, of the host metasedimentary rocks (Figure 3.1e). Locally within supracrustal rocks, granitic injection dykes, dykelets, and sills are boudinaged. In some localities, there is injection into boudin necks, suggesting that injection and boudinage are roughly coeval. Orthoamphibole, indicative of upper-amphibolite facies metamorphism and found primarily in the injection material, is also found in boudin necks suggesting that this metamorphism is coeval with injection and boudinage (Figure 3.1d, 4.15c). In some localities, it appears as though boudins are folded by F2 (Figure 4.15d), whereas in other localities the boudinage of layers and granitic material may be related to the folding itself (Figure 4.15e). In these cases, the boudin necks are not observed, and consequently it is difficult to discern whether the folding or the boudinage came first. Therefore, boudinage is either pre- or syn-F2. Based on all of the field observations, boudinage throughout the Gull Rapids area is interpreted as being approximately late-G1 or early-G2.

The westernmost zone of orthogneiss in the Gull Rapids map area is dominated by L>S- and L-tectonite (where the strain ellipsoid is of constrictional type, with K»1; Figure 3.3d, 4.16a). Moving across strike from east to west within the orthogneiss, the structure changes from S- and S-L-tectonite (with K = 0.85; Figure 4.16b) to L- and L>S-tectonite over 30 metres. Strain analyses were completed on stretched grains of K-feldspar. Due to the small amount of available outcrop (only along the shores of the Nelson River), proper boundary conditions cannot be placed on the formation of this L-tectonite zone (cf. Knee Lake Shear Zone of Lin and Jiang, 2001). Regardless, the lineation in the L-tectonite trends subparallel to lineation throughout the map area, suggesting that all stretching lineations at Gull Rapids are kinematically related.

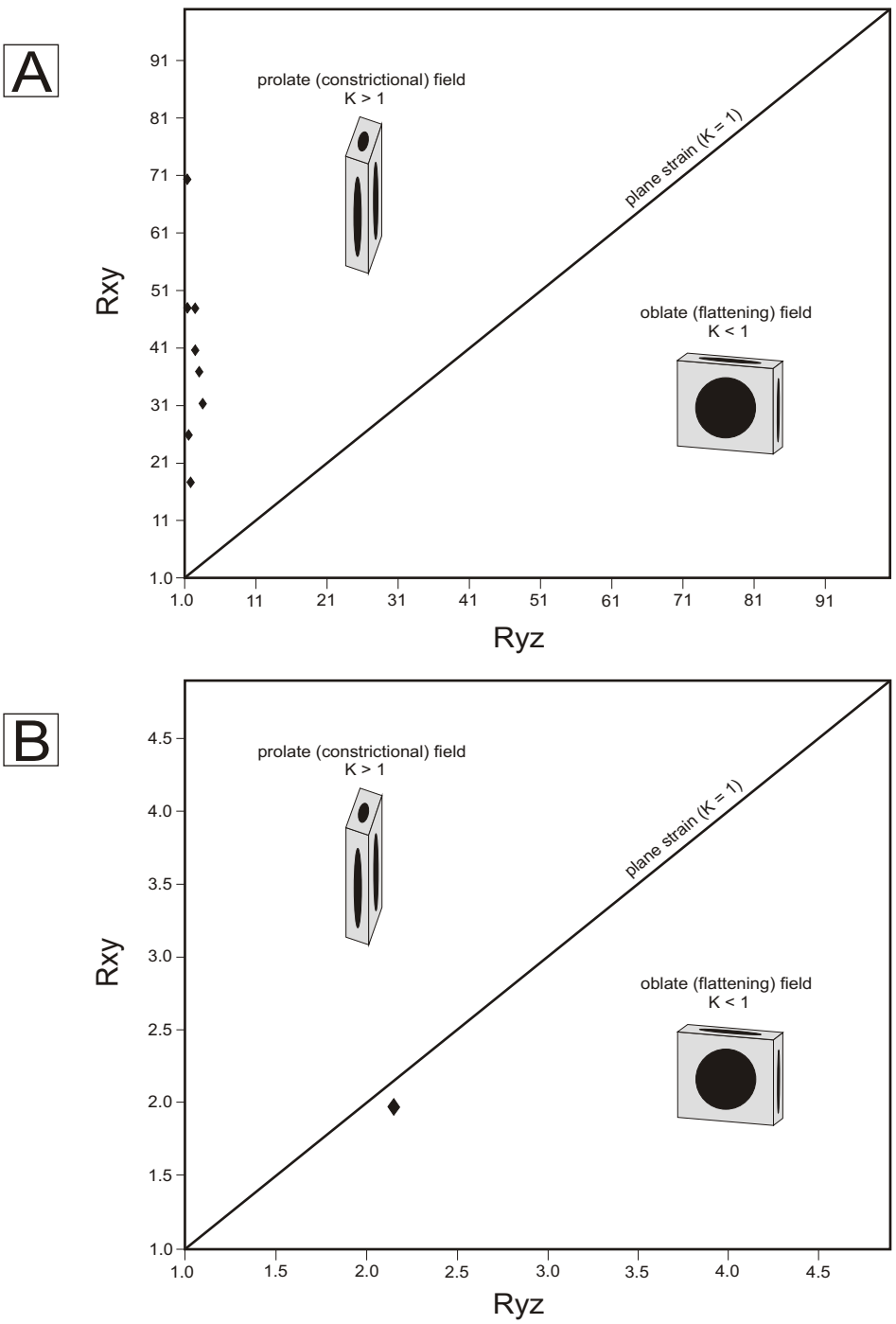

Figure 4.16. Strain analysis of selected rock types from the Gull Rapids orthogneiss assemblage, using Flinn diagrams. A. Flinn diagram of small outcrop (50 centimetres by 50 centimetres) of L-tectonite. Diamonds represent stretched grains of K-feldspar. Note that K>>1, and points lie in the field of constriction, typical for such an L-tectonite. B. Flinn diagram of small outcrop (2 metres by 2 metres) of stretched and flattened augen gneiss. Diamond represents average Rxy and Ryz for 20 augen. (An average was taken because augen on the XY plane could not be correlated to the same augen on the YZ plane.) Note that K = 0.85, close to the field of plane strain, typical for an S-L tectonite.

4.2.3 G3 Structures

Evidence for a third structural generation, G3, is sparse. It is only recognized as a refolding event in supracrustal rocks. This third generation of folding, F3, is a metre- to kilometre-scale open style of folding with an axial surface oriented approximately east-northeast (075–080°). The F3 generation rotates S1 (and S2) strike orientations from 345–000° in the northern portion of the supracrustal sequence to 030–050° in the southern portion (see Figure 1.3 and 4.2). This major fold has an amplitude of approximately 1 kilometre. The F3 generation also refolds minor tight to isoclinal F2 axial planes and fold axes in a more open style of folding (Figure 4.17a–c). This small-scale refolding is only seen in a few localities within the supracrustal rocks, and is parasitic to the much larger F3 fold. Unfortunately, neither F3 fold axes nor axial planes were observed to allow for proper measurement.

4.3 FAULTING AND SHEARING IN THE GULL RAPIDS AREA

Generally, shearing is late and comprises the structural generations G4 and G5. Early shearing is related to sheath fold development during G1-G2. Crosscutting relationships between ca. 2.1 Ga mafic dykes and G4-G5 shear zones are the key to the separation of shearing events into the G4 and G5 generations. G4 shear zones are those that are cut by mafic dykes, whereas G5 shear zones are those that cut mafic dykes.

4.3.1 Early Shearing and Kinematics

An early shearing event is related to the development of a sheath fold system in the Gull Rapids supracrustal assemblage, and is related to F2 tight to isoclinal folding. This shearing may also be responsible for F1 isoclinal folding, and for the development of the S1 foliation. Since the S1 foliation generally dips to the northeast, the L2 lineation plunges southeast, Z-folds plunge northwest in the northeastern portion of the map area, and S- and Z-folds both plunge southeast in the southern and western portions of the map area, this shearing event has southwest-side-up, dextral sense of

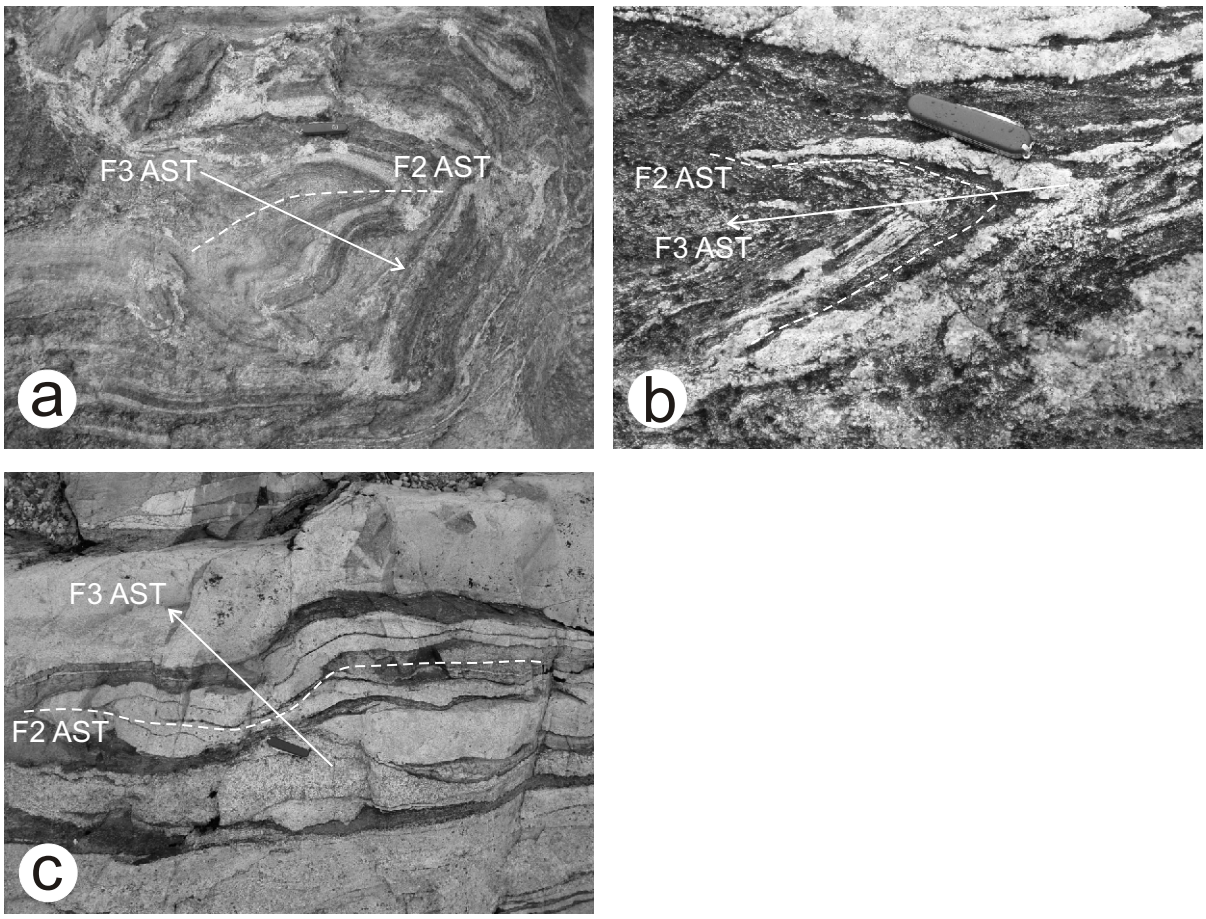

Figure 4.17. Minor F3 structures in metasedimentary rocks at Gull Rapids. These are more open-style folds that refold tight to isoclinal F2 folds. The F3 folds have an axial trace striking approximately east-northeast. The dip of the axial plane, as well as F3 fold axes, were not observed and thus not measurable. AST = axial surface trace. Arrows on F3 axial trace point towards the east-northeast strike direction. F2 axial traces are dotted.

shear (Figures 4.12, 4.13). No microscale kinematic indicators were found. This shearing event pre-dates any later, more brittle shearing and faulting in the Gull Rapids supracrustal assemblage, as well as the G3 generation of folding.

4.3.2 G4/G5 Shearing and Kinematics

Throughout the map area it is difficult to distinguish between G4 and G5 shears unless crosscutting relationships with mafic dykes are seen. Differentiating between G4 and G5 cannot be readily done based on shear sense or shear zone trend orientation alone. Also, since many of the shear zones are semibrittle, it is accordingly difficult to separate the shears and faults of Gull Rapids into G4 or G5 based on cohesiveness. On the whole, G4/G5 shear zones strike west-northwest (Figure 4.18a). Dextral shear zones have a major set trending west-northwest and a minor set trending north-northwest (Figure 4.18b), and sinistral shear zones have a major set trending west-northwest and a minor set trending northwest (Figure 4.18c). A certain number of shear zones have an unknown shear sense, but also strike northwest (Figure 4.18d). All shear zones are steeply dipping to vertical.

Strike slip components for G4 and G5 are both dextral and sinistral, and dip slip components are generally southwest-side-up, when shear surfaces are seen. In the supracrustal rocks, G4 and G5 shearing is largely semibrittle (either ductile-brittle or brittle-ductile) and cuts all foliations, lineations, and folds, and all rock types with the exception of late pegmatite and mafic dykes (Figure 4.19a–c). In the orthogneiss, ductile shearing, typical of Archean gneissic bodies, is observed (Figure 4.19d, e). It is also relatively late, as it cuts the gneissosity. The difference between the shearing in the supracrustal rocks being semibrittle and in the gneiss being ductile is most likely due to a compositional or rheological contrast between the supracrustals and the orthogneiss, and is probably not related to depth. This is because both the orthogneiss and the supracrustal rocks were at the same crustal level during deformation and metamorphism, as evidenced by the fact that both assemblages underwent a similar structural and metamorphic evolution, as well as by the fact that the shearing in both cuts all previous structures.

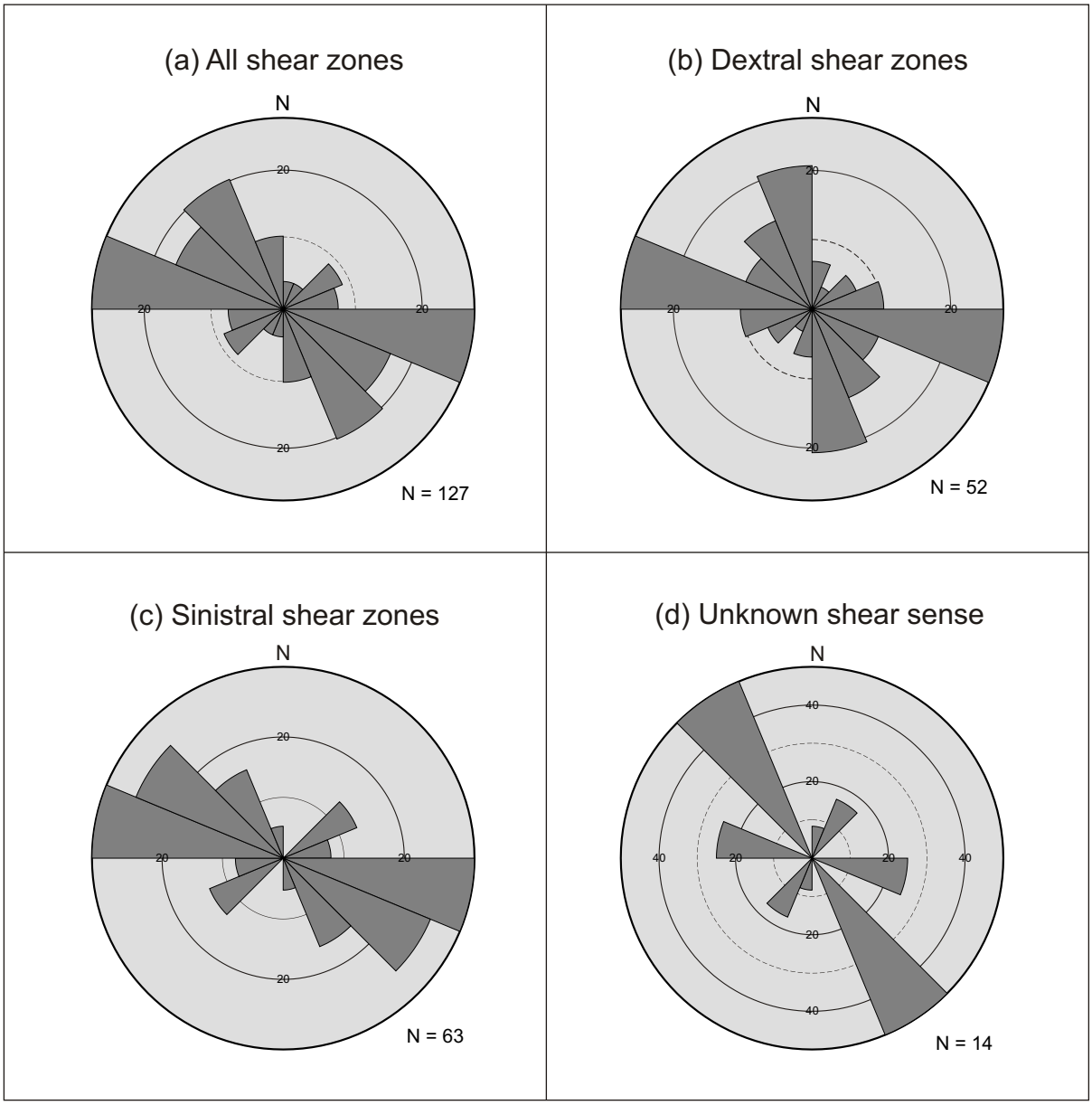

Figure 4.18. Rose diagrams of strike orientations of shears and faults, Gull Rapids map area. a) All shear zones in Gull Rapids map area. The main concentration of shear zones strikes west-northwest. b) All dextral shear zones. Dextral shear zones have a major set striking west-northwest and a minor set striking north-northwest. c) All sinistral shear zones. Sinistral shear zones have a major set striking west-northwest and a minor set striking northwest. d) Shear zones with unknown sense of shear. Main concentration strikes northwest.

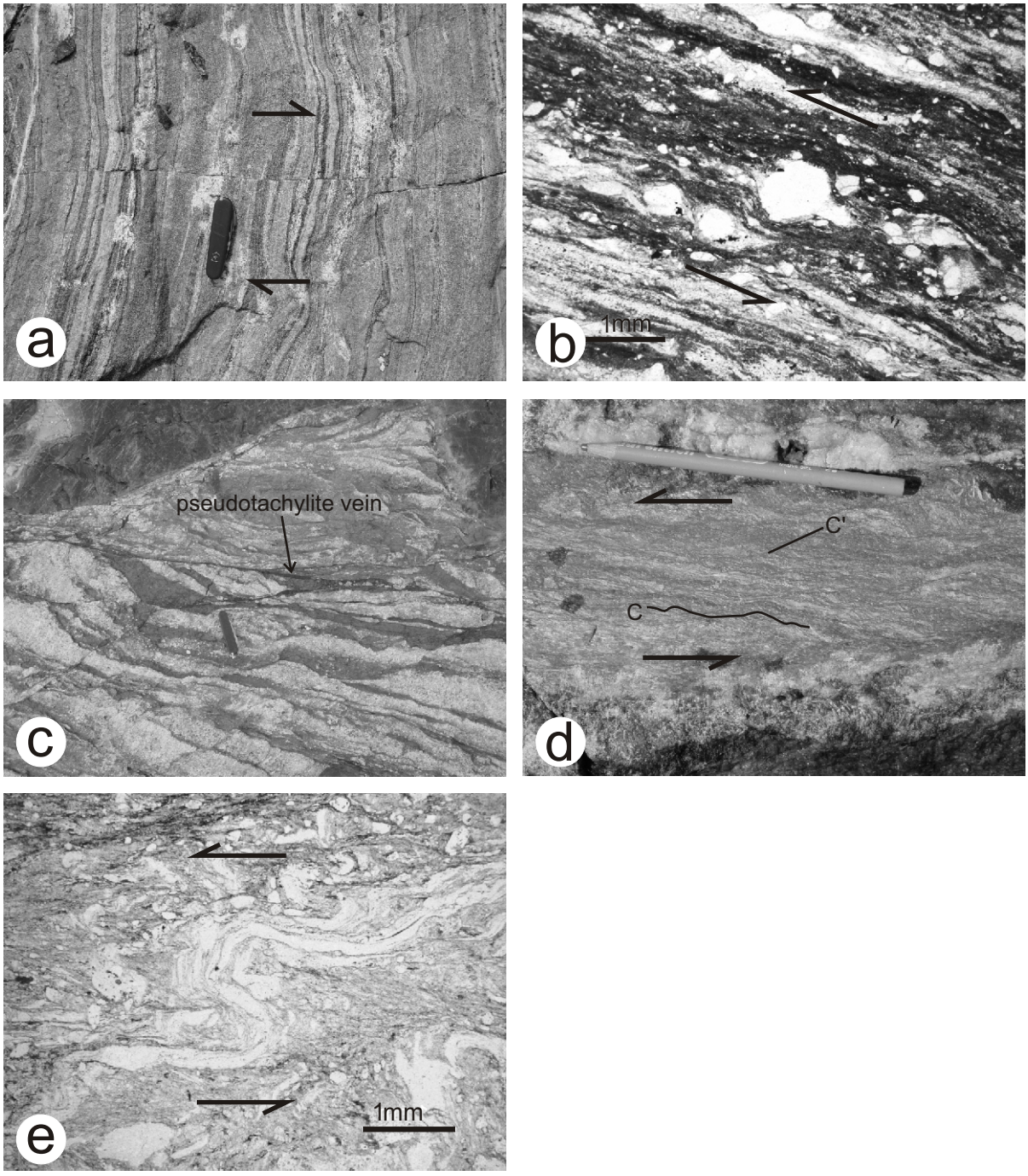

Figure 4.19. G4/G5 shearing at Gull Rapids. a) Dextral, brittle shear zone in amphibolite, showing offset of foliation. Shear zone is 230/90 (strike/dip). b) Photomicrograph of a small sinistral ductile mylonite zone in metasedimentary rock. Shear zone is 110/85 (strike/dip). Sigma clast in shear zone indicates sinistral sense. Horizontal surface. Plane polarized light. c) Pseudotachylite vein in shear zone, indicating brittle nature of shear zone. In proximity to mafic dyke at top of photo. Shear zone strikes 335 and dips 90. d) Sinistral, ductile shear zone in orthogneiss, showing C-C' shear bands. Shear zone is 253/77 (strike/dip). Horizontal surface. e) Photomicrograph of shear zone in d), showing shear-related S-fold, which indicates sinistral sense. Plane polarized light.

4.3.2.1 G4 shearing and kinematics

The G4 shearing event predates mafic dyke emplacement, as mafic dykes cut across G4 shear zones (Figure 4.20a). G4 shear zones are ductile-brittle (more ductile than brittle; local and discrete brittle and mylonite shear zones are present), and have components of strike slip and dip slip. This dip-slip component has the same shear sense as the early G1-G2 shearing event, suggesting that both shearing events could have formed in a similar kinematic regime.

In one subdomain within the metasedimentary rocks, a ductile-brittle sinistral shear zone is truncated by a mafic dyke, and is accompanied by pegmatite dyke emplacement (Figure 4.20b). A dip-slip component of this faulting is not evident. Bookshelf-style faulting accompanies this shearing and results in an overall sinistral sense for the shear zone (Figure 4.20c). In a subdomain within the amphibolite, a granitic dyke is offset by a brittle-ductile sinistral shear zone. Pegmatitic material also flows into and along the shear plane, suggesting that the emplacement of the pegmatite is contemporaneous with this shearing. In fact, pegmatite dykes throughout the Gull Rapids supracrustal and orthogneissic assemblages are commonly associated with shear zones (Figure 4.20d). These dykes are parallel to shear zones and have shear fabrics that are parallel to dyke margins, and these shear zones offset foliations, folds, and older dykes and sills. However, it is common for pegmatite dyke emplacement to be accompanied by shearing of the host rock (Figure 4.20d). Since these pegmatite dykes are always cut by late mafic dykes, and since G5 shear zones are those that cut mafic dykes, it is inferred that pegmatite dyke emplacement is synchronous with G4 shearing.

4.3.2.2 G5 shearing and kinematics

The G5 shearing seems to have occurred during greenschist facies metamorphism, as evidenced by chlorite slickenlines on brittle shear surfaces (Figure 4.21a), and largely postdates mafic dyke emplacement, as mafic dykes are cut and deformed by G5 shears (Figure 4.21b). Since mafic dyke emplacement pre-dates G5 shearing, G5 shearing and related greenschist facies metamorphism is most likely related to Hudsonian deformation and metamorphism at ca. 1.8 Ga. A late Hudsonian

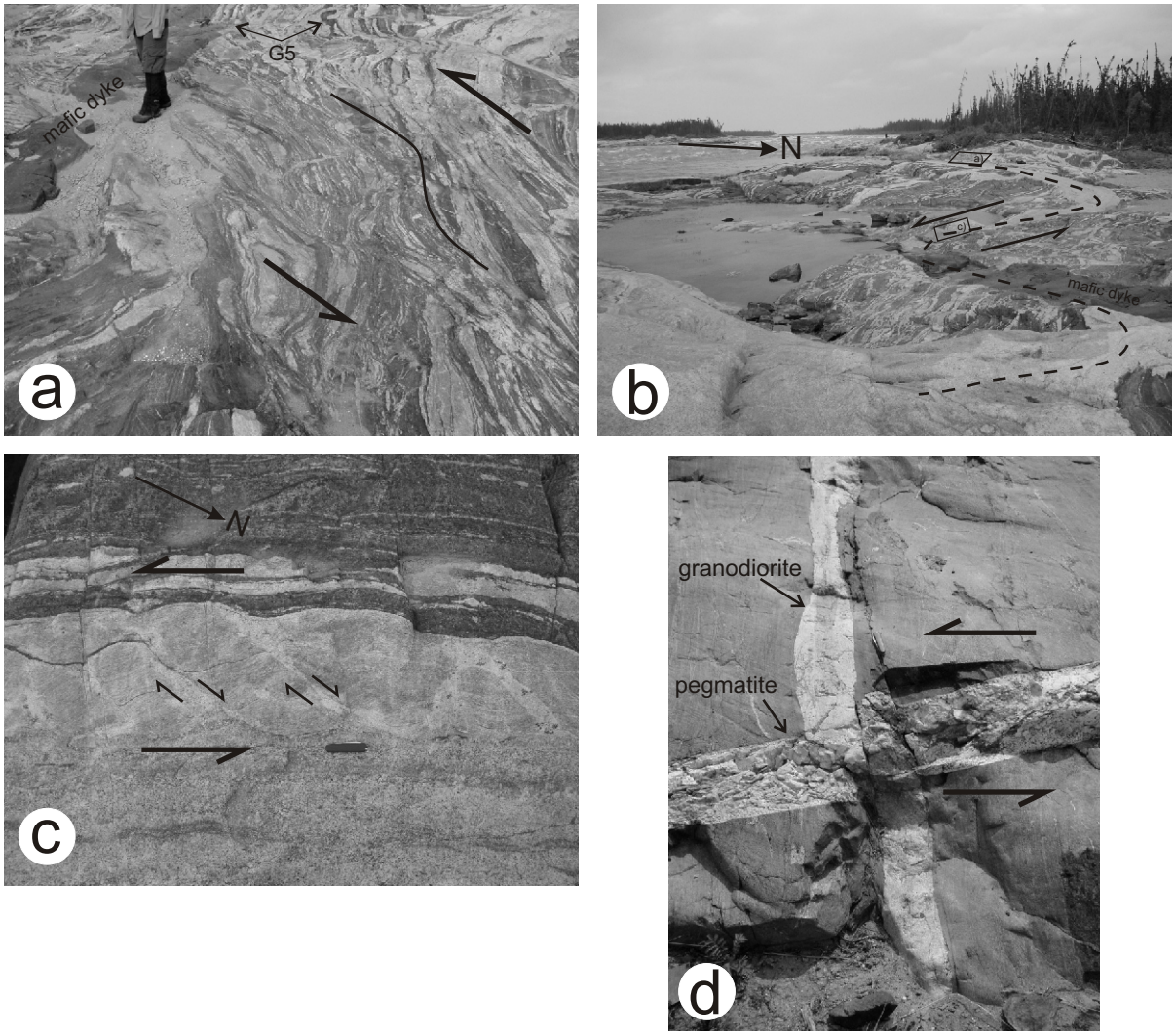

Figure 4.20. G4 shearing. a) Sinistral, semibrittle shear zone in metasedimentary rock, striking 330. Shear zone is cut by straight-walled mafic dyke (top left hand side of photo). Note a G5 shear zone across the top of the photo; this shear zone is only determined as such because it offsets the mafic dyke (top side of mafic dyke in photo). b) Sinistral shear zone. Shear zone is contemporaneous with pegmatite emplacement, and mafic dyke postdates shearing. c) Bookshelf-style faulting on one side of shear zone in b) indicates sinistral sense for this shear zone. Nearby S-folds on same side also indicate sinistral sense. d) Pegmatite dyke crosscutting and offsetting earlier, S1-subparallel granitic injection sill. Shear zone is semibrittle, sinistral, and contemporaneous with pegmatite dyke emplacement. Shear zone is 250/90 (strike/dip). Granodiorite dyke is approximately 30 centimentres wide. See text for discussion.

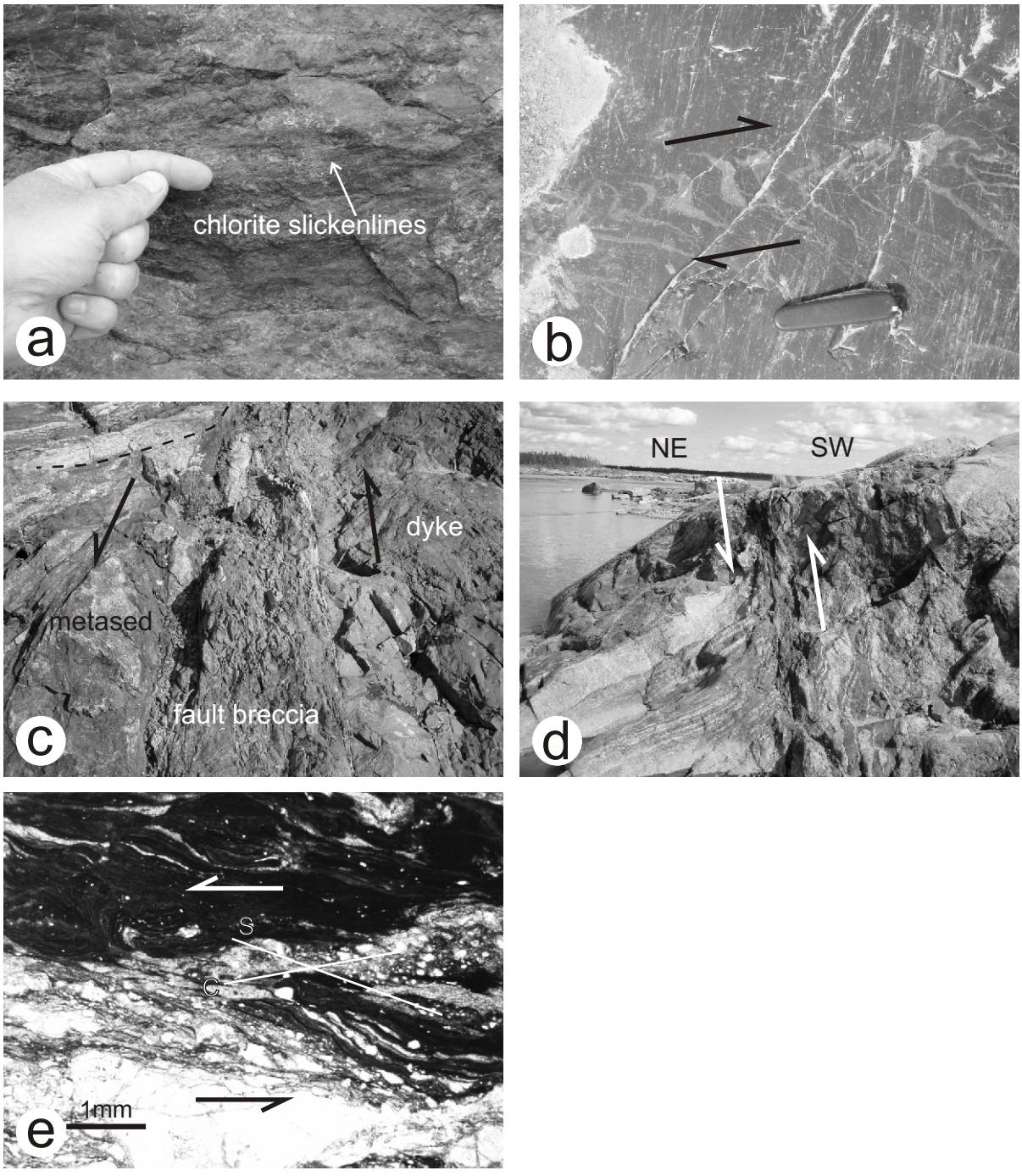

Figure 4.21. G5 shearing. a) Chlorite slickenlines on a brittle shear surface, indicating that greenschist facies retrograde metamorphism is contemporaneous with G5 shearing. This shear zone strikes 225 and dips 75NE. b) Dextral tension gashes in a shear zone that cuts through a mafic dyke, implying that G5 shear zones are post-mafic dyke emplacement. Shear zone strikes 150. c) Fault breccia in sinistral shear zone running along a mafic dyke contact with host metasedimentary rock. Shear zone strikes 140 and dips 70SW. d) Continuation of the same shear zone as in c), further to the south, in the metasediments. Note southwest-side-up movement component (as indicated by shearing of granitic dyke). e) Photomicrograph of same shear zone as in e). S-C shear bands provide sinistral sense of shear. Horizontal surface. Plane polarized light.

tectonic overprint is not observed elsewhere in the map area. G5 shear zones are generally brittle-ductile, and are dominantly strike slip, with local dip slip components. At mafic dyke contacts within the metasedimentary rocks, shearing can be entirely brittle, as evidenced by the presence of pseudotachylite veining and fault breccia, subparallel to some contacts (Figure 4.19c and 4.21c, respectively). In other localities, it can be more brittle-ductile, as evidenced by the presence of S-C shear bands (Figure 4.21d, e). In the case of some smaller dykes, the entire dyke is sheared, and a strong shear fabric is developed parallel to dyke contacts. Mafic dyke contacts are zones of weakness that facilitate the concentration of late brittle, or brittle-ductile shearing at or near those contacts. Shearing can also be ductile-brittle, as discrete mylonite zones exist in small shear zones that cut through mafic dykes, close to their contact (Figure 4.22a–d). These mylonite zones display clear C-C' and S-C fabrics and thereby provide good shear sense indicators. Some shear zones have conjugate sets of shears, with the major being sinistral and the minor being dextral (e.g. Figure 4.22b).

4.4 STRUCTURAL SUMMARY OF THE GULL RAPIDS AREA

The Gull Rapids area records three generations of ductile deformation, followed later by two generations of ductile and brittle shearing. The current geometry, and interpreted kinematics, are summarized in Figure 4.23, and below.

1. G1 produced the main foliation that is seen to be subparallel throughout the orthogneiss and supracrustal assemblages (S1). F1 isoclinal folding is rarely observed and therefore poorly constrained. The nature of the foliation, and the presence of F1 isoclinal folds, suggests that this generation of deformation was produced while an unknown amount of ductile shearing was going on (Figure 4.23a).
2. G2 is the strongest generation in the map area, and produced widespread, tight to isoclinal F2 folds in the supracrustal assemblages. An S2 foliation is rarely observed, but is axial-planar to the tight to isoclinal F2 folds. This S2 foliation may be a transposition foliation, but it is difficult to discern between S1 and S2 if this is the case. Overall, this structural generation is

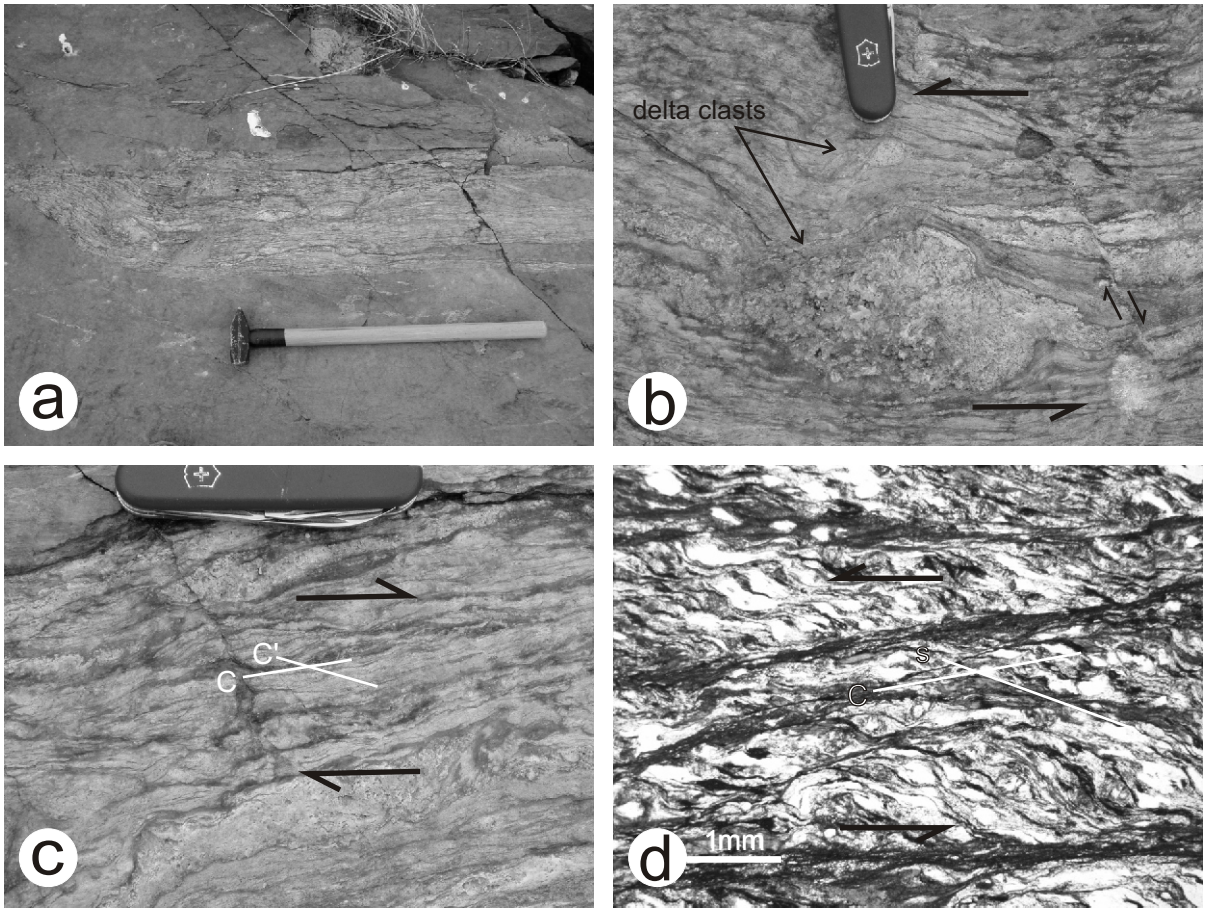

Figure 4.22. G5 shearing (continued). a) Discrete mylonite zone in a mafic dyke near its contact with the host rock. This shear zone has both sinistral and dextral conjugate sets, with the sinistral set being the major one. Shear zone strikes 225 and dips 90. b) Close-up of a portion of the shear zone from a), with delta clasts that indicate a sinistral sense. On the right hand side of the photo, a conjugate minor dextral shear zone is seen. Main sinistral set strikes 225 and dips 90, parallel to the mylonite zone it lies in. The minor dextral set strikes approximately 325. c) Close up of a different portion of the mylonite zone from a). C-C' shear bands indicate a dextral sense, and the shear zone strikes nearly 310. d) Photomicrograph of the same mylonite zone from c). S-C shear bands indicate a sinistral sense. Plane polarized light.

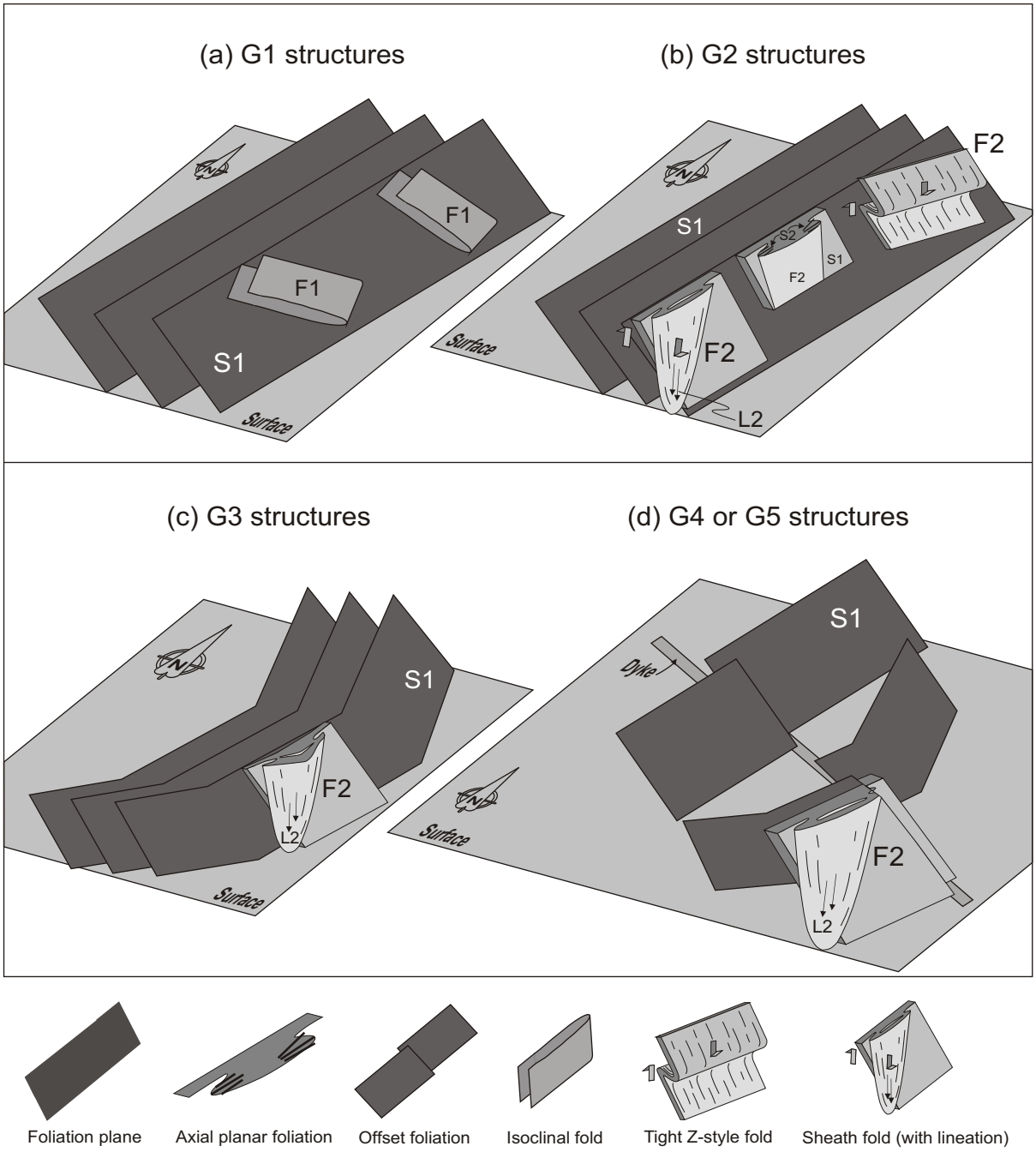

Figure 4.23. Schematic diagrams of the structures found in the Gull Rapids map area. a) G1 generation, showing average S1 foliation (approximately north-south striking, moderately east dipping) and F1 isoclinal folds (approximately plunging to the south). Folding is only observed in the supracrustal rocks. b) G2 generation, showing average S1 foliation, Z-shaped F2 drag folds (plunging approximately north), and F2 sheath folds in the supracrustal rocks, with L2 subparallel to the long axis of the sheath fold (with fold axes and lineation approximately south plunging). Shear sense is dextral, southwest-side-up. Rare S2 foliations are axial planar to F2. c) G3 generation, showing average S1 foliation being folded by open F3 folds (axial plane approximately east-west striking. F2 folds are refolded by F3 in same manner. d) G4 or G5 generation, showing average S1 foliation and F2 folds being offset by G4 or G5 shears, respectively. Sinistral shear sense is shown, however, dextral sense is also seen in the field, as are dip slip components. Trace of dyke (pegmatite for G4, mafic for G5) along shear zone plane is also shown.

related to the development of a sheath fold system, which developed as a result of an early, southwest-side-up, dextral shearing event. This sheath folding/shearing event also produced a strong regional L2 stretching lineation, which is parallel to the long axis of the sheath folds. This early shearing event may have begun earlier, during G1, and may be responsible for the production of the S1 foliation and F1 folds. In turn, this suggests that G1 and G2 may be continuous (Figure 4.23b). In conclusion, a large shear zone was developed and active during the G1-G2 generations.

3. G3 is a weak folding generation (F3) that only re-folds F2 folds and the S1 foliation in an open-style (Figure 4.23c).
4. G4 is a ductile-brittle, southwest-side-up (occasionally south-side-up), dextral and sinistral shearing event that affects all older ductile structures in all rock types (except mafic dykes), and predates ca. 2.1 Ga mafic dyke emplacement. G4 shearing is contemporaneous with pegmatite dyke emplacement (Figure 4.23d).
5. G5 is a brittle-ductile, dextral and largely sinistral shearing event that again affects all older structures in all rock types. The G5 shearing may be related to Hudsonian deformation, as G5 shears cut the ca. 2.1 Ga mafic dykes (Figure 4.23d).

4.4.1 Relationship of Deformation Between Orthogneiss and Supracrustal Rocks

Based on field observations alone, the orthogneiss and supracrustal assemblages at Gull Rapids are deformed in different ways. The orthogneiss was subjected to S1 foliation and L2 lineation development but does not appear to be folded in any way (due to a lack of markers), whereas the supracrustals were subjected to S1 foliation and L2 lineation development as well as widespread F2 folding (which is sheath folding related to shearing). Both assemblages were subjected to late G4/G5 shearing, the supracrustal shearing being brittle-ductile whereas the orthogneiss shearing is more ductile.

If the orthogneiss is interpreted to solely represent the basement to the supracrustal rocks, there would need to be some sort of detachment between the two assemblages. This is not observed. The orthogneiss was originally intruded into a portion of the supracrustal assemblage (the metavolcanic rocks), and then the orthogneiss and volcanic rocks became the basement for the deposition of the sedimentary rocks. The supracrustal assemblage is autochthonous to the orthogneiss assemblage (i.e. the two assemblages were probably not brought together by faulting). Since late shearing affects both assemblages, they would have been together by the onset of G4/G5 shearing. Lineation (L2) is approximately parallel in both assemblages, suggesting that both assemblages were together by the onset of G2, but that later folding rotated the lineation in the supracrustals and not in the orthogneiss (Figure 4.9a, b). S1 foliation is subparallel throughout both assemblages, suggesting they were together by the onset of G1 (Figure 4.1a, b). All of the above evidence suggests that the orthogneiss and supracrustals were together at the onset of deformation at Gull Rapids, and that the orthogneiss is not always deformed in the same manner as the supracrustal rocks. Since foliation is not well developed in all parts of the orthogneiss, folding similar to that in the supracrustal assemblage is simply not observed in the orthogneiss. Shear-related folding in the orthogneiss, on the other hand, is relatively common.

Chapter 5

TIMING OF DEFORMATION AND GEOCHRONOLOGY

5.1 INTRODUCTION

Relative timing constraints on deformation at Gull Rapids are based on critical crosscutting relationships between structures and late felsic intrusive phases, and the absolute timing of deformation is constrained by applying zircon and titanite U-Pb geochronology to selected felsic intrusive samples. These felsic intrusive phases help to constrain the age of stages G1 through G4, and late crosscutting mafic dykes help to constrain the age of the last stage (G5) of deformation at Gull Rapids. The timing of deformation can also be related to the timing of metamorphism. This is accomplished through the use of textural relationships between felsic intrusive phases, metamorphic assemblages typical of certain metamorphic facies, and deformation fabrics. Determining the timing of deformation and metamorphism through relative and absolute age dating is the key to unravelling the tectonic history of the Gull Rapids area.

5.2 TIMING OF DEFORMATION

5.2.1 Number and Type of Intrusive Phases

Based on field observations, five main crosscutting intrusive phases can be distinguished within the map area. The first three phases are felsic and are dominantly tonalitic, granodioritic, or granitic in composition, similar to the older orthogneisses (see Chapter 3.4). They form from melting of the host rock (leucosome) or they intruded as dykes or they formed from a combination of the two processes (melting and injection). The last two phases are mafic and are gabbroic to diabasic in composition. They intruded as dykes and in places are observed to crosscut each other. Most localities display only the second and third intrusive phases. Separation of the various phases can be done within single exposures where crosscutting phases are seen. However, it is difficult to extend these

crosscutting and textural relationships across the entire map area, in particular from the supracrustal to the orthogneissic assemblages.

The first phase is tonalitic and is only found locally as irregularly shaped bodies in supracrustal rocks and orthogneiss (Figure 3.4e). It is fine- to medium-grained and is largely massive, generally lacking a deformation fabric. The second phase is granodioritic to granitic, and occurs as dykes (metre-scale), dykelets and sills (millimetre- to centimetre-scale), and irregularly shaped leucosome pods (metre- to centimetre-scale), all of which intrude rocks throughout the map area (Figure 3.4a–d). It is medium- to coarse-grained and locally pegmatitic. It also locally contains orthoamphibole not seen in the host rock and in the first intrusive phase (Figure 3.1c, 3.4e), and it is weakly foliated. Pegmatitic cores are common in the larger dykes. The third phase is pegmatitic granite, is coarse- to very coarse-grained, and occurs as straight-walled dykes (metre-scale) and dykelets (millimetre- to centimetre-scale) that intrude the host rock and earlier intrusive phases (Figure 3.4f). These pegmatites do not have a foliation; however, they do locally have a shear-related fabric. The fourth phase is gabbroic, coarse-grained and massive, and occurs as dykes (centimetre- to metre- to outcrop-scale) that intrude the host rock and all earlier phases (Figure 3.5c, d). The fifth phase is diabasic, fine-grained and massive, and crosscuts all earlier phases as well, including the fourth phase (Figure 3.5a, b, d). The fourth and fifth intrusive phases are grouped as late mafic dykes.

5.2.1.1 Pluton emplacement mechanisms

Some studies of intrusive emplacement mechanisms focus on the space-making problem (Cruden 1990, 1998; Paterson and Fowler 1993; Morgan et al. 1998). The second and third felsic intrusive phases at Gull Rapids form a large volume of felsic magmatism. This material can be interpreted as either injection or partial melt. However it should be noted that the morphology of much of this leucocratic material suggests injection via dykes, dykelets, and sills: these intrusive bodies are generally long, thin to wide, laterally continuous, subconcordant to discordant bodies of material that have been emplaced into the pre-existing rocks (Figure 3.1a–b, 3.2a–b, 3.4a–d, 5.1a).

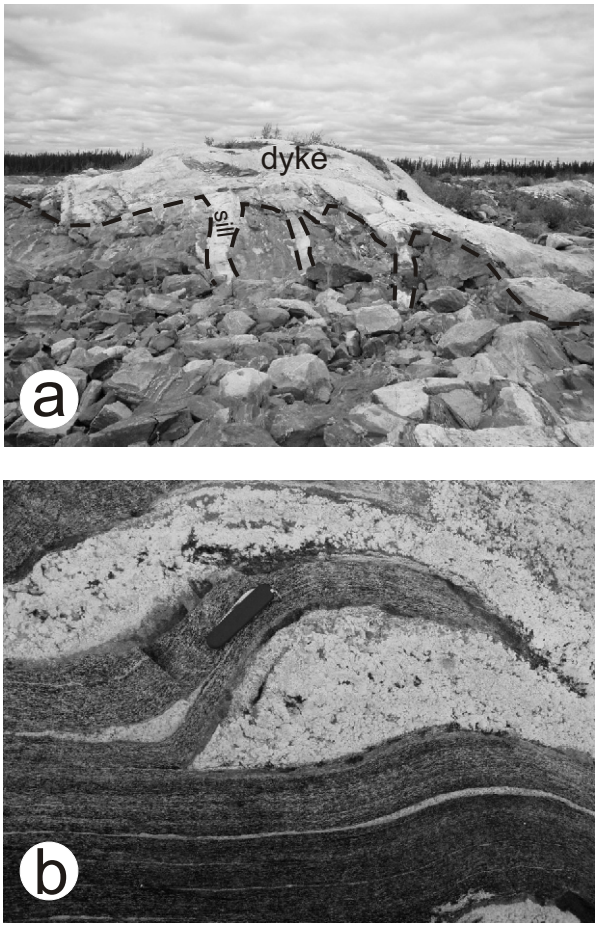

Figure 5.1. Pluton emplacement at Gull Rapids. a) Outcrop photo of granodiorite dyke crosscutting metasedimentary rocks. Dyke crosscuts foliation, and sills that branch off from the main dyke are subparallel to S1 foliation planes. b) Forceful emplacement of granodiorite dyke into amphibolite. Note that the dyke forced apart pre-existing S1 foliation planes, and intruded in between them, making room for itself in a forceful manner.

Dyke contacts are generally sharp and have chilled margins, and there is a lack of intrusion-related ductile deformation in the host rock at these contacts. The emplacement of these dykes, dykelets, and sills requires that space be made for that intrusive material in the crust. One possible mechanism is passive emplacement along faults or in fold hinges. Another possible mechanism is forceful emplacement (e.g., a dyke forces the wall rocks aside as it intrudes). Emplacement of the felsic dykes locally affects structure in a forceful way in the amphibolite (Figure 5.1b). These dykes push aside the foliation and force their way into the zones of weakness between foliation planes. Elsewhere in the map area, pods of leucosome are observed, suggesting some degree of partial melting of the host rock. These leucosome pods have the same crosscutting relationship with the host rock as do the dykes, dykelets, and sills, suggesting that the injection and melting are related to each other. There is a most likely a degree of partial melting associated with the injection, as many of the dykes and dykelets show melt segregation along their margins (quartzofeldspathic-rich cores and hornblende-rich rims; Figure 3.1d). In reality, the injection could have formed by partial melting, and thus there could be a gradation between the two (Figure 3.1d, 3.4a).

5.2.2 Crosscutting Relationships

The first intrusive phase is tonalitic and crosscuts the S1 foliation in the supracrustal assemblage. Locally it is weakly foliated, with the foliation in the tonalite subparallel to that in the host rock. This tonalite is not observed to be folded by F2. This may be because of a lack of exposure of the tonalite. Dykes of the second and third phases crosscut this phase (e.g. Figure 3.4e).

The second intrusive phase is granodioritic to granitic (locally pegmatitic), and is a widespread phase throughout Gull Rapids. Crosscutting relationships of this phase are best viewed in the supracrustal assemblages. Large dykes (metre-scale) cut across the S1 foliation, but dykelets and sills that branch off from the larger dykes are subparallel to S1 foliation planes and have a weak foliation (Figure 5.1a, 5.2a, b). These dykelets and sills are then folded by F2 (Figure 5.2c, d), boudinaged (Figure 4.15a, d, e), and offset by faulting. Locally, this phase is observed in boudin

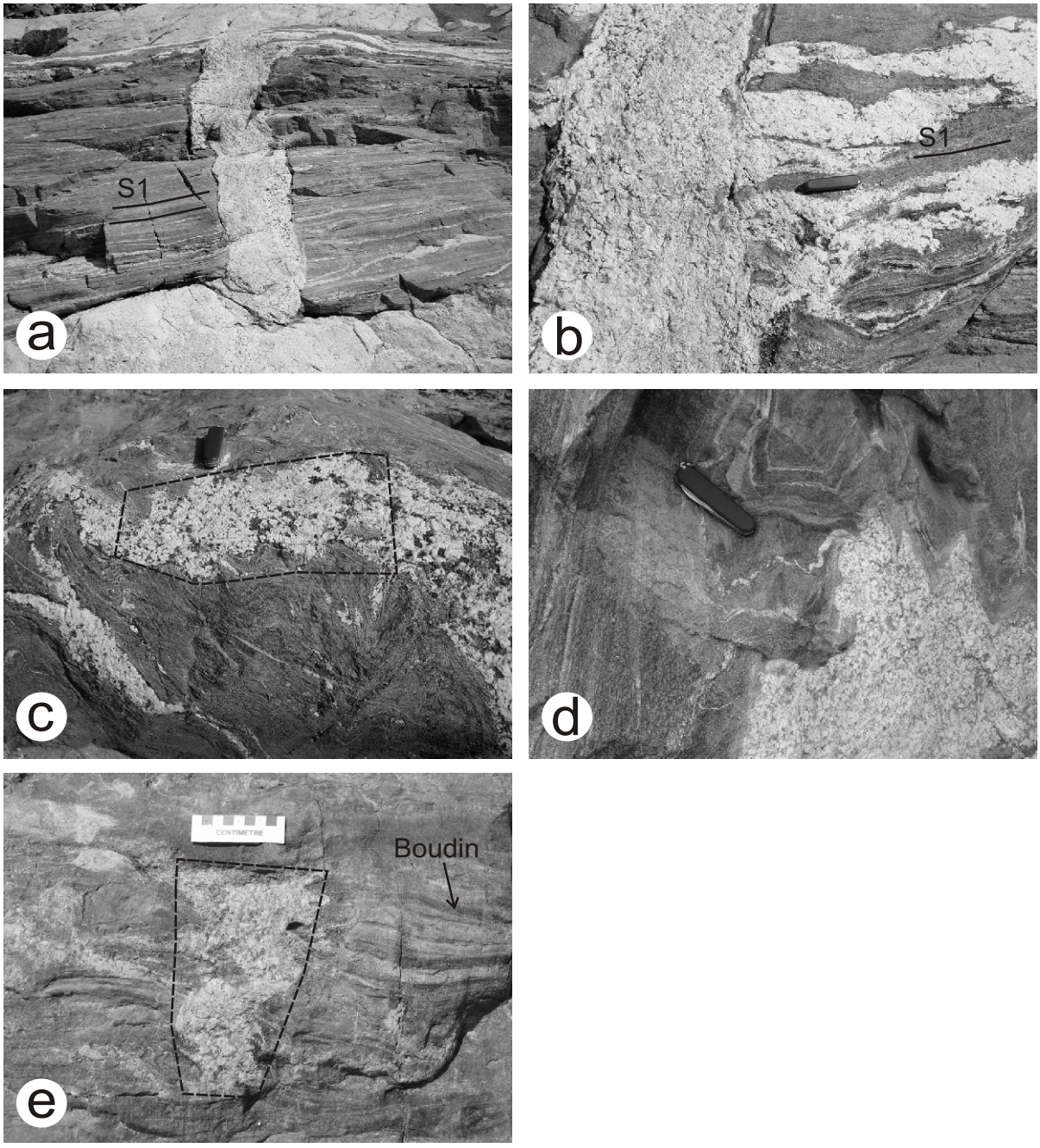

Figure 5.2. Crosscutting relationships of the second intrusive phase, used to constrain the timing of deformation in the Gull Rapids map area. a) Granodiorite dyke crosscutting S1 in amphibolite. Dykelets and sills that branch off from the dyke are subparallel to S1. Granodiorite dyke is approximately 50 centimetres wide. b) Granodiorite dyke (left side of photo) crosscutting S1 in amphibolite. Dykelets and sills that branch off from the dyke are subparallel to S1, and are locally boudinaged. c) Leucosome dyke-like body crosscuts S1 in amphibolite. Dykelets and sills that branch off from the dyke are subparallel to S1 and are folded by F2. Black dashed polygon indicates sample 097-04-5218A (GSC #8384), taken for geochronological analysis. d) Granodiorite dyke crosscutting S1 in amphibolite; branching dykelets are folded by F2. e) Pegmatitic granite injection into boudin neck in amphibolite. Injection is therefore syn-boudinage. Black dashed polygon indicates sample 097-03-4008A (GSC #8315), taken for geochronological analysis. See text for discussion.

necks, suggesting that emplacement is (locally) syn-boudinage (Figure 4.15c, 5.2e). Therefore, emplacement is either pre- or syn-boudinage; the boudinage is either pre- or syn-F2 (see Chapter 4.2.2). All of this evidence combined indicates that this second intrusive phase was emplaced during the period between the end of S1 foliation development (late- G1) and the onset of F2 folding (early-G2). In the orthogneiss, this phase crosscuts amphibolite rafts and the gneissosity (Figure 5.3a, b).

The third intrusive phase is pegmatitic granite and is also widespread. This phase crosscuts all foliations, lineations, and folds, and the earlier intrusive phases (Figure 5.4a, b, 3.4f), and is crosscut by the later mafic dykes. These pegmatites do not have a foliation, but do have local shear-related fabrics. Pegmatite dyke emplacement is commonly contemporaneous with shearing (see Chapter 4.3.2.1; Figure 5.4c). Pegmatite dykes are everywhere crosscut by late mafic dykes (Figure 5.4d). Since G5 shearing is post-mafic dyke emplacement, the shearing associated with this third intrusive phase emplacement is therefore G4.

The fourth and fifth intrusive phases are grouped as mafic dykes, and both phases crosscut all earlier structures and intrusive phases. Mafic dyke emplacement pre-dates G5 shearing (dykes are cut and deformed by shearing; Figure 4.21b, c, 4.22a–d, see Chapter 4.3.2.2). This mafic dyke emplacement and the associated shearing are the last intrusive and structural events to affect the map area, respectively.

5.2.3 Timing of Metamorphism versus Deformation

The biotite and hornblende that are consistently found throughout the supracrustal assemblage are typical of prograde regional mid-amphibolite facies metamorphism (M1a; Corkery 1985). Subhedral to euhedral crystal shapes and host rock protolith type imply that most biotite and hornblende grew during metamorphism, and are not primary (see Chapter 3.1, 3.2). These minerals define the S1 foliation and do not overprint it. Also, all biotite and hornblende grains have similar orientations but do not have similar extinction angles throughout the thin sections. This implies that they originally grew in random orientations and were rotated towards parallelism with each other

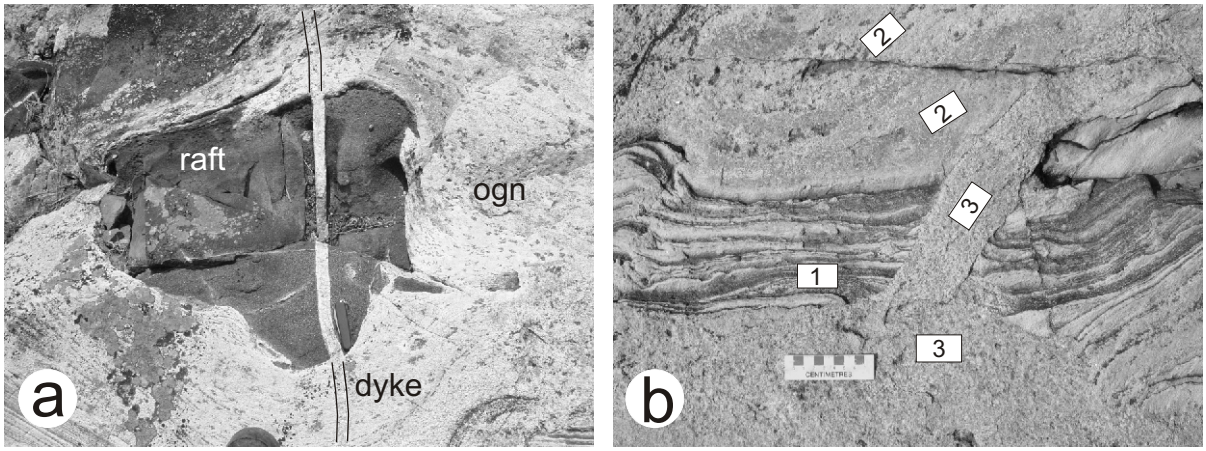

Figure 5.3. Crosscutting relationships of the second intrusive phase, used to constrain the timing of deformation in the Gull Rapids map area. a) Amphibolite raft in orthogneiss (ogn). Both are cut by a granitic dyke of the second intrusive phase. b) Strongly foliated augen gneiss xenolith ('1') in orthogneiss ('2') cut by granitic dyke of the second intrusive phase ('3').

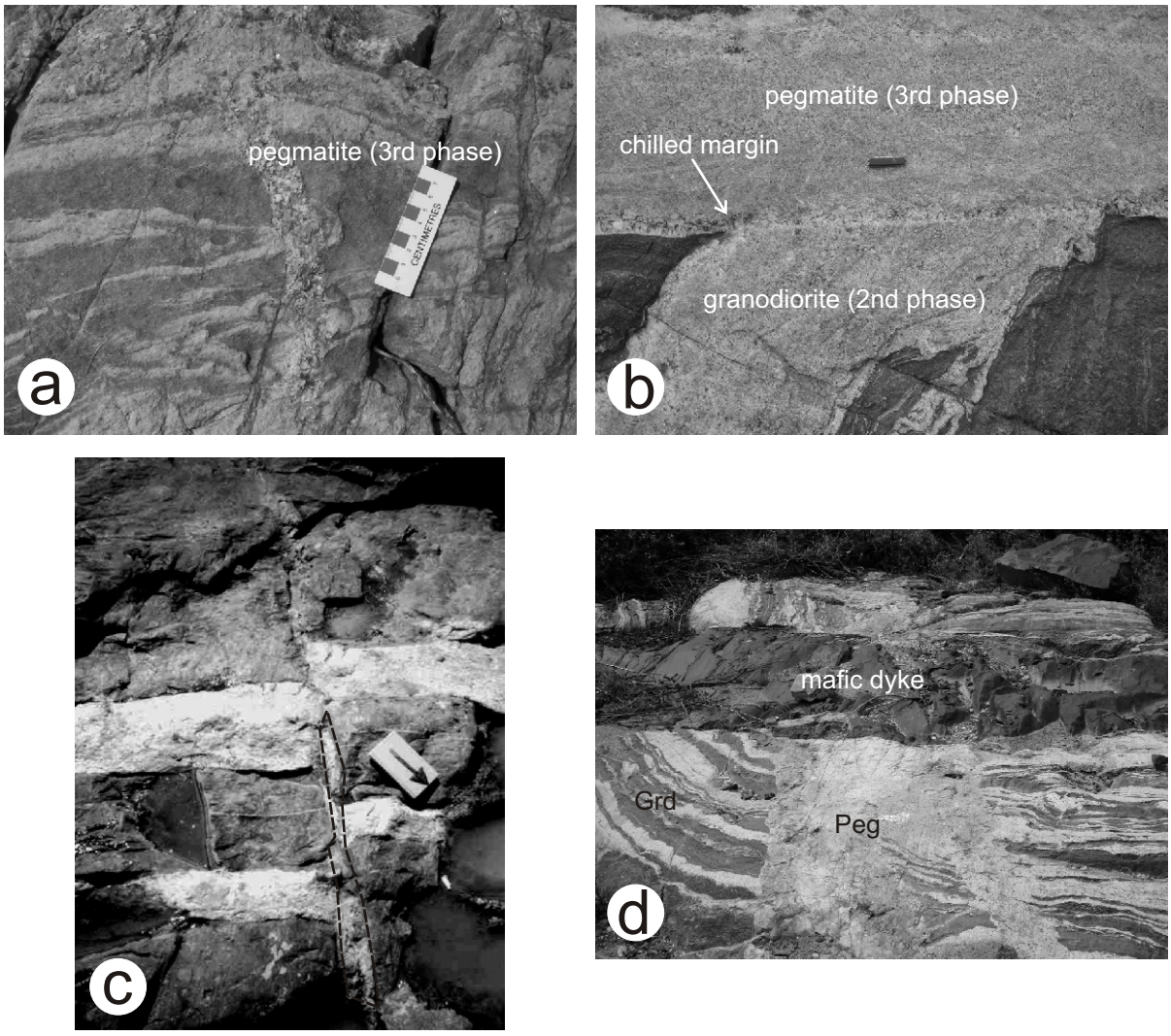

Figure 5.4. Crosscutting relationships of the third intrusive phase, used to constrain the timing of deformation in the Gull Rapids map area. a) Straight-walled pegmatite dyke crosscutting F2 fold of granitic dykelets (second intrusive phase) and S1 in metasedimentary rocks. b) Straight-walled pegmatite dyke crosscutting S1-subparallel granodiorite sill (second phase) in metasedimentary rocks. c) Pegmatite dyke offset by shear zone in amphibolite. Note that pegmatite is also injected along the shear plane, suggesting the emplacement of this pegmatite is syn-shearing. Black dashed polygon indicates sample 097-03-4008C (GSC #8317), taken for geochronological analysis. Book points south. d) Mafic dyke crosscutting a pegmatite dyke of the third intrusive phase (Peg), which is crosscutting granodiorite sills of the second intrusive phase (Grd). See text for discussion.

during S1 deformation. Therefore, these grains grew before, or more likely during the early stages of G1. Since these minerals grew during M1a metamorphism and during the early stages of S1 foliation development, M1a metamorphism is therefore roughly synchronous with G1 deformation.

The presence of orthoamphibole in the second intrusive phase indicates that this phase reached upper-amphibolite peak metamorphic grade (M1b; Corkery 1985; Figure 3.1c, 4.15c). Orthoamphibole-bearing intrusive material is only observed in the second phase, indicating that the intrusion of this phase is roughly coeval with the peak of metamorphism in the area (M1b). Dykes and sills of this second phase crosscut the S1 foliation defined by biotite and hornblende in the supracrustal assemblages, and consequently overprint the M1a metamorphism. An S1 foliation is not developed in these dykes and sills. However, sills that branch off from larger dykes are subparallel to the foliation, and are then folded by F2. Since this material was emplaced late-G1 to early-G2, the M1b metamorphism is synchronous with the end of G1 to the beginning of G2 deformation. Locally, clinoamphibole pseudomorphs (from orthoamphibole) are observed (orthoamphibole cores and clinoamphibole rims). Since clinoamphibole is indicative of mid-amphibolite facies metamorphism, these rocks experienced retrogression from upper- to mid-amphibolite facies metamorphism (M1b to M2; Corkery 1985). No specific structural generation can be correlated to this M2 metamorphism.

Chlorite slickenlines, indicative of prograde greenschist metamorphism, are only observed in G5 shear zones. This suggests that G5 shearing is coeval with, or pre-dates greenschist metamorphism (Figure 4.21a). Retrograde greenschist facies metamorphism is moderate to strong and pervasive throughout the map area (M3; Corkery 1985). This greenschist metamorphism may in fact be a late hydrothermal event that altered the rocks to the extent seen.

The above paragraphs describe the timing of metamorphism at Gull Rapids, and this information agrees with the observations by Corkery (1985) for the Split Lake Block. In the Split Lake Block, regional upper-amphibolite facies metamorphism is observed in most rocks (M1a). These rocks are cut by orthopyroxene-bearing rocks, characteristic of granulite facies metamorphism (M1b). Retrogression of orthopyroxene to amphibole during upper-amphibolite facies metamorphism

(M2) is followed by greenschist facies metamorphism (M3). At Gull Rapids, G1 deformation is synchronous with M1a metamorphism (M1a at Gull Rapids is mid-amphibolite facies; M1a in the Split Lake Block is upper-amphibolite facies), and late-G1 to early-G2 deformation is synchronous with M1b metamorphism (M1b at Gull Rapids is upper-amphibolite facies and only locally granulitic in the orthogneiss; M1b in the Split Lake Block is granulite facies). This was followed shortly thereafter by retrograde M2 metamorphism, and G5 deformation is roughly synchronous with M3 metamorphism.

5.3 U-PB GEOCHRONOLOGY

Uranium-lead geochronology is used in this study to constrain the absolute timing of deformation at Gull Rapids. This study deals only with samples dated for the timing of deformation. Other samples collected and dated by other Gull Rapids workers (e.g. Böhm et al. 2003a; Bowerman et al. 2004) have been briefly discussed in previous sections and chapters, and will be summarized at the end of this chapter.

5.3.1 Sample Collection and Analytical Procedures

Three samples of the felsic intrusive phases outlined in section 5.2.1 were dated using the U-Pb zircon and titanite geochronology methods. The samples chosen provide the clearest crosscutting relationships in the map area, and importantly, they can be correlated across the entire map area. The samples were collected from dykes, sills, and irregularly shaped leucosome pods that crosscut fine-grained amphibolitic rocks (Figure 1.3, Appendix A). All three samples (two pegmatitic granites and one granodiorite) were approximately 50cm x 15cm x 15cm in dimension and 5-7kg in weight. Samples were cut out of the outcrop using a rocksaw, and any host rock was removed. Relatively small samples were taken in order to obtain the best constrained crosscutting relationship with the deformation.

All crushing and analytical work was performed at the Geological Survey of Canada Geochronology Laboratory in Ottawa, Ontario. Zircons were extracted from the rock sample using standard crushing, heavy-liquid, and magnetic-separation techniques. Zircons were dated using the Sensitive High-Resolution Ion MicroProbe (SHRIMP II). SHRIMP analytical procedures followed those described by Stern (1997), with standards and U-Pb calibration methods following Stern and Amelin (2003). Briefly, zircons were cast in 2.5 cm diameter epoxy mounts (GSC #341) along with fragments of the GSC laboratory standard zircon (z6266, with $^{206}Pb/^{238}U$ age = 559 Ma). The internal features of the zircons (such as zoning, structures, alteration, etc.) were characterized with back-scattered electrons (BSE) using a Cambridge Instruments scanning electron microscope. Mount surfaces were evaporatively coated with 10 nm of high purity Au. Analyses were conducted using an $^{16}O^-$ primary beam, projected onto the zircons at 10 kV. The sputtered area used for analysis was ca. 16 μm in diameter with a beam current of ca. 4 nA. The count rates of ten isotopes of Zr^+, U^+, Th^+, and Pb^+ in zircon were sequentially measured over 5 scans with a single electron multiplier and a pulse counting system with deadtime of 30 ns. Off-line data processing was accomplished using customized in-house software. The 1σ external errors of $^{206}Pb/^{238}U$ ratios reported in the data tables (Tables 5.2, 5.4, 5.5) incorporate a ±1.4 % error in calibrating the standard zircon (see Stern and Amelin 2003). No fractionation correction was applied to the Pb-isotope data. Common Pb correction utilized the Pb composition of the surface blank (Stern 1997). Isoplot v. 3.00 (Ludwig 2003) was used to generate concordia plots (error ellipses 2σ). Titanite was dated using the Isotope Dilution - Thermal Ionization Mass Spectrometry (ID-TIMS) technique. ID-TIMS analytical procedures followed those of Parrish et al. (1992) and Davis et al. (1997).

5.3.2 Sample Descriptions, Crystal Morphology, and U-Pb Results

Zircons from two samples of pegmatitic granite (097-03-4008A and 097-03-4008C) and from one sample of coarse-grained granodiorite (097-04-5218A) were dated by U-Pb SHRIMP methods. Titanite from sample 097-03-4008A was dated by U-Pb ID-TIMS methods. Table 5.1

Sample and mineral dated	***Rock type***	***UTM E***	***UTM N***	***Intrusive Phase***	***Cross-cutting relationships***	***Fabric development***	***Timing constraints***
097-03-4008A Zircon (SHRIMP) Titanite (ID-TIMS)	Pegmatitic granite (pod)	363766	6247141	2nd	Intrusive material fills into boudin neck (syn-boudinage). Boudinage is late-G1 to early-G2	Weak foliation	Late-G1 to early-G2
097-04-5218A Zircon (SHRIMP)	Granodiorite (sill)	363727	6247316	2nd	Intrusive material crosscuts S1 foliation, and is folded by F2	Weak foliation	Late-G1 to early-G2
097-03-4008C Zircon (SHRIMP)	Pegmatitic granite (dyke)	363776	6247141	3rd	Intrusive material fills into shear zone plane. Pegmatite is older than mafic dykes, thus shear zone is G4	Weak shear-related fabric	Syn-G4 shearing

Table 5.1. Summary of locations and field relationships of U-Pb geochronology samples from the Gull Rapids area. See Appendix A for a sample location map.

outlines the crosscutting relationships and samples dated, and Appendix A displays the sample locations.

5.3.2.1 Sample 097-03-4008A

Sample 097-03-4008A (GSC #8315) is from a pegmatitic granite pod of the second intrusive phase (Figure 5.2e; Appendix A). It is relatively homogeneous (plagioclase–K-feldspar–quartz; Chapter 3.4). Biotite and hornblende are minor, and define a weak foliation. Quartz and feldspar also display evidence for intracrystalline deformation. Orthoamphibole was not observed in this sample. This pegmatitic granite was injected into a boudin neck in the amphibolite and is therefore syn-boudinage (Table 5.1). Nearby, similar pegmatitic material crosscuts the S1 foliation and is folded by F2. The age of this pegmatitic granite will thereby provide a constraint on late-G1 to early-G2 deformation. Since M1b (peak) metamorphism is coeval with late-G1 to early-G2 deformation, the age of this pegmatitic granite will also constrain the age of M1b (peak) metamorphism.

Zircon morphology and U-Pb age results

Zircon crystal size is mostly small (<200 μm), with length to width ratios that vary from 2 to 3 (Figure 5.5). All of the zircons exhibit a subhedral-euhedral prismatic external morphology with rounded edges and corners, and have been recrystallized as indicated by abundant alteration along fractures in the grain and in patchy spots throughout the grain (Figure 5.5). Also, internal zoning is relatively uncommon, but cores and rims are relatively distinguishable in grains 14, 24, 30, and 34. Favourable spots (possible rims, possible cores) away from alteration zones and fractures were chosen for SHRIMP U-Pb spot analysis.

A total of 35 zircons were found in the sample, and 10 spots were analyzed from 8 grains. The U-Pb results are presented in Table 5.2 and on concordia diagrams in Figure 5.6. The zircons have anomalously high uranium concentrations (2000-7000 ppm) and are discordant (0.5 to 5%) to highly discordant (10-26.5%). They give a wide range of $^{207}Pb/^{206}Pb$ ages, from 1832 ± 7 Ma to 2686

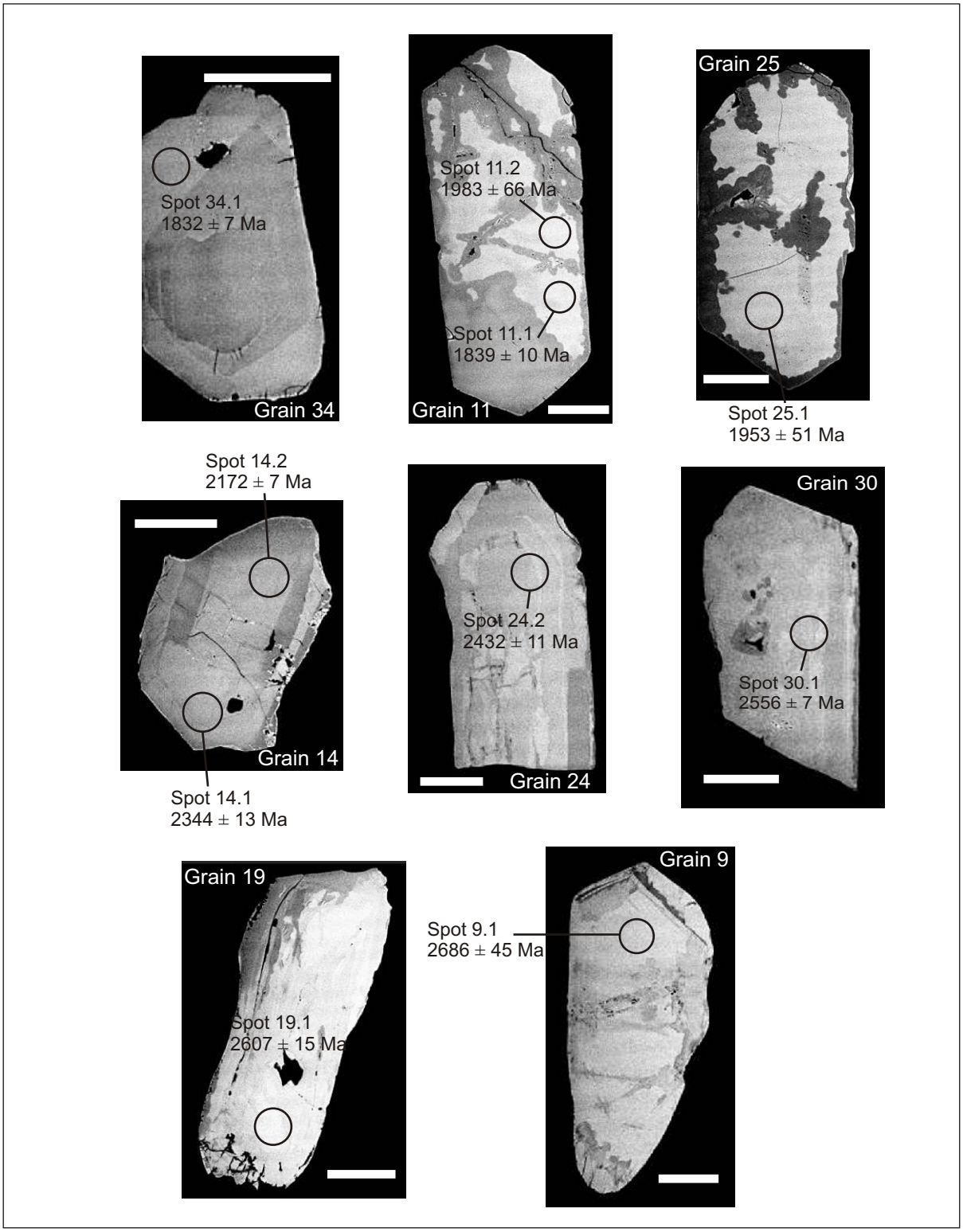

Figure 5.5. Backscattered electron images of zircons from sample 097-03-4008A (GSC #8315; Figure 5.2e). Note subhedral-euhedral prismatic form, abundant alteration (darker blebs in pods and along fractures) in all grains, and general lack of magmatic zoning. White scale bars represent 50 μm. Circles represent ion beam pits analyzed on the SHRIMP. Spot ages are $^{207}Pb/^{206}Pb$ ages from Table 5.2.

Spot name	U (ppm)	Th (ppm)	Th/U	Pb* (ppm)	^{204}Pb (ppb)	$^{204}Pb/^{206}Pb$	$\pm ^{204}Pb/^{206}Pb$	$f(206)^{204}$	$^{208*}Pb/^{206*}Pb$	$\pm ^{208}Pb/^{206}Pb$	$^{207*}Pb/^{235}U$	$\pm ^{207}Pb/^{235}U$
8315-9.1	2544	44	0.02	1337	1	1.01E-06	2.12E-06	2.00E-05	0.00501	0.00018	13.024	0.5625
8315-19.1	2025	96	0.05	1009	32	3.73E-05	1.07E-05	0.00065	0.01354	0.00044	11.775	0.24065
8315-30.1	2450	145	0.06	1135	57	6.03E-05	6.79E-06	0.00104	0.01747	0.0004	10.625	0.20532
8315-24.2	2992	153	0.05	1229	195	1.87E-04	9.36E-06	0.00323	0.01525	0.00048	8.8552	0.1761
8315-14.1	2758	213	0.08	1016	73	8.46E-05	6.86E-06	0.00147	0.02247	0.00036	7.5479	0.17269
8315-14.2	3109	245	0.08	1013	197	2.25E-04	1.48E-05	0.00391	0.02317	0.00087	6.1116	0.12423
8315-11.2	6682	810	0.13	1923	100	6.02E-05	2.08E-05	0.00104	0.03475	0.00116	4.8604	0.24963
8315-25.1	6417	414	0.07	1797	27	1.71E-05	2.52E-06	0.0003	0.02042	0.0003	4.7163	0.18723
8315-11.1	6779	692	0.11	1677	18	1.21E-05	2.83E-06	0.00021	0.02998	0.00027	3.903	0.09718
8315-34.1	5310	422	0.08	1206	15	1.46E-05	6.04E-06	0.00025	0.02474	0.00031	3.5875	0.07214

Spot name	$^{206*}Pb/^{238}U$	$\pm ^{206}Pb/^{238}U$	Corr Coeff	$^{207*}Pb/^{206*}Pb$	$\pm ^{207}Pb/^{206}Pb$	Apparent Ages (Ma) $^{206}Pb/^{238}U$	$\pm ^{206}Pb/^{238}U$	$^{207}Pb/^{206}Pb$	$\pm ^{207}Pb/^{206}Pb$	Disc. (%)
8315-9.1	0.51433	0.01582	0.7895	0.18365	0.00491	2675	68	2686	45	0.4
8315-19.1	0.48772	0.00836	0.8948	0.1751	0.00161	2561	36	2607	15	1.8
8315-30.1	0.45373	0.00834	0.9774	0.16984	0.0007	2412	37	2556	7	5.6
8315-24.2	0.40701	0.00736	0.9486	0.15779	0.001	2201	34	2432	11	9.5
8315-14.1	0.36528	0.00755	0.9446	0.14986	0.00113	2007	36	2344	13	14.4
8315-14.2	0.3269	0.00637	0.9819	0.13559	0.00053	1823	31	2172	7	16
8315-11.2	0.2894	0.00926	0.7116	0.12181	0.00443	1639	46	1983	66	17.4
8315-25.1	0.28561	0.00705	0.7107	0.11976	0.00337	1620	35	1953	51	17.1
8315-11.1	0.2518	0.00596	0.9771	0.11242	0.0006	1448	31	1839	10	21.3
8315-34.1	0.23232	0.00447	0.9806	0.112	0.00045	1347	23	1832	7	26.5

Notes (see Stern, 1997):

* = radiogenic Pb

Uncertainties reported at 1 sigma (absolute) and are calculated by numerical propagation of all known sources of error

f(206)204 refers to mole fraction of total 206Pb that is due to common Pb, calculated using the 204Pb-method; common Pb composition used is the surface blank

Discordance relative to origin = 100 * (1-(206Pb/238U age)/(207Pb/206Pb age))

Table 5.2. SHRIMP U-Pb zircon results for sample 097-03-4008A (GSC #8315)

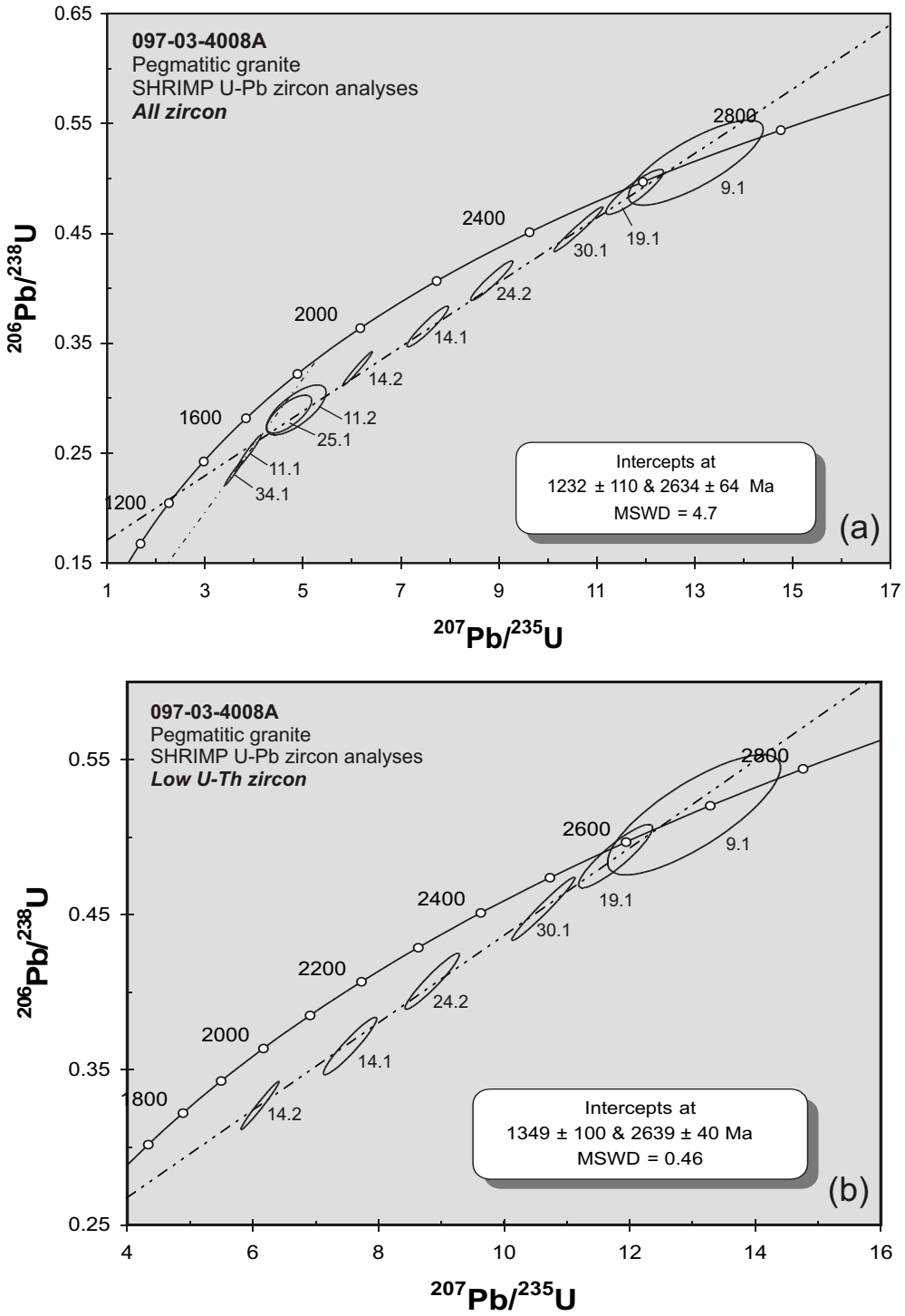

Figure 5.6. Concordia diagrams for the SHRIMP U-Pb analyses of 8 zircons (10 spots) from sample 097-03-4008A (GSC #8315; Figure 5.2e, 5.5). Numbers correspond to spot number; data presented in Table 5.2. a) All zircons yield an upper intercept age of 2634 ± 64 Ma. A second discordia line, through spots 11.1 and 34.1, has an upper intercept at ca. 1850 Ma, suggesting Hudsonian thermo-activity. There are two zircon populations: a high U-Th and a low U-Th population. The $^{207}Pb/^{206}Pb$ ages (youngest) of the high U-Th population are geologically meaningless. b) Low U-Th zircons yield an upper intercept age of 2639 ± 40 Ma. High U-Th zircons were not used in this diagram. See text for discussion.

± 45 Ma (Figure 5.6a). The cores and rims in the grains show no predictable core-rim age relationships. Their Th/U ratios range from 0.02 to 0.13, suggestive of metamorphic zircon (Williams and Claesson 1987; Pidgeon and Compston 1992; Williams et al. 1996; Mezger and Krogstad 1997; Nemchin and Pidgeon 1997; Böhm et al. 2003c). On the other hand, the subhedral-euhedral crystal shape to all of the grains suggests magmatic zircon (Figure 5.6). High uranium concentrations (i.e. few 1000 ppm) are common in zircons in coarse-grained and pegmatitic granitoid rocks, and are thought to be characteristic of magmatic zircons (Williams and Claesson 1987; Heaman and Parrish 1991; Pidgeon 1992; Williams 1992; Pidgeon and Compston 1992; Mezger and Krogstad 1997; Nemchin and Pidgeon 1997; Kuiper 2003). Magmatic zircon in coarse-grained and pegmatitic granitoid rocks may have lower than normal expected Th/U ratios (Williams and Claesson 1987; Pidgeon 1992; Williams 1992; Pidgeon and Compston 1992; Mezger and Krogstad 1997; Nemchin and Pidgeon 1997). Therefore, the evidence suggests that these zircons are most likely magmatic.

Grain #9 is the most concordant, and grains get consistently more discordant the younger they are (Figure 5.6a). A regression of the zircon analyses yields a discordia with an upper intercept at 2634 ± 64 Ma and a lower intercept at 1232 ± 110 Ma, with an MSWD (mean square of weighted deviates) of 4.7 (Figure 5.6a). The data suggests the existence of a complex Pb-loss event or polymetamorphism. An event associated with the young lower intercept age is not known from the Superior Province or neighbouring Trans-Hudson Orogen, however, a possibility would be the emplacement of the Mackenzie mafic dyke swarm at 1270 Ma (Heaman 2005). More likely, the original lower intercept to the discordia was near ca. 1835 Ma, and was pulled down to 1232 Ma by a late Pb-loss event. Therefore, the lower intercept most likely is associated with a Pb-loss event related to Hudsonian thermo-activity at ca. 1835 Ma (e.g. Machado et al. 1999; Zwanzig 1999, 2005).

As illustrated in Table 5.2, distributions of $^{207}Pb/^{206}Pb$ ages can be separated into high U-Th (grains 11, 25, and 34; 5000-7000 ppm U, 400-800 ppm Th) and low U-Th (2000-3000 ppm U, 50-250 ppm Th) zircon populations. High U-Th zircons have $^{207}Pb/^{206}Pb$ ages ranging from 1832–1983 Ma, are highly altered and fractured, and have poor internal zoning. Low U-Th zircons range from

2172–2686 Ma, are less altered and fractured, and have better developed internal zoning (Figure 5.5). Both populations have similar Th/U ratios. The very high concentrations of uranium in grains 11, 25, and 34, nearly double that of the older grains, cause radiation damage in the grains, and Pb is lost along fractures. This indicates that the system in these grains was not closed, so the data obtained was very discordant (17.1-26.5%), thus rendering geologically meaningless $^{207}Pb/^{206}Pb$ ages. As a result, the high U-Th zircons were not included in the calculation of a better constrained upper intercept age (Figure 5.6b). A regression of the low U-Th zircon analyses yields a discordia with an upper intercept at 2639 Ma, with a rather large uncertainty of 40 Ma, and an MSWD of 0.46. A lower intercept is at 1349 ± 100 Ma, again this lower intercept age is not known from the Superior Province, and therefore such a Pb-loss event is most likely related to Hudsonian thermo-activity. The upper intercept age of 2639 ± 40 Ma on Figure 5.6b is interpreted as the best age estimate for the zircon growth in this pegmatitic granite and represents the crystallization age of the rock. In order to better constrain the age of this sample, titanite was dated by the ID-TIMS method.

Titanite morphology and U-Pb age results

Titanite is generally light brown to pinkish brown. Crystal size is generally <300 µm, with length to width ratios that vary from 1 to 3 (Figure 5.7 inset). Some titanite are roughly prismatic, with rounded edges, whereas others have ovoid or stubby morphologies. Fractures are present in most crystals.

Three 11-grain titanite fractions were analyzed. The U-Pb results are presented in Table 5.3 and on a concordia diagram in Figure 5.7. These three fractions yield concordant results (0.2-1% discordant) and were low in uranium, especially when compared to the uranium concentrations in zircon from the sample. Two of the analyses are concordant (T1, T3), and one is reversely discordant (T2), but all have a similar $^{207}Pb/^{206}Pb$ age. Fraction T2 is reversely discordant because of analytical problems (either dissolution or the result of the common Pb composition chosen; N. Rayner, pers. comm., 2005). The analyses yield a weighted mean $^{207}Pb/^{206}Pb$ age of 2686.1 ± 2.8 Ma. This 2686 Ma

Fraction	Wt. (µg)	U^2 (ppm)	Pb^{*2} (ppm)	$\frac{^{206}Pb^1}{^{204}Pb}$	Pbc^1 (pg)	$\frac{^{208}Pb^2}{^{206}Pb}$	$\frac{^{207}Pb^2}{^{235}U}$	$\pm\frac{^{207}Pb}{^{235}U}$	$\frac{^{206}Pb^2}{^{238}U}$	$\pm\frac{^{206}Pb}{^{238}U}$	Corr Coeff
T1	33	176	106	1317.2	144	0.17	13.079	0.017	0.5161	0.0005	0.8854377
T2	44	192	117	1348	204	0.17	13.222	0.017	0.5225	0.0005	0.8773407
T3	57	161	96	1146.1	260	0.16	13.115	0.029	0.5181	0.0008	0.8847539

Fraction	$\frac{^{207}Pb^2}{^{206}Pb}$	$\pm\frac{^{207}Pb}{^{206}Pb}$	Apparent Ages (Ma) $\frac{^{206}Pb}{^{238}U}$	$\pm\frac{^{206}Pb}{^{238}U}$	$\frac{^{207}Pb}{^{235}U}$	$\pm\frac{^{207}Pb}{^{235}U}$	$\frac{^{207}Pb}{^{206}Pb}$	$\pm\frac{^{207}Pb}{^{206}Pb}$	Disc. (%)
T1	0.18378	0.00012	2682.8	4	2685.4	2.5	2687.3	2.2	0.21
T2	0.18354	0.00012	2709.7	4	2695.7	2.5	2685.1	2.2	-1.12
T3	0.18359	0.00021	2691.1	6.5	2688	4.2	2685.6	3.7	-0.25

Mean age = 2686.1 ± 2.8 Ma (0.10%) with 95% confidence (1 sigma). Wtd by data-point errors only, 0 of 3 rejected. MSWD = 0.26, probabilty = 0.77

Notes:

1: SE absolute on ratios

2: SE Ma on ages

[1] = spike and fractionation corrected only

[2] = spike, fractionation and blank corrected

Table 5.3. ID-TIMS U-Pb titanite results for sample 097-03-4008A (GSC #8315)

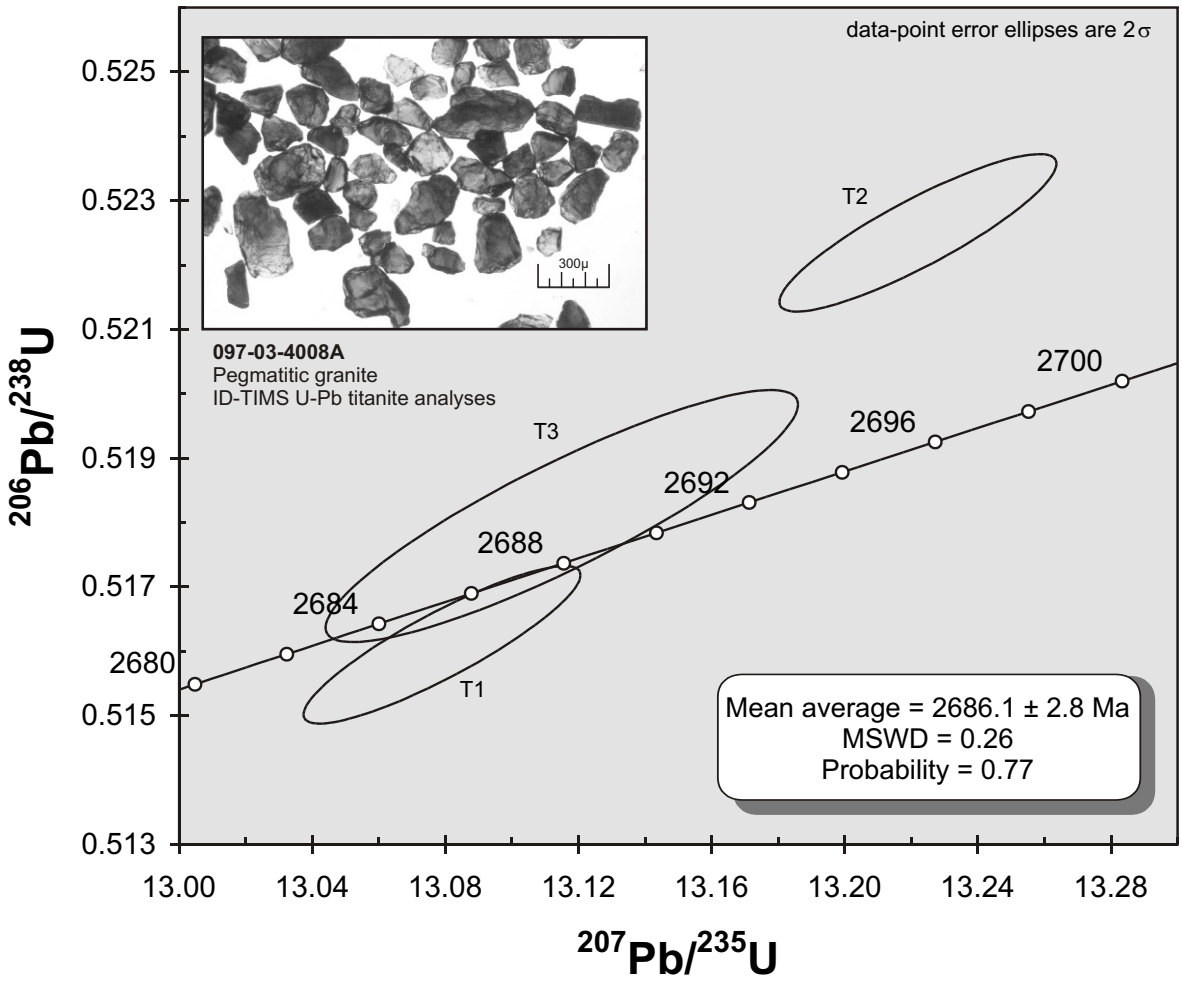

Figure 5.7. Concordia diagram and photomicrograph (inset) for the ID-TIMS U-Pb analyses of three titanite fractions from sample 097-03-4008A (GSC #8315). Numbers correspond to fraction number; data presented in Table 5.3. These three fractions yield relatively concordant results: two of the analyses are concordant (T1, T3), and one is reversely discordant (T2; due to analytical procedures). All have a similar $^{207}Pb/^{206}Pb$ age. These analyses give a weighted mean $^{207}Pb/^{206}Pb$ age of 2686.1 ± 2.8 Ma.

age fits closely within error of the zircon $^{207}Pb/^{206}Pb$ age for the same sample (2639 ± 40 Ma). The weighted mean $^{207}Pb/^{206}Pb$ age of 2686.1 ± 2.8 Ma is thereby interpreted as the best age estimate for the titanite growth in this pegmatitic granite and represents either the crystallization age of the rock, or a Neoarchean metamorphic event.

5.3.2.2 Sample 097-04-5218A

Sample 097-04-5218A (GSC #8384) is from a granodiorite sill of the second intrusive phase (Figure 5.2c; Appendix A). It is relatively homogeneous (plagioclase–K-feldspar–quartz; Chapter 3.4). Biotite and hornblende are minor, and define a weak foliation. Quartz and feldspar also display evidence for intracrystalline deformation. Orthoamphibole was observed in this sample. This granodiorite was injected along an S1 foliation plane and was then folded by F2 (Table 5.1). Nearby, similar granodiorite dykes crosscut S1. The age of this granodiorite will thereby provide a constraint on late-G1 to early-G2 deformation. This sample has the same timing relationship as 097-03-4008A, and was dated in addition to 097-03-4008A in order to better constrain the age of late-G1 to early-G2 deformation and M1b (peak) metamorphism.

Zircon morphology and U-Pb age results

Zircon crystal size is rather small (<100 μm), with length to width ratios that vary from 1 to 3 (Figure 5.8). The zircon morphology of this sample is similar to zircons of sample 097-03-4008A. Zircons exhibit a subhedral-euhedral, roughly prismatic form with rounded corners and edges. Internal zoning is developed in grains 1, 6, and 11, and is very well developed in grain 3 (Figure 5.8). Varying degrees of fracturing and alteration are also evident. Favourable spots (possible rims, possible cores) away from alteration zones and fractures were chosen for SHRIMP U-Pb spot analysis.

A total of 13 zircons were found in the sample, and 10 spots were analyzed from 8 grains. The U-Pb results are presented in Table 5.4 and on concordia diagrams in Figure 5.9. The zircons are

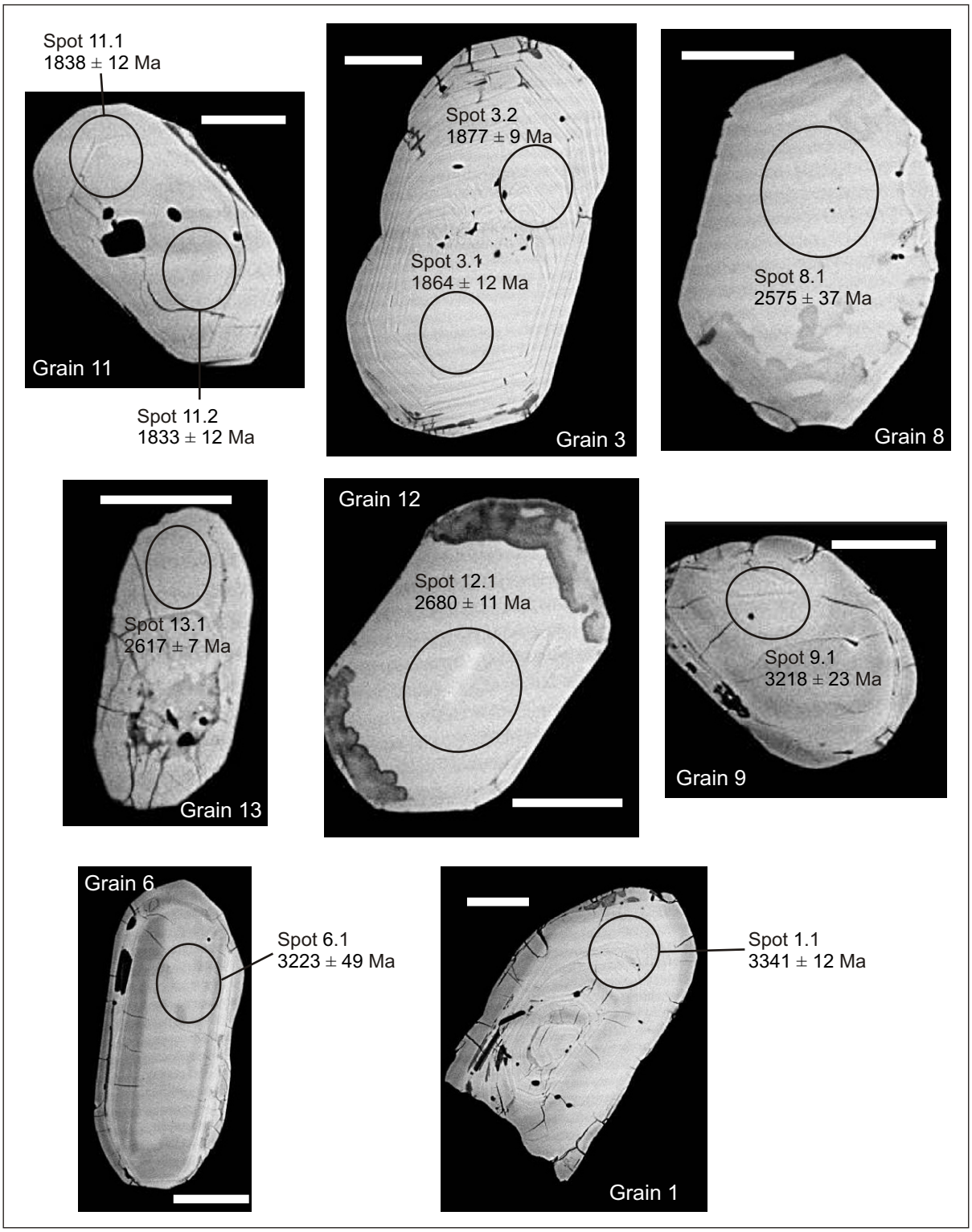

Figure 5.8. Backscattered electron images of zircons from sample 097-04-5218A (GSC #8384; Figure 5.2c). Note subhedral-euhedral prismatic form, large amount of alteration (darker blebs in pods and along fractures) in all grains, and general lack of magmatic zoning in some. Grain 3 shows well developed magmatic zoning. White scale bars represent 25 μm. Circles represent ion beam pits analyzed on the SHRIMP. Spot ages are $^{207}Pb/^{206}Pb$ ages from Table 5.4.

Spot name	U (ppm)	Th (ppm)	Th/U	Pb* (ppm)	^{204}Pb (ppb)	$^{204}Pb/^{206}Pb$	$\pm\ ^{204}Pb/^{206}Pb$	$f(206)^{204}$	$^{208*}Pb/^{206*}Pb$	$\pm\ ^{208}Pb/^{206}Pb$	$^{207*}Pb/^{235}U$	$\pm\ ^{207}Pb/^{235}U$
8384-1.1	576	65	0.12	360	2	7.79E-06	6.36E-06	0.00013	0.03392	0.00061	21.106	0.3982
8384-6.1	268	173	0.66	199	1	1.00E-05	1.00E-05	0.00017	0.18527	0.00337	21.108	0.80272
8384-9.1	428	86	0.21	298	34	1.51E-04	1.78E-05	0.00261	0.05341	0.00153	21.74331	0.55089
8384-12.1	1524	144	0.10	849	8	1.19E-05	3.59E-06	0.00021	0.02597	0.00064	13.52241	0.28458
8384-13.1	690	63	0.09	345	6	1.94E-05	1.75E-05	0.00034	0.02843	0.00077	11.73406	0.18976
8384-8.1	2083	254	0.13	1094	1	1.05E-06	2.76E-06	0.00002	0.03481	0.0008	11.986	0.45638
8384-3.2	1025	325	0.33	348	3	9.01E-06	8.23E-06	0.00016	0.0961	0.00183	5.169	0.08218
8384-3.1	1152	381	0.34	395	5	1.60E-05	6.65E-06	0.00028	0.09778	0.0009	5.1619	0.08822
8384-11.1	423	264	0.64	155	1	1.00E-05	1.00E-05	0.00017	0.19034	0.00168	5.05236	0.08665
8384-11.2	376	281	0.77	131	3	3.21E-05	2.68E-05	0.00056	0.21921	0.00269	4.7064	0.08482

Spot name	$^{206*}Pb/^{238}U$	$\pm\ ^{206}Pb/^{238}U$	Corr Coeff	$^{207*}Pb/^{206*}Pb$	$\pm\ ^{207}Pb/^{206}Pb$	Apparent Ages (Ma) $^{206}Pb/^{238}U$	$\pm\ ^{206}Pb/^{238}U$	$^{207}Pb/^{206}Pb$	$\pm\ ^{207}Pb/^{206}Pb$	Disc. (%)
8384-1.1	0.55454	0.00912	0.9208	0.27604	0.00205	2844	38	3341	12	14.9
8384-6.1	0.59775	0.01155	0.6079	0.25611	0.00779	3021	47	3223	49	6.3
8384-9.1	0.6178	0.0117	0.8198	0.25525	0.00373	3101	47	3218	23	3.6
8384-12.1	0.53603	0.0102	0.9453	0.18296	0.00127	2767	43	2680	11	-3.2
8384-13.1	0.48305	0.00728	0.9653	0.17618	0.00075	2541	32	2617	7	2.9
8384-8.1	0.50611	0.01453	0.825	0.17177	0.00373	2640	62	2575	37	-2.5
8384-3.2	0.32653	0.00476	0.9547	0.11481	0.00055	1822	23	1877	9	2.9
8384-3.1	0.32844	0.00487	0.917	0.11398	0.00078	1831	24	1864	12	1.8
8384-11.1	0.32606	0.00492	0.9272	0.11238	0.00073	1819	24	1838	12	1
8384-11.2	0.3046	0.00482	0.926	0.11206	0.00077	1714	24	1833	12	6.5

Notes (see Stern, 1997):

* = radiogenic Pb

Uncertainties reported at 1 sigma (absolute) and are calculated by numerical propagation of all known sources of error

f(206)204 refers to mole fraction of total 206Pb that is due to common Pb, calculated using the 204Pb-method; common Pb composition used is the surface blank

Discordance relative to origin = 100 * (1-(206Pb/238U age)/(207Pb/206Pb age))

Table 5.4. SHRIMP U-Pb zircon results for sample 097-04-5218A (GSC #8384)

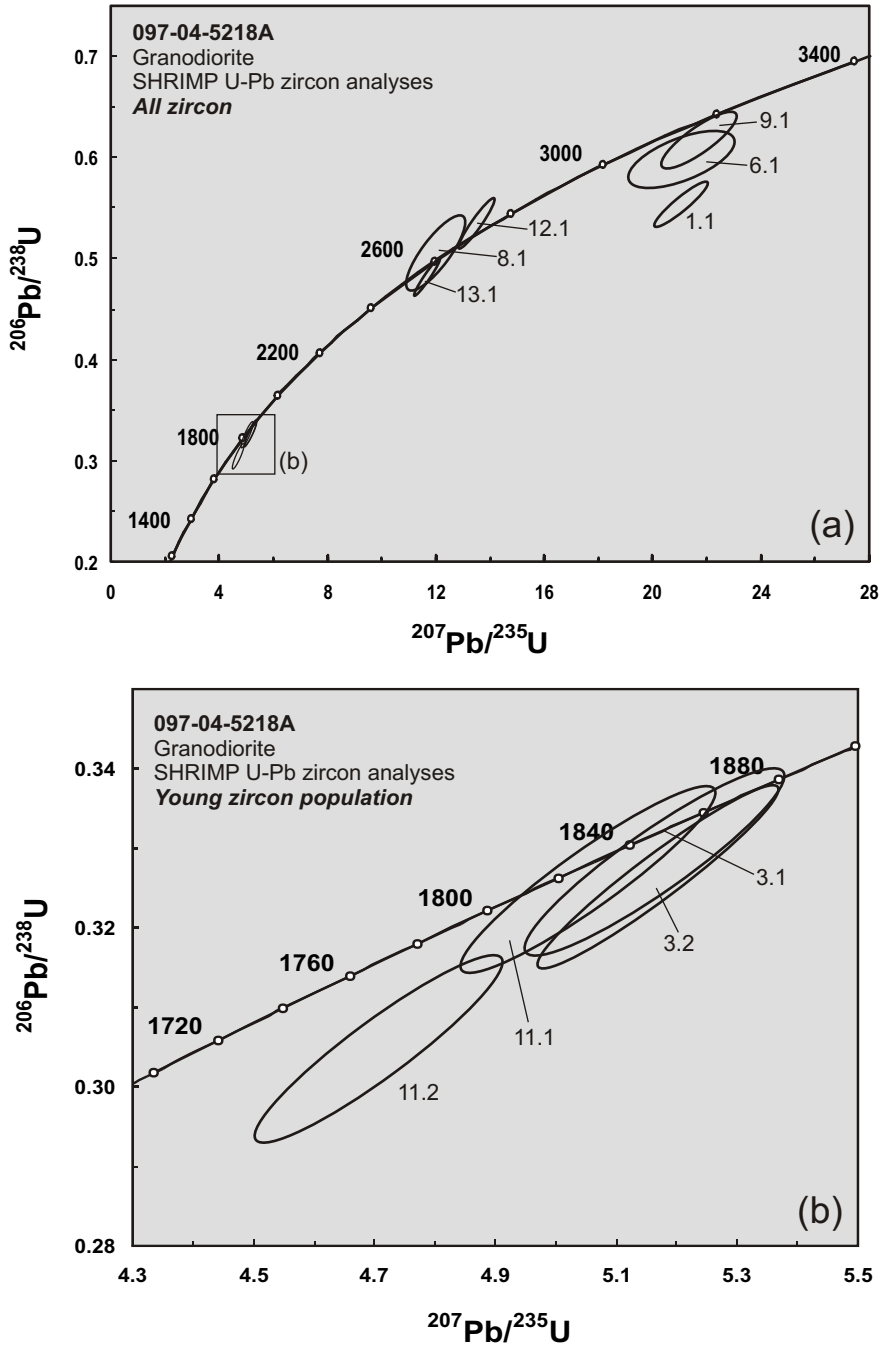

Figure 5.9. Concordia diagrams for the SHRIMP U-Pb analyses of 8 zircons (10 spots) from sample 097-04-5218A (GSC #8384; Figure 5.2c, 5.8). Numbers correspond to spot number; data presented in Table 5.4. B is an inset of A. These 10 spots yield concordant results. From this it is apparent that a discordia line and upper intercept age cannot be placed on the diagram. Two concordant zircon populations are evident: 2575-2680 Ma (grains 8, 12, and 13), and 1833-1877 Ma (grains 3 and 11, figure b). An older discordant population (3218-3341 Ma, grains 1, 6, and 9) is relatively discordant and therefore most likely represents older, inherited grains. The crystallization age of this rock could lie in the 1833-1877 Ma range or in the 2575-2680 Ma range. See text for discussion.

low in uranium when compared to sample 097-03-4008A (average of 600 ppm, maximum of 2000 ppm), have a consistent amount of thorium (~200 ppm), and are concordant (with the exception of grain #1, the grains have an average of 3% discordancy). They give a wide range of $^{207}Pb/^{206}Pb$ ages, from 1833 ± 12 Ma to 3341 ± 12 Ma (Figure 5.9a). The cores and rims in the grains show no predictable core-rim age relationships. Their Th/U ratios range from 0.09 to 0.77, suggestive of metamorphic and magmatic zircon, respectively. However, magmatic zircon in coarse-grained and pegmatitic granitoid rocks may have lower than normal expected Th/U ratios (Williams and Claesson 1987; Pidgeon and Compston 1992; Williams et al. 1996; Mezger and Krogstad 1997; Nemchin and Pidgeon 1997; Böhm et al. 2003c). The subhedral-euhedral crystal shape to all of the grains suggests magmatic zircon (Figure 5.8). Therefore, the evidence suggests that these zircons are most likely magmatic.

As illustrated on Figure 5.9a, the data cannot be regressed to produce a discordia line anywhere, or an upper intercept age. However, it is evident that there are two concordant zircon $^{207}Pb/^{206}Pb$ age populations, one in the 2575–2680 Ma range (grains 8, 12 and 13), and one in the 1833–1877 Ma range (grains 3 and 11). An older zircon $^{207}Pb/^{206}Pb$ age population, in the 3218–3341 Ma range (grains 1, 6, and 9), is relatively discordant. Zircons in the 1833–1877 Ma range are concordant (1-6.5%), have well developed internal zoning and a general lack of alteration and fracturing, uranium concentrations ranging from 400 to 1000 ppm, and Th/U ratios ranging from 0.33 to 0.77. Zircons in the 2575–2680 Ma range are concordant (2.5-3.2%), have no evident internal zoning, and have a significant amount of alteration and fracturing, uranium concentrations ranging from 700 to 2000 ppm, and Th/U ratios ranging from 0.09 to 0.13. Zircons in the 3218–3341 Ma range are relatively discordant (3-15%), have weak internal zoning and some alteration and fracturing, uranium concentrations ranging from 270 to 580 ppm, and Th/U ratios ranging from 0.12 to 0.66. This population most likely represents older, inherited grains. These old $^{207}Pb/^{206}Pb$ ages are not known from the Gull Rapids orthogneiss complex, nor from the Split Lake Block, and may be indicative of older Mesoarchean crust beneath the Split Lake Block. It is evident that no specific

zircon population has a specific amount of uranium, i.e. zircons with uranium concentrations of ~400-600 ppm are both young and old. Also, the 1833–1877 Ma population does not have an anomalously high uranium concentration, as it did in sample 097-03-4008A.

From the data presented above, it is apparent that the rock could have a crystallization age in the 2575–2680 Ma range, or in the 1833–1877 Ma range. The discordancy between the zircons in the older of the two concordant populations is very similar, and any one of the three zircons could represent the best-fit $^{207}Pb/^{206}Pb$ age. However, when in comparison to the upper intercept zircon age from sample 097-03-4008A (2639 ± 40 Ma), either grain #13, with a $^{207}Pb/^{206}Pb$ age of 2617 ± 7 Ma, or grain #12, with a $^{207}Pb/^{206}Pb$ age of 2680 ± 11 Ma, both of which are within error of 2639 ± 40 Ma, most likely represents the best-fit $^{207}Pb/^{206}Pb$ age for this population. These two samples (097-03-4008A and 097-04-5218A) can be compared to each other in such a manner because they have similar crosscutting relationships with the host rock deformation. Zircons in this population have Th/U ratios suggestive of metamorphic zircon. However, high uranium concentrations and subhedral-euhedral crystal shapes provide stronger evidence that these zircons are magmatic and not metamorphic.

The least discordant zircon in the younger of the two concordant populations is grain #3, with an $^{207}Pb/^{206}Pb$ age of ca. 1870 Ma. Zircons in this population have well developed internal zoning, and Th/U ratios suggestive of magmatic zircon. It is interesting to note that this age population is similar to the age of Hudsonian thermo-activity (e.g. Machado et al. 1999; Zwanzig 1999, 2005), and similar to the age of high U-Th zircons from sample 097-03-4008A. Therefore, this age population could be related to some Hudsonian thermo-activity. Regardless, it is evident from the results presented above this rock could either have a Neoarchean (ca. 2640 Ma) or a Paleoproterozoic (ca. 1870 Ma) crystallization age.

5.3.2.3 Sample 097-03-4008C

Sample 097-03-4008C (GSC #8317) is from a pegmatitic granite dyke of the third intrusive phase (Figure 5.4c; Appendix A). It is homogeneous (plagioclase–quartz; Chapter 3.4) and does not have a fabric. Biotite is minor, and quartz and plagioclase display evidence for intracrystalline deformation. This pegmatite dyke is parallel to a shear zone. It was first offset by the shear zone, and was then injected into and along the shear plane, implying that the pegmatite emplacement is syn-shearing (Table 5.1). Such shearing associated with pegmatite dyke emplacement is of the G4 generation (see Chapter 4.3.2.1 and 5.2.2). The age of this pegmatite will thereby provide a constraint on G4 deformation (as well as providing a constraint on earlier deformation).

Zircon morphology and U-Pb age results

Zircon crystal size is generally <200 μm, with length to width ratios that vary from 1 to 4 (Figure 5.10). The zircon morphology of this sample is similar to that of samples 097-03-4008A and 097-04-5218A. Zircons exhibit a subhedral-euhedral, roughly prismatic form with rounded corners and edges. Internal zoning is developed in grains 26, 29, 74, 90, 94, and 108 (Figure 5.10). Varying degrees of fracturing and alteration are also evident. Favourable spots (possible rims, possible cores) away from alteration zones and fractures were chosen for SHRIMP U-Pb spot analysis.

A total of 108 zircons were found in the sample, and 15 spots were analyzed from 13 grains. The U-Pb results are presented in Table 5.5 and on concordia diagrams in Figure 5.11. Some zircons have high uranium (~2000-5000 ppm), whereas others are lower in uranium (~100-1000 ppm). These zircons have a relatively consistent amount of thorium (~200-300 ppm), and are concordant (with the exception of grains #29, 43, 74, and 96, the grains have an average of 2% discordancy). They give a wide range of $^{207}Pb/^{206}Pb$ ages, from 1458 ± 9 Ma to 3279 ± 5 Ma (Figure 5.11a). The cores and rims in the grains show no predictable core-rim age relationships. The zircon Th/U ratios range from 0.03 to 0.83, suggestive of metamorphic and magmatic zircon, respectively (Williams and Claesson 1987; Pidgeon and Compston 1992; Williams et al. 1996; Mezger and Krogstad 1997; Nemchin and

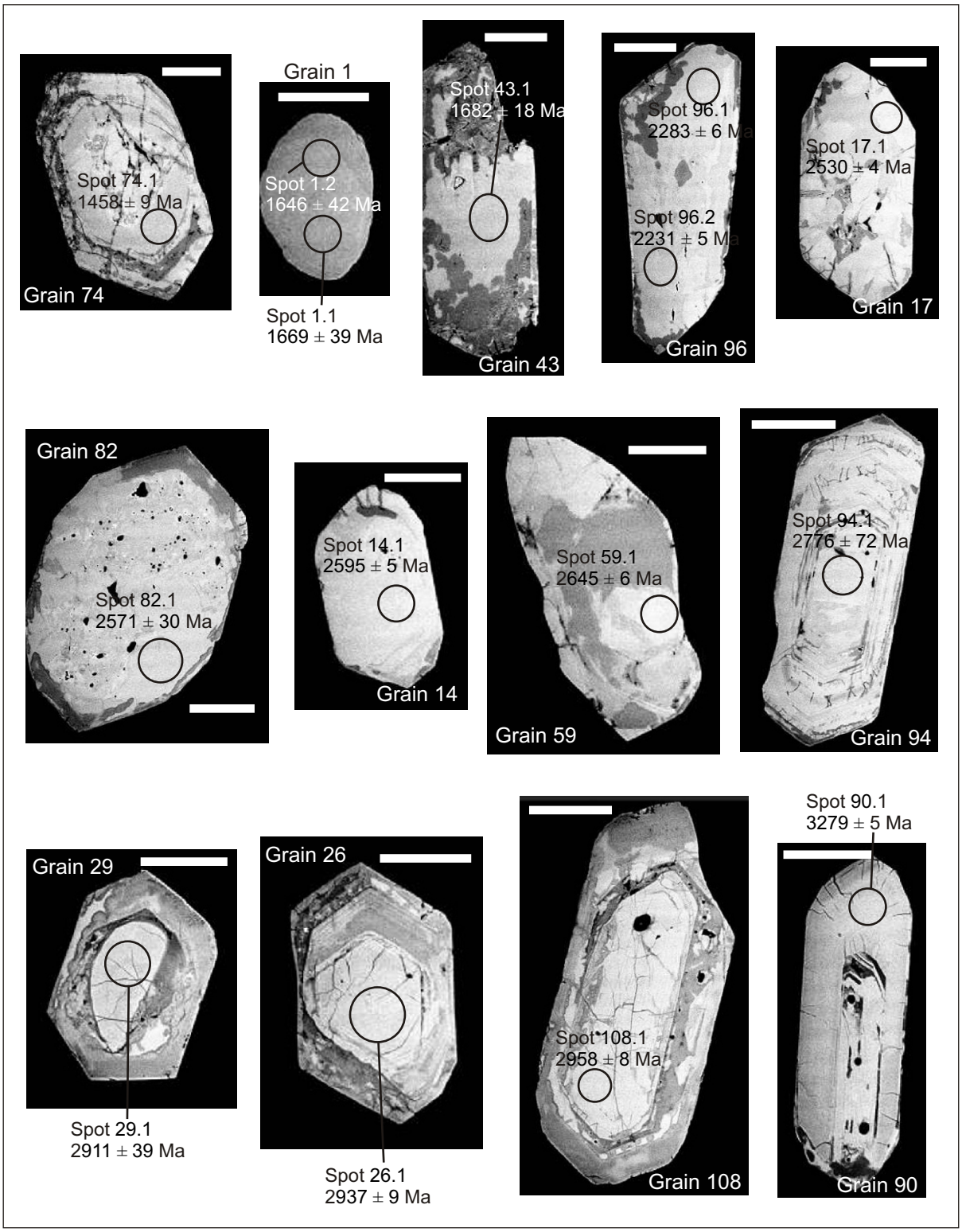

Figure 5.10. Backscattered electron images of zircons from sample 097-03-4008C (GSC #8317; Figure 5.4c). Note subhedral-euhedral prismatic form, large amount of alteration (darker blebs in pods and along fractures) in all grains, and general lack of magmatic zoning in some. Some zircons display well developed zoning. White scale bars represent 50 μm. Circles represent ion beam pits analyzed on the SHRIMP. Spot ages are $^{207}Pb/^{206}Pb$ ages from Table 5.5.

Spot name	U (ppm)	Th (ppm)	Th/U	Pb* (ppm)	^{204}Pb (ppb)	$^{204}Pb/^{206}Pb$	$\pm\ ^{204}Pb/^{206}Pb$	f(206)^{204}	$^{208*}Pb/^{206*}Pb$	$\pm\ ^{208}Pb/^{206}Pb$	$^{207*}Pb/^{235}U$
8317-90.1	910	629	0.71	756	4	7.93E-06	4.64E-06	0.00014	0.18713	0.00086	24.315
8317-108.1	736	364	0.51	485	4	1.26E-05	4.68E-06	0.00022	0.13673	0.00105	16.911
8317-26.1	516	291	0.58	338	2	1.00E-05	1.00E-05	0.00017	0.16354	0.00113	16.299
8317-29.1	259	98	0.39	142	9	8.46E-05	1.57E-04	0.00147	0.12164	0.006	13.917
8317-94.1	2333	154	0.07	1345	141	1.28E-04	4.89E-05	0.00222	0.02995	0.00308	14.642
8317-59.1	1763	59	0.03	947	74	9.36E-05	8.22E-06	0.00162	0.01171	0.00036	12.953
8317-14.1	2274	118	0.05	1104	50	5.35E-05	7.53E-06	0.00093	0.01404	0.00033	11.391
8317-82.1	2776	114	0.04	1398	25	2.10E-05	4.79E-06	0.00036	0.01169	0.00025	11.695
8317-17.1	2705	153	0.06	1276	54	5.06E-05	9.86E-06	0.00088	0.01572	0.00042	10.691
8317-96.1	5090	327	0.07	1954	546	3.24E-04	9.72E-06	0.00562	0.01862	0.00055	7.6504
8317-96.2	4790	335	0.07	1766	603	3.94E-04	1.03E-05	0.00684	0.01917	0.00044	7.1536
8317-43.1	5226	274	0.05	1289	89	7.71E-05	7.39E-06	0.00134	0.01565	0.00037	3.6492
8317-1.1	139	111	0.83	46	3	9.28E-05	5.29E-05	0.00161	0.24228	0.00705	4.0612
8317-1.2	122	72	0.61	38	3	9.90E-05	4.60E-05	0.00172	0.18083	0.00447	3.9611
8317-74.1	4095	187	0.05	813	129	1.75E-04	1.07E-05	0.00304	0.01332	0.00045	2.6369

Spot name	$\pm\ ^{207}Pb/^{235}U$	$^{206*}Pb/^{238}U$	$\pm\ ^{206}Pb/^{238}U$	Corr Coeff	$^{207*}Pb/^{206*}Pb$	Apparent Ages (Ma) $\pm\ ^{207}Pb/^{206}Pb$	$^{206}Pb/^{238}U$	$\pm\ ^{206}Pb/^{238}U$	$^{207}Pb/^{206}Pb$	$\pm\ ^{207}Pb/^{206}Pb$	Disc. (%)
8317-90.1	0.37838	0.66448	0.00984	0.9781	0.2654	0.00087	3285	38	3279	5	-0.2
8317-108.1	0.30211	0.56553	0.00943	0.9657	0.21687	0.00101	2889	39	2958	8	2.3
8317-26.1	0.2907	0.55202	0.00899	0.952	0.21415	0.00118	2834	37	2937	9	3.5
8317-29.1	0.41818	0.47904	0.00768	0.631	0.21071	0.00495	2523	34	2911	39	13.3
8317-94.1	0.96766	0.54748	0.02464	0.7625	0.19397	0.00836	2815	103	2776	72	-1.4
8317-59.1	0.21148	0.52457	0.00815	0.9776	0.17909	0.00062	2719	35	2645	6	-2.8
8317-14.1	0.18276	0.4753	0.0073	0.9815	0.17382	0.00054	2507	32	2595	5	3.4
8317-82.1	0.32367	0.49503	0.00959	0.779	0.17135	0.003	2592	41	2571	30	-0.8
8317-17.1	0.18174	0.46356	0.00763	0.9878	0.16726	0.00045	2455	34	2530	4	3
8317-96.1	0.15481	0.38375	0.00747	0.9843	0.14459	0.00052	2094	35	2283	6	8.3
8317-96.2	0.15555	0.36975	0.00786	0.9925	0.14032	0.00038	2028	37	2231	5	9.1
8317-43.1	0.07832	0.2565	0.00463	0.8973	0.10318	0.00099	1472	24	1682	18	12.5
8317-1.1	0.11332	0.2875	0.00459	0.6661	0.10245	0.00215	1629	23	1669	39	2.4
8317-1.2	0.12134	0.28391	0.00527	0.6959	0.10119	0.00224	1611	26	1646	42	2.1
8317-74.1	0.04345	0.20891	0.00317	0.9566	0.09154	0.00044	1223	17	1458	9	16.1

Notes (see Stern, 1997):

* = radiogenic Pb

Uncertainties reported at 1 sigma (absolute) and are calculated by numerical propagation of all known sources of error

f(206)204 refers to mole fraction of total 206Pb that is due to common Pb, calculated using the 204Pb-method; common Pb composition used is the surface blank

Discordance relative to origin = 100 * (1-(206Pb/238U age)/(207Pb/206Pb age))

Table 5.5. SHRIMP U-Pb zircon results for sample 097-03-4008C (GSC #8317)

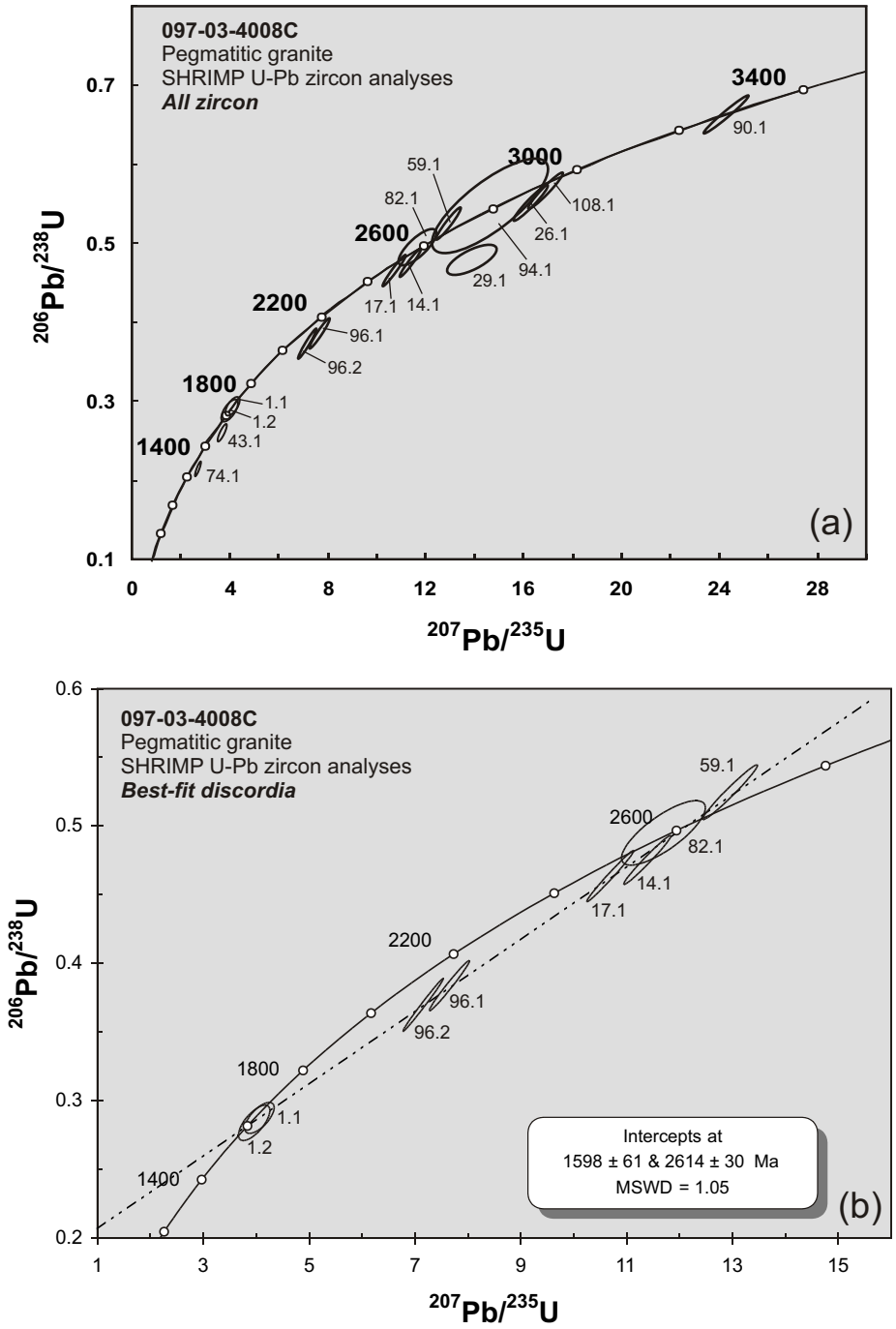

Figure 5.11. Concordia diagrams for the SHRIMP U-Pb analyses of 13 zircons (15 spots) from sample 097-03-4008C (GSC #8317; Figure 5.4c, 5.10). Numbers correspond to spot number; data presented in Table 5.5. a) All zircons yield three concordant (grain #1; grains 14, 17, 59, and 82; grains 26, 94, and 108) and one discordant (grain #96) age populations. b) A best-fit discordia line through two concordant populations (grain #1 and grains 14, 17, 59, and 82) and through one discordant population (grain #96) yields an upper intercept age of 2614 ± 30 Ma. See text for discussion.

Pidgeon 1997; Böhm et al. 2003c). On the other hand, the subhedral-euhedral crystal shape to all of the grains suggests magmatic zircon (Figure 5.10). Therefore, the evidence suggests that these zircons are most likely magmatic.

As illustrated on Figure 5.11a, three concordant zircon $^{207}Pb/^{206}Pb$ age populations can be described: the first at 1646–1669 Ma (2% discordancy; grain #1), the second in the 2530–2645 Ma range (0.8-3.4% discordancy; grains 14, 17, 59, and 82), and the third in the 2776–2958 Ma range (1.4-3.5% discordancy; grains 26, 94, and 108; grain 94 has a 72 Ma error associated with it). An older concordant zircon has a $^{207}Pb/^{206}Pb$ age of 3279 ± 5 Ma (0.2% discordancy; grain #90). A discordant zircon $^{207}Pb/^{206}Pb$ age population lies in the 2231–2283 Ma range (8-9% discordancy; grain #96), and young discordant zircons have $^{207}Pb/^{206}Pb$ ages of 1458 ± 9 Ma (16% discordancy; grain #74) and 1682 ± 18 Ma (12.5% discordancy; grain #43). An older discordant zircon has a $^{207}Pb/^{206}Pb$ age of 2911 ± 39 Ma (13.3% discordancy; grain #29).

The zircon in the 1646–1669 Ma range (grain #1; the two replicates on that grain are equivalent within error) has no visible internal zoning, has a rounded subhedral crystal shape, and has a significant amount of alteration, a uranium concentration of ~100 ppm, and a Th/U ratio of 0.61-0.83. The evidence suggests that this zircon is magmatic. Zircons in the 2530–2645 Ma range (grains 14, 17, 59, and 82) have no evident internal zoning, subhedral-euhedral crystal shapes, and have a significant amount of alteration, uranium concentrations ranging from 1700 to 2700 ppm, and Th/U ratios ranging from 0.03 to 0.06. Zircons in the 2776–2958 Ma range (grains 26, 94, and 108) have well developed internal zoning and subhedral-euhedral crystal shapes, but also a significant amount of alteration, uranium concentrations ranging from 500 to 2300 ppm, and Th/U ratios ranging from 0.07 to 0.58. Thus, zircons in the 2530–2958 Ma range are most likely magmatic. The older zircon with a concordant age of 3279 Ma (grain #90) has weak internal zoning, and is relatively altered and fractured. This old zircon is most likely inherited, and may be indicative of older Mesoarchean crust beneath the Split Lake Block. The zircon in the discordant 2231–2283 Ma range (grain #96) is largely altered and no internal zoning is visible. It has a very high uranium concentration (4700-5000 ppm),

and a Th/U ratio of 0.07. The very high concentrations of uranium in grains 43 (1682 Ma) and 74 (1458 Ma) and consequent high discordancy renders these $^{207}Pb/^{206}Pb$ ages geologically meaningless. The 2911 Ma discordant zircon (grain #29) is most likely inherited, and may be from the orthogneiss complex at Gull Rapids.

From the data presented above and on Figure 5.11a, it is apparent that the rock has a crystallization age in the 2530–2958 Ma range. In order to produce a best-fit discordia, a regression was completed using the concordant zircon populations of 1646–1669 Ma and 2530–2645 Ma, and the discordant population of 2231–2283 Ma. The younger of the two older concordant zircon populations (2530–2645 Ma and 2776–2958 Ma) was used in such a regression in order to obtain a best-fit discordia with the smallest error and MSWD. As well, it is known that the maximum crystallization age of this rock must be younger than ca. 2640 Ma, because the emplacement of this felsic intrusive rock is synchronous with G4 deformation, whereas the emplacement of the felsic intrusive rock 097-03-4008A (age of ca. 2640 Ma) is synchronous with late-G1 to early-G2 deformation. From this, it is assumed that the 2776–2958 Ma population represents inherited zircon. These ages are similar to rocks from the Gull Rapids orthogneiss complex, or from the Split Lake Block. The regression of these analyses yields a discordia with an upper intercept at 2614 ± 30 Ma, with a lower intercept of 1598 ± 61 Ma, and an MSWD of 1.05 (Figure 5.11b). An event associated with the young lower intercept age is not known from the Superior Province or neighbouring Trans-Hudson Orogen. The upper intercept age of 2614 ± 30 Ma on Figure 5.11b is interpreted as the best age estimate for the zircon growth in this pegmatitic granite and represents the crystallization age of the rock.

5.3.3 Age Interpretations

5.3.3.1 Late-G1 to early-G2 deformation

Felsic intrusive samples 097-03-4008A and 097-04-5218A were emplaced late-G1 to early-G2. Zircon from sample 097-03-4008A yields an upper intercept age of 2639 ± 40 Ma (Figure 5.6b)

which is interpreted to represent the crystallization age of the rock. The low Th/U ratios are suggestive of metamorphic growth, but the high uranium concentrations (few 1000 ppm) and subhedral-euhedral crystal shapes are suggestive of magmatic zircon growth, and Th/U ratios in such coarse-grained and pegmatitic felsic intrusive rocks may not always be useful in discerning between metamorphic and magmatic zircon. Zircon growth from sample 097-04-5218A yields an age of either ca. 2640 Ma (which is the same age as sample 097-03-4008A) or ca. 1870 Ma (Figure 5.9a). Zircons from these populations are interpreted to represent magmatic growth.

In the case of sample 097-03-4008A, titanite was dated in addition to zircon to better constrain the age of the rock (Figure 5.7). Since this pegmatitic granite was emplaced late-G1 to early-G2 (section 5.2.2), and since orthoamphibole is present in the second intrusive phase, to which sample 097-03-4008A belongs (section 5.2.3), this pegmatitic granite was emplaced during peak (M1b) metamorphism. It is known that at Gull Rapids the metamorphism reached peak conditions of upper-amphibolite facies, which is between 600ºC and ~700ºC (Yardley 1989). The closure temperature of titanite is relatively high, up to 700ºC (Frost et al. 2000), but normally near 600ºC (Cherniak 1993). This is lower than that of zircon, which is ~900–1000ºC (Cherniak and Watson 2001). Therefore, the titanite could have grown during this high-grade metamorphism, or was inherited and its age reset as the rock cooled through ~600-700ºC. Regardless, the age of the titanite (2686 ± 3 Ma) represents the age of peak metamorphism. Since the pegmatitic granite was emplaced during peak metamorphism, and since the titanite age represents the age of such metamorphism, the crystallization age of the pegmatitic granite of sample 097-03-4008A cannot be younger than the titanite age, and is most likely ca. 2680 Ma This age agrees with the pegmatitic granite zircon age (2639 ± 40 Ma).

In the case of sample 097-04-5218A, the Paleoproterozoic zircon age population can be ruled out as a possible zircon growth age because ca. 2100 Ma mafic dykes crosscut all of the felsic intrusive phases at Gull Rapids. Therefore, the ca. 1870 Ma zircons grew during some late silicate-

rich metamorphic fluid event, which may be related to Hudsonian thermo-activity. The zircon age of ca. 2640 Ma fits within error of the titanite age from 097-03-4008A.

All of the above evidence implies that a ca. 2680 Ma age represents the age of peak metamorphism at Gull Rapids, and the emplacement age of the second intrusive phase. Therefore, late-G1 to early-G2 deformation occurred at ca. 2680 Ma.

5.3.3.2 G4 deformation

The felsic intrusive sample 097-03-4008C was emplaced during G4 deformation. Zircon from sample 097-03-4008C yields an upper intercept age of 2614 ± 30 Ma (Figure 5.11b). This pegmatite must be younger than that of samples 097-03-4008 and 097-04-5218A (ca. 2680 Ma), which date late-G1 to early-G2 deformation. Therefore, the age of 2614 ± 30 Ma is interpreted to represent the crystallization age of this pegmatite, and therefore the age of G4 deformation. The age of this deformation agrees with ages obtained for G5 deformation, that is, that ca. 2100 Ma mafic dykes are deformed by G5. Therefore, G5 shear zones must be younger than 2100 Ma (and most likely ca. 1.8 Ga).

5.4 SUMMARY AND DISCUSSION OF GEOCHRONOLOGICAL RESULTS FROM GULL RAPIDS

A number of age dates have been collected from Gull Rapids, and have been briefly discussed in Chapter 3. The oldest rocks are amphibolite rafts in orthogneiss. These were not isotopically age dated, but the orthogneiss that hosts them has rock crystallization ages ranging from 3.18 Ga for the L-tectonite, to 2.85 Ga for the augen gneiss (Böhm et al. 2003a). Since the main amphibolite (mafic volcanic) assemblage at Gull Rapids has a similar geochemistry to these amphibolite rafts (Bowerman et al. 2004), it is inferred that they are related, and therefore the amphibolite assemblage must be older than the orthogneiss. The metasedimentary rocks have a ca.

2.70-2.68 Ga age (Bowerman et al. 2004; this thesis), and were likely deposited on top of pre-existing orthogneiss and amphibolite (see Chapter 3, and 4.4.1).

Granitoid dykes and sills were dated for this thesis work in order to constrain the timing of deformation. The second intrusive phase (samples 097-03-4008A and 097-04-5218A) has an age of ca. 2.68 Ga. The third intrusive phase (sample 097-03-4008C) has an age of ca. 2.61 Ga. Mafic dykes in the area were dated by L. Heaman (unpublished data), and have ages of 2102 ± 2 and 2073 ± 2 Ma (see Chapter 3.5, 4.3.2.2, and 5.2.2).

Regional studies on the metamorphism in the Split Lake Block (see Chapter 2.3.1) area have shown that the first metamorphic event, a mid- to upper-amphibolite facies event, occurred at ca. 2705 Ma (M1a; Corkery 1985; Böhm et al. 1999). This was followed closely by an upper-amphibolite to granulite facies event at 2695–2685 Ma (M1b), and by a later mid- to upper-amphibolite event at ca. 2640 Ma (M2; Corkery 1985; Böhm et al. 1999). These ages agree with ages obtained for the timing of deformation and metamorphism at Gull Rapids. Based on the age of the second intrusive phase (ca. 2680 Ma; age of late-G1 to early-G2 deformation), the main phase of G1 deformation must be older, to an unknown extent, than ~2680 Ma. Since G1 deformation is synchronous with M1a metamorphism, G1 deformation must have occurred at ca. 2705 Ma. A further constraint on G1 deformation is the age of sedimentation. Sedimentation occurred between 2700 (youngest detritus) and 2680 Ma (crosscutting intrusion). Therefore, G1 deformation must have occurred sometime around 2700 Ma. The emplacement of the second intrusive phase at ca. 2680 Ma was synchronous with upper-amphibolite facies peak metamorphism (M1b) and late-G1 to early-G2 deformation. The third intrusive phase is synchronous with G4 deformation, which occurred shortly thereafter, at ca. 2610 Ma, but no specific metamorphic event is associated with G4 deformation. The fourth and fifth intrusive phases (mafic dykes), emplaced at ca. 2100 Ma, pre-date G5 deformation and retrograde greenschist facies metamorphism (M3) which are most likely Hudsonian (ca. 1.8 Ga). Table 5.6 summarizes the above.

Age	*Intrusive Event*	*Deformation*	*Metamorphism at Gull Rapids*	*Metamorphism In Split Lake Block*
pre-2705 Ma	Trondhjemite-Tonalite-Granodiorite Gneissic complex (TTG)	Pre-G1 fabric development Possible early development of S1	Mid-amphibolite (M1a)	Upper-amphibolite to granulite (M1a)
ca. 2705 Ma	None recognized	Main pulse of G1	Mid-amphibolite (M1a)	Upper-amphibolite to granulite (M1a)
ca. 2680 Ma	Tonalite-granodiorite-granite Dykes, dykelets, sills, leucosome pods Locally pegmatitic 2nd intrusive phase (1st phase occurred some unknown time before this)	Late-G1 to early-G2 Foliation (S1), folding (F2), Shearing and sheath folding	Upper-amphibolite (M1b) Local granulite in orthogneiss	Granulite (M1b)
ca. 2640 Ma	None recognized	Possible continuation of G2	Mid-amphibolite (M2)	Upper- to mid- -amphibolite (M2)
None recognized	None recognized	G3 folding (F3)	None recognized	None recognized
ca. 2610 Ma	Pegmatite Dykes and dykelets 3rd intrusive phase	G4 shearing	None recognized	None recognized
ca. 2102-2073 Ma	Gabbro, diabase Dykes and dykelets 4th and 5th intrusive phases	None recognized	None recognized	None recognized
ca. 1800 Ma	None recognized	G5 shearing	Greenschist (M3)	Greenschist (M3)

Table 5.6. Summary of absolute ages of intrusive events, metamorphism, and deformation in the Gull Rapids area.

Chapter 6

SUMMARY AND REGIONAL SIGNIFICANCE

6.1 INTRODUCTION

This chapter presents a summary of the previous chapters, and a geological and tectonic history of the Gull Rapids area, using lithology, magmatism, structure, metamorphism, kinematics, and timing of deformation and intrusion using relative and absolute age dating. The history and development of the Gull Rapids area is then discussed in a regional context.

6.2 SUMMARY

The geological and tectonic events that took place at Gull Rapids are chronologically summarized below, and in Figure 6.1.

1. Pre–3.18 Ga: Eruption of mafic volcanic sequence; interpreted as early mafic crust through which Tonalite-Trondhjemite-Granodiorite (TTG) intrusive complex intrudes. This mafic volcanic sequence has an εNd value of +1.0, suggesting a juvenile-mantle origin with only small amounts of crustal contamination (Bowerman et al. 2004). These mafic rocks are geochemically similar to granulites of the Split Lake Block (Bowerman et al. 2004).
2. 3.18–2.85 Ga: Intrusion of TTG complex and formation of gneisses. Rafts of amphibolite occur throughout all different zones (L-tectonite, straight-layered, and augen gneiss) in this orthogneiss complex. Samples of orthogneiss have εNd values of –4 to –7, suggesting significant contamination from the early mafic crust. These orthogneisses are geochemically similar to orthogneisses in the nearby Split Lake Block (Bowerman et al. 2004).

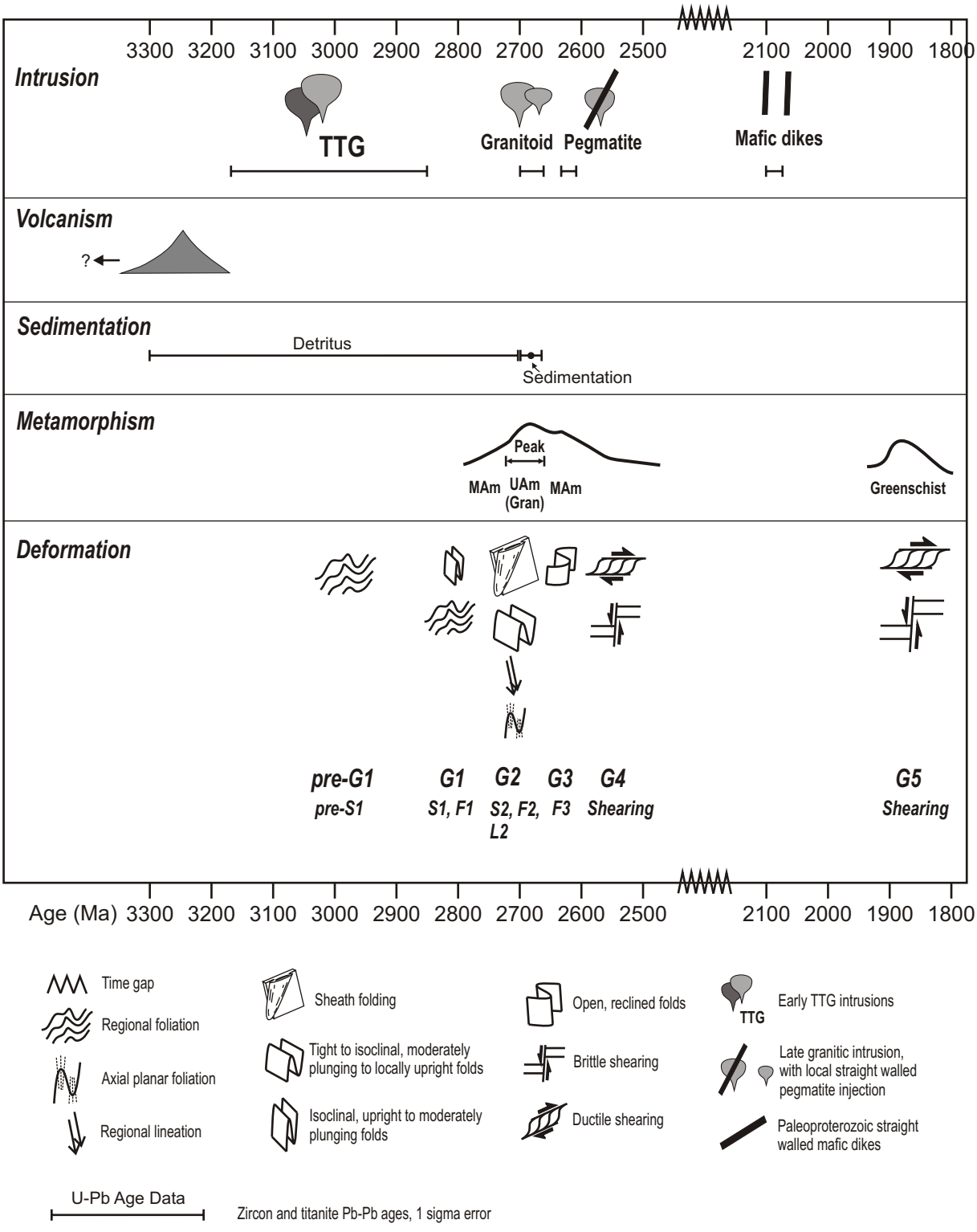

Figure 6.1. Diagram summarizing the magmatic, volcanic, sedimentary, metamorphic, and deformational history of Gull Rapids. MAm = mid-amphibolite grade metamorphism, UAm = upper-amphibolite grade metamorphism, (Gran) = local granulite grade metamorphism in orthogneiss assemblage. See text for discussion.

3. Ca. 2.70 Ga: Deposition of metasedimentary sequence. The metasedimentary rocks contain detritus ranging from 2.7 to 3.3 Ga; the mafic volcanic rocks and orthogneiss were the sources of the detritus. These metasedimentary rocks underwent M1a and G1 deformation. This metasedimentary sequence was deposited in a basin in, or near the margin of the Split Lake Block (Böhm et al. 2003a; Bowerman et al. 2004). A significant amount of granitoid magmatism also occurred during this time (Böhm et al. 1999, 2001, 2003c).
4. ca. 2.70: Mid-amphibolite facies prograde metamorphism (M1a; Corkery 1985; Böhm et al. 1999, 2001, 2003c). The main pulse of G1 deformation (S1 foliation development) occurred around this time. This metamorphic event is observed in the Split Lake Block and Assean Lake Crustal Complex as well (Corkery 1985; Böhm et al. 1999, 2001, 2003c). At Gull Rapids, this metamorphosed the supracrustal and orthogneissic rocks to mid-amphibolite facies conditions.
5. Ca. 2.68 Ga: Upper-amphibolite facies peak metamorphic conditions were attained at Gull Rapids, and granulite facies metamorphism occurred between 2.695 and 2.685 Ga in the Split Lake Block and Pikwitonei Granulite Domain (M1b; Corkery 1985; Böhm et al. 1999, 2001, 2003c). Orthopyroxene, indicative of granulite facies metamorphism, is rare in the Gull Rapids orthogneiss. During this time period at Gull Rapids, the S1 foliation was (further) developed, as was F1 isoclinal folding (and related shearing). F2 sheath folding (and related shearing) began during this time as well. Two phases of felsic intrusion were emplaced during this period, with the second phase being synchronous with peak metamorphism during late-G1 to early-G2 deformation. G3 deformation (F3 folding) would have developed sometime after this G1-G2 deformation. Late-G1 and early-G2 deformation is synchronous with M1b metamorphism. The shearing that took place during this period at Gull Rapids has a southwest-side-up component, suggesting that the west side of Gull Rapids (the Split Lake Block) moved up relative to the east side

(supracrustal assemblage). This would suggest that the Split Lake Block was uplifted at this time. It has also been suggested that the exotic Assean Lake Crustal Complex was juxtaposed to the Split Lake Block post-M1 and prior to M2 (Corkery 1985; Böhm et al. 1999, 2001, 2003c; Kuiper et al. 2003, 2004a, b). This is consistent with regional data (although there is a lack of cooling ages for the Split Lake Block and Assean Lake Crustal Complex). M2 retrograde metamorphism to mid-amphibolite facies conditions were attained sometime after M1b peak metamorphism, but before 2.61 Ga (the age of pegmatite dykes).

6. Ca. 2.61 Ga: G4 shearing at Gull Rapids. This shearing is southwest-side-up, and is associated with pegmatite dyke emplacement (third intrusive phase). This shearing has a similar dip-slip component to the earlier G1-G2 shearing at Gull Rapids. No specific metamorphic event associated with G4 deformation is recognized at Gull Rapids.
7. 2.102–2.073 Ma: Mafic dyke emplacement along the margin of Superior craton (Gull Rapids, Split Lake Block; Heaman and Halls 2000; L. Heaman, unpublished data).
8. 1.8 Ga: Hudsonian deformation. G5 shearing and M3 greenschist facies retrogressive metamorphism at Gull Rapids (M3; Corkery 1985). This metamorphism may be hydrothermal alteration. Greenschist facies retrograde metamorphism (M3 of Corkery 1985) throughout Pikwitonei Granulite Domain, Split Lake Block, and Assean Lake Crustal Complex. A strong Hudsonian deformational overprint is not recognized at Gull Rapids, as only the G5 shear zones are recognized. However, the metamorphic overprint (M3) was much stronger, as is evidenced by pervasive greenschist retrogression of all rocks at Gull Rapids, and by the Paleoproterozoic metamorphic zircon growth observed in the samples dated.

6.3 REGIONAL SIGNIFICANCE

The Gull Rapids area is host to a spectacularly exposed sequence of multiply deformed Neoarchean rocks that have been mapped and studied in detail. The excellent crosscutting relationships between magmatism and deformation, as well as metamorphism, provide tight constraints on the timing of deformation and metamorphism at this portion of the Superior Boundary Zone. Despite the detailed analysis that could be made at Gull Rapids, the area is small (10 km^2), and not much outcrop exists outside of the study area. Therefore, reliable regional correlations cannot always be made, and when they are, such regional correlations require a certain amount of speculation.

The Gull Rapids area evolved through three generations of ductile deformation (G1 to G3) and two generations of ductile and brittle shearing (G4 to G5). The structural development (ductile to brittle transition) is consistent with transitions from prograde (mid- to upper-amphibolite) to retrograde (upper- to mid-amphibolite, and then to greenschist) metamorphism. There may have been an early, pre-G1 deformation in the area, which would have created an initial gneissosity in the amphibolite rafts in orthogneiss. G1 was a widespread event that created a regional foliation (S1) in the Gull Rapids supracrustal and orthogneiss assemblages, and local isoclinal folding (F1) in the supracrustal assemblage. M1a prograde metamorphism is roughly synchronous with G1 deformation. The foliation and folding may have been due to an early shearing event, which would have also been responsible for the development of a sheath fold system (F2) during G2 deformation. The regional lineation (L2) would have been created at this time as well, and would have moved older lineations in the orthogneiss (L-tectonite) into near parallelism with it. A local and rare S2 foliation was developed at this time in the supracrustal rocks. M1b peak metamorphism in the area is approximately synchronous with the transition between G1 and G2 deformation. The tectonism during G1-G2 created a kilometre-scale, north-northwest oriented, southwest-side-up, dextral shear zone. This shear zone is parallel to the orthogneiss-supracrustal contact (Figure 6.2). Since the orthogneiss assemblage at Gull Rapids is interpreted to belong to the Split Lake Block, this Gull Rapids shear zone lies at the

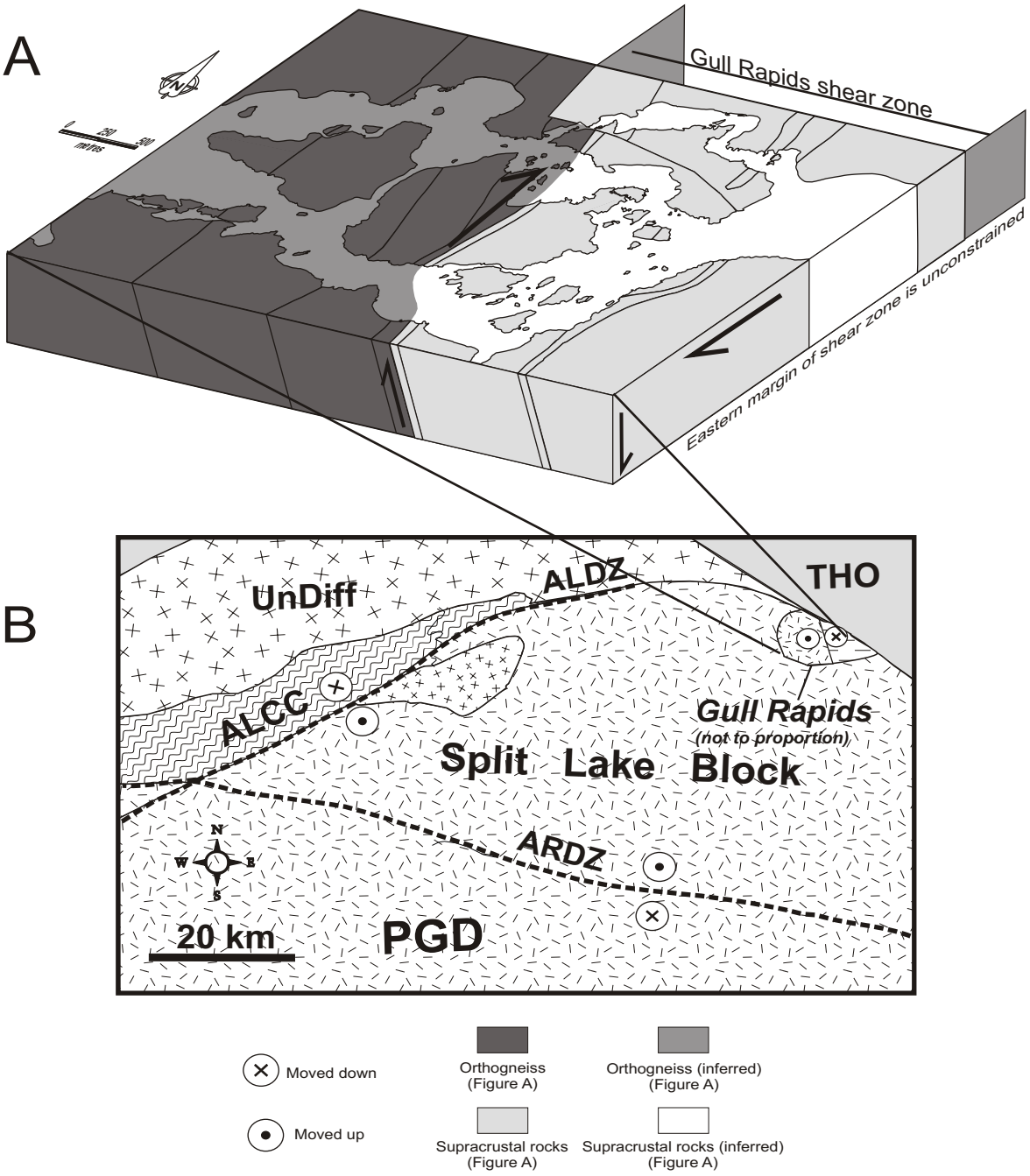

Figure 6.2. A. Schematic block diagram of Gull Rapids, showing large southwest-side-up shear zone in the supracrustal assemblage. The supracrustal assemblage is in juxtaposition with the orthogneiss assemblage, this juxtaposition is post-sedimentary deposition (see Chapter 3, 4). Contacts of the various units within each assemblage are shown. The Gull Rapids orthogneiss assemblage is interpreted to belong to the Split Lake Block, and thus this shear zone represents the uplift of the Split Lake Block at Gull Rapids. The eastern margin of the shear zone is unconstrained due to a lack of exposure. B. Superior craton margin, showing uplift of Split Lake Block along the Assean Lake and Aiken River deformation zones. Figure A zooms down to figure B; Gull Rapids area in B is not to sscale. PGD = Pikwitonei Granulite Domain; THO = Trans-Hudson Orogen; ALCC = Assean Lake Crustal Complex; Undiff = Reworked and juvenile Archean and Proterozoic rocks, respectively (undifferentiated); ALSZ = Assean Lake Deformation Zone; ARSZ = Aiken River Deformation Zone.

edge of the Split Lake Block and the shearing represents the uplift of the Split Lake Block. Ages of metamorphism obtained from this study at Gull Rapids agree well with those obtained for the Split Lake Block (e.g. Corkery 1985; Böhm et al. 1999).

The Assean Lake deformation zone, which strikes 050°, bounds the Split Lake Block to the south and older Archean rocks to the north (Kuiper et al. 2004a). This deformation zone has a significant component of southeast-side-up, dextral shearing, and in combination with north-side-up, dextral shearing along the Aiken River deformation zone (which lies at the southern boundary of the Split Lake Block; Kuiper et al. 2004b; Figure 6.2), signifies the uplift of the Split Lake Block. The shear zone at Gull Rapids has similar Split Lake Block-side-up shearing, and agrees with the regional information that indicates that the Split Lake Block was uplift during this time (ca. 2.68 Ga). The emplacement of granitoid bodies in the area during this time may be due to crustal extension associated with such uplift. Further cooling ages are required from the Split Lake Block and bounding Assean Lake and Aiken River deformation zones to provide better evidence that such uplift occurred during this time.

M2 metamorphism may be synchronous with the later stages of G2 deformation, or may be entirely post-G2. G3 deformation was later, and re-folded older foliations and folds. This was followed by G4 shearing and much later by G5 shearing associated with the Trans-Hudson orogeny. At Gull Rapids, M3 metamorphism is associated with G5 shearing. A supposed mylonitic-cataclastic shear zone exists just to the east and north of Gull Rapids, and supposedly represents the Superior craton margin itself (Hudsonian deformation). However, this young shear zone is no longer exposed at Gull Rapids.

The Gull Rapids area records a complex tectonic history, the bulk of which occurred during Neoarchean orogenesis, rather than during Paleoproterozoic (Hudsonian) orogenesis. Other portions of the Superior Boundary Zone, especially the Thompson belt, have experienced much greater thermotectonic overprinting due to the collisional tectonics of the Trans-Hudson Orogeny (Green et al. 1985; Bleeker 1990a; Weber 1990; Norquay 1997). It is known that deformation and

metamorphism at Gull Rapids largely post-dates emplacement and deposition of gneissic and supracrustal rocks, respectively. This deformation and metamorphism, aside from G5 and M3, is Neoarchean (ca. 2.68–2.61 Ga), and may represent a significant movement of crustal blocks (e.g. uplift of Split Lake Block). Late, weak deformation and strong metamorphism (G5, M3) is most likely related to the Paleoproterozoic Trans-Hudson orogeny. A weak Hudsonian deformational and strong Hudsonian metamorphic overprint is typical for many crustal segments of the Superior Boundary Zone, including the Split Lake Block. The Neoarchean and Paleoproterozoic zircon populations in the geochronological data also suggest that the Gull Rapids area largely experienced Neoarchean deformation and metamorphism with a weak Paleoproterozoic overprint. All of the evidence presented above suggests that the Gull Rapids area lies in a part of the Superior Boundary Zone, yet does not lie at the exact margin of the Superior craton, and therefore does not mark the exact Archean-Proterozoic boundary (i.e. Superior craton margin proper) in northeastern Manitoba.

REFERENCES

Ansdell, K.M., and Norman, A.R., 1995. U-Pb geochronology and tectonic development of the southern flank of the Kisseynew Domain, Trans-Hudson Orogen, Canada. Precambrian Research, **72**: 147-167.

Baragar, W.R.A., and Scoates, R.F.J., 1981. The Circum-Superior belt; a Proterozoic plate margin? *In* Precambrian Plate Tectonics. *Edited by* A. Kröner. Elsevier, Amsterdam, pp. 297-330.

Bleeker, W., 1990*a*. New structural-metamorphic constraints on Early Proterozoic oblique collision along the Thompson Nickel Belt, Manitoba, Canada. *In* The Early Proterozoic Trans-Hudson Orogen of North America. *Edited by* J.F. Lewry and M.R. Stauffer. Geological Association of Canada, Special Paper **37**, pp. 57-73.

Bleeker, W., 1990*b*. Evolution of the Thompson Nickel Belt and its nickel deposits, Manitoba, Canada. Ph.D. Thesis, University of New Brunswick, Fredericton, 400 p.

Böhm, C.O., Heaman, L.M., and Corkery, M.T., 1999. Archean crustal evolution of the northwestern Superior craton margin: U-Pb zircon results from the Split Lake Block. Canadian Journal of Earth Sciences, **36**: 1973-1987.

Böhm, C.O., Heaman, L.M., Creaser, R.A., and Corkery, M.T., 2000. Discovery of pre-3.5 Ga exotic crust at the northwestern Superior Province margin, Manitoba. Geology, **28**: 75-78.

Böhm, C.O., Heaman, L.M., Creaser, R.A., Corkery, M.T., and Stern, R.A., 2001. Two billion years of crustal evolution preserved at the NW Superior Craton margin. *In* Western Superior Lithoprobe Transect / Western Superior NATMAP 2001 Joint Annual Meeting. *Edited by* R.M. Harrap and H.H. Helmstaedt. Lithoprobe Report **80**, pp. 29-35.

Böhm, C.O., Bowerman, M.S., and Downey, M.W., 2003*a*. Bedrock mapping in the Gull Rapids area, northern Manitoba (NTS 54D6). *In* Report of Activities, 2003. Manitoba Industry, Economic Development and Mines, Manitoba Geological Survey, Winnipeg, pp. 92-104.

Böhm, C.O., Bowerman, M.S., and Downey, M.W., 2003*b*. Geology of the Gull Rapids area, Manitoba (NTS 54D6). Manitoba Industry, Economic Development and Mines, Manitoba Geological Survey, Preliminary Map PMAP2003-3, scale 1:5 000.

Böhm, C.O., Heaman, L.M., Stern, R.A., Corkery, M.T., and Creaser, R.A., 2003*c*. Nature of Assean lake ancient crust, Manitoba: a combined SHRIMP–ID-TIMS U–Pb geochronology and Sm–Nd isotope study. Precambrian Research, **126**: 55-94.

Böhm, C.O., Corkery, M.T., Bowerman, M.S., Downey, M.W., Hartlaub, R.P., Kuiper, Y.D., Heaman, L.M., and Lin, S., 2003*d*. Superior margin programs in the lower Nelson River region, Manitoba (parts of NTS 54D and 64A): year one. *In* Report of Activities, 2003. Manitoba Industry, Economic Development and Mines, Manitoba Geological Survey, Winnipeg, pp. 86-91.

Böhm, C.O., Bowerman, M.S., Downey, M.W., Hartlaub, R.P., and Kuiper, Y.D., 2004. Superior Margin Program News. *Abstract for oral presentation* at 2004 Manitoba Mines and Minerals Convention, Manitoba Industry, Economic Development and Mines, Manitoba Geological Survey, Winnipeg, November 15-18th, 2004.

Bowerman, M. S., Böhm, C.O., Hartlaub, R.P., Heaman, L.M., and Creaser, R.A., 2004. Preliminary geochemical and isotopic results from the Gull Rapids area of the eastern Split Lake Block, northwestern Superior Province, Manitoba (parts of NTS 54D5 and 6). *In* Report of Activities, 2004. Manitoba Industry, Economic Development and Mines, Manitoba Geological Survey, Winnipeg, pp. 156-170.

Card, K.D., 1990. A review of the Superior Province of the Canadian Shield, a product of Archean accretion. Precambrian Research, **48**: 99-156.

Cherniak, D.J., 1993. Lead diffusion in titanite and preliminary results on the effects of radiation damage on Pb transport. Chemical Geology, **110**: 177-194.

Cherniak, D.J., and Watson, E.B., 2001. Pb diffusion in zircon. Chemical Geology, **173**: 5-24.

Corkery, M.T., 1975. Lower Nelson River Project (54D-5, 6, 11, 12). *In* Manitoba Mineral Resources Division, Summary of Geological Fieldwork 1975. Geological Paper (Winnipeg), **75-3**: 36-37.

Corkery, M.T., 1985. Geology of the Lower Nelson River Project area, Manitoba. Manitoba Energy and Mines, Geological Report **GR82-1**, 66 p.

Corkery, M.T., Davis, D.W., and Lenton, P.G., 1992. Geochronological constraints on the development of the Cross Lake greenstone belt, northwest Superior Province, Manitoba. Canadian Journal of Earth Sciences, **29**: 2171-2185.

Corrigan, D., 2004*a*. Evolutionary Tectonic Development of the Trans-Hudson Orogen – a tale of three cratons, a large ocean, accretionary and collisional tectonics. *In* LITHOPROBE Celebratory Conference Oral and Poster Presentations. *Compiled by* R.M. Clowes and C. Li. Published by the LITHOPROBE Secretariat, University of British Columbia, Vancouver, Canada, E-Publication No. 5, CD vol. 2.

Corrigan, D., 2004*b*. The Middle Earth I: Ancient oceanic crust in the middle of the Prairies and formation of the Canadian Shield 2000 to 1800 million years ago. *In* LITHOPROBE Celebratory Conference Oral and Poster Presentations. *Compiled by* R.M. Clowes and C. Li. Published by the LITHOPROBE Secretariat, University of British Columbia, Vancouver, Canada, E-Publication No. 5, CD vol. 2.

Cruden, A.R., 1990. Flow and fabric development during the diapiric rise of magma. Journal of Geology, **98**: 681-698.

Cruden, A.R., 1998. On the emplacement of tabular granites. Journal of the Geological Society, London, **155**: 853-862.

Davis, W.J., McNicoll, V.J., Bellerive, D.L., Santowski, K., and Scott, D.J., 1997. Modified chemical procedures for the extraction and purification of uranium from titanite, allanite, and rutile in the Geochronology Laboratory, Geological Survey of Canada. *In* Radiogenic Age and Isotopic Studies, Report 10. Geological Survey of Canada, Current Research **1997-F**, pp. 33-35.

Downey, M.W., Lin, S., and Böhm, C.O., 2004. New insights into the structural geology and timing of deformation at the Superior craton margin, Gull Rapids, Manitoba (NTS 54D6). *In* Report of

Activities 2004. Manitoba Industry, Economic Development and Mines, Manitoba Geological Survey, Winnipeg, pp. 171–186.

Elphick, S.C., 1970. Metamorphic petrology of the Gillam area (Archean), Manitoba. MSc. Thesis, University of Manitoba, Winnipeg, 75 p.

Frost, B.R., Chamberlain, K.R., and Schumacher, J.C., 2000. Sphene (titanite): phase relations and role as a geochronometer. Chemical Geology, **172**: 131-148.

Green, A.G., Hajnal, Z., and Weber, W., 1985. An evolutionary model of the western Churchill Province and western margin of the Superior Province of Canada and the north-central United States. Tectonophysics, **116**: 281-322.

Halls, H.C., and Heaman, L.M., 2000. The paleomagnetic significance of new U-Pb age data from the Molson dyke swarm, Cauchon Lake area, Manitoba. Canadian Journal of Earth Sciences, **37**: 957-966.

Hartlaub, R.P., Heaman, L.M., Böhm, C.O., and Corkery, M.T, 2003. Split Lake Block revisited: new geological constraints from the Birthday to Gull rapids corridor of the lower Nelson River (NTS 54D5 and 6). *In* Report of Activities 2003, Manitoba Industry, Economic Development and Mines, Manitoba Geological Survey, Winnipeg, pp. 114-117.

Hartlaub, R.P., Böhm, C.O., Kuiper, Y.D., Bowerman, M.S. and Heaman, L.M. 2004. Archean and Paleoproterozoic geology of the northwestern Split Lake Block, Superior Province, Manitoba (parts of NTS 54D4, 5, 6 and 64A1). *In* Report of Activities 2004. Manitoba Industry, Economic Development and Mines, Manitoba Geological Survey, Winnipeg, pp. 187-194.

Haugh, I., and Elphick, S.C., 1968. Kettle Rapids-Moose Lake area. *In* Manitoba Mines Branch, Summary of Geological Fieldwork 1968. Geological Paper (Winnipeg), **68-3**: 29-37.

Heaman, L.M., Machado, N., and Krogh, T.E., 1986*a*. Preliminary U-Pb zircon results from the Pikwitonei granulite terrain, Manitoba. Geological Association of Canada – Mineralogical Association of Canada, Joint Annual Meeting, Program with Abstracts, **Vol. 11**, p. 79.

Heaman, L.M., Machado, N., Krogh, T.E., and Weber, W., 1986*b*. Precise U-Pb zircon ages for the Molson dyke swarm and the Fox River sill; constraints for early Proterozoic crustal evolution in northeastern Manitoba, Canada. Contributions to Mineralogy and Petrology, **94**: 82-89.

Heaman, L.M., and Parrish, R.R., 1991. U-Pb geochronology of accessory minerals. *In* Applications of Radiogenic Isotope Systems to Problems in Geology. *Edited by* L.M. Heaman and J.N. Ludden. Mineralogical Association of Canada, Short Course Handbook **19**, pp. 59-102.

Heaman, L.M., and Corkery, M.T., 1996. U-Pb geochronology of the Split Lake Block, Manitoba; preliminary results. *In* Trans-Hudson Orogen Lithoprobe Transect, Sixth Transect Meeting. *Edited by* Z. Hajnal and J. F. Lewry. Lithoprobe Report **55**, pp.60-68.

Heaman, L.M., 2005. Precambrian mafic magmatism: contribution to the growth of continental roots. *In* LITHOPROBE Celebratory Conference Oral and Poster Presentations. *Compiled by* R.M. Clowes and C. Li. Published by the LITHOPROBE Secretariat, University of British Columbia, Vancouver, Canada, E-Publication No. 5, CD vol. 2.

Hoffman, P.F., 1988. United plates of America, the birth of a craton; early Proterozoic assembly and growth of Laurentia. Annual Review of Earth and Planetary Sciences, **16**: 543-603.

Hoffman, P.F., 1990. Subdivision of the Churchill Province and extent of the Trans-Hudson Orogen. *In* The Early Proterozoic Trans-Hudson Orogen of North America. *Edited by* J.F. Lewry and M.R. Stauffer. Geological Association of Canada, Special Paper **37**, pp. 15-39.

Hubregtse, J.J.M.W., 1980. The Archean Pikwitonei granulite domain and its position at the margin of the northwestern Superior Province (central Manitoba). Geological Paper (Winnipeg), **80-3**, 16 p.

Kuiper, Y.D., 2003. Isotopic constraints on timing of deformation and metamorphism in the Thor-Odin dome, Monashee Complex, southeastern British Columbia. Ph.D. Thesis, University of New Brunswick, Fredericton, 321 p.

Kuiper, Y.D., Lin, S., Böhm, C.O., and Corkery, M.T., 2003. Structural geology of the Assean Lake and Aiken River deformation zones, northern Manitoba (NTS 64A1, 2 and 8). *In* Report of Activities 2003. Manitoba Industry, Economic Development and Mines, Manitoba Geological Survey, Winnipeg, pp. 105–113.

Kuiper, Y.D., Lin, S., Böhm, C.O., and Corkery, M.T., 2004*a*. Structural geology of Assean Lake, Manitoba (NTS 64A1, 2 and 8). *In* Report of Activities 2004. Manitoba Industry, Economic Development and Mines, Manitoba Geological Survey, Winnipeg, pp. 195–200.

Kuiper, Y.D., Lin, S., Böhm, C.O., and Corkery, M.T., 2004*b*. Structural geology of the Aiken River deformation zone, Manitoba (NTS 64A1 and 2). *In* Report of Activities 2004. Manitoba Industry, Economic Development and Mines, Manitoba Geological Survey, Winnipeg, pp. 201–208.

Kuiper, Y.D., Lin, S., Böhm, C.O., and Corkery, M.T., 2005. Shear zones of the Superior Boundary Zone northeast of Thompson, Manitoba. Canadian Tectonics Group, 25th Anniversary Meeting, Orillia, Ontario, Canada, 28th-30th October, 2005. Program with Abstracts, p. 25.

Lewry, J.F., and Collerson, K.D., 1990. The Trans-Hudson Orogen; extent, subdivision, and problems. *In* The Early Proterozoic Trans-Hudson Orogen of North America. *Edited by* J.F. Lewry and M.R. Stauffer. Geological Association of Canada, Special Paper **37**, pp. 1-14.

Lewry, J.F., Thomas, D.J., Macdonald, R., Chiarenzelli, J.R., 1990. Structural relations in accreted terranes of the Trans-Hudson Orogen, Saskatchewan; telescoping in a collisional regime? *In* The Early Proterozoic Trans-Hudson Orogen of North America. *Edited by* J.F. Lewry and M.R. Stauffer. Geological Association of Canada, Special Paper **37**, pp. 75-94.

Lin, S., and Jiang, D., 2001. Using along-strike variation in strain and kinematics to define the movement direction of curved transpressional shear zones; an example from northwestern Superior Province, Manitoba. Geology, **29**: 767-770.

Lindal, D., 1992. Kettle Rapids (NTS 54D). Manitoba Energy and Mines, Manitoba Geological Survey, Bedrock Geology Compilation Map Series, scale 1:250 000.

Ludwig, K.R., 2003. User's manual for Isoplot/Ex rev. 3.00: a Geochronological Toolkit for Microsoft Excel. Special Publication, 4, Berkeley Geochronology Center, Berkeley, 70 p.

Machado, N., Zwanzig, H.V., and Parent, M., 1999. U-Pb ages of plutonism, sedimentation, and metamorphism of the Paleoproterozoic Kisseynew metasedimentary belt, Trans-Hudson Orogen (Manitoba, Canada). Canadian Journal of Earth Sciences, **36**: 1829-1842.

Mawer, C.K., and Williams, P.F., 1991. Progressive folding and foliation development in a sheared, coticule-bearing phyllite. Journal of Structural Geology, **13**: 539-555.

Mezger, K., Hanson, G.N., and Bohlen, S.R., 1986. Investigations of metamorphism in the Pikwitonei Domain. *In* Report of Field Activities 1986. Mineral Resources Division, Manitoba Geological Survey, Winnipeg, pp.204-205.

Mezger, K., Bohlen, S.R., and Hanson, G.N., 1990. Metamorphic history of the Archean Pikwitonei granulite domain and the Cross Lake Subprovince, Superior Province, Manitoba, Canada. Journal of Petrology, **31**: 483-517.

Mezger, K., and Krogstad, E.J., 1997. Interpretation of discordant U-Pb zircon ages: An evaluation. Journal of Metamorphic Geology, **15**: 127-140.

Morgan, S.S., Law, R.D., and Nyman, M.W., 1998. Laccolith-like emplacement model for the Papoose Flat pluton based on porphyroblast-matrix analysis. Geological Society of America Bulletin, **110**, 96-110.

Nemchin, A.A., and Pidgeon, R.T., 1997. Evolution of the Darling Range Batholith, Yilgarn Craton, Western Australia: a SHRIMP zircon study. Journal of Petrology, **38**: 625-649.

Norman, A.R., Williams, P.F., and Ansdell, K.M., 1995. Early Proterozoic deformation along the southern margin of the Kisseynew gneiss belt, Trans-Hudson Orogen; a 30 Ma progressive deformation cycle. Canadian Journal of Earth Sciences, **32**: 875-894.

Norquay, L.I., 1997. Structural and metamorphic evolution of the North Star Lake area, Manitoba. MSc. Thesis, University of Manitoba, Winnipeg, 244 p.

Parks, J., Lin, S., Davis, D., and Corkery, T., *submitted*. Geochronological constraints on the history of the Island Lake greenstone belt and the relationship of terranes in the northwestern Superior Province.

Parmenter, A.C., 2002. The structural evolution of the Pipestone Lake area in the Cross Lake Greenstone Belt, northwestern Superior Province, Manitoba. MSc. Thesis, University of Waterloo, Waterloo, Ontario, 91 p.

Parrish, R.R., Bellerive, D.L., and Sullivan, R.W., 1992. U-Pb chemical procedures for titanite and allanite in the Geochronology Laboratory, Geological Survey of Canada. *In* Radiogenic Age and Isotopic Studies, Part 5. Geological Survey of Canada, Paper **91-2**, pp. 187-190.

Passchier, C.W., Myers, J.S., and Kröner, A., 1990. Field Geology of High-Grade Gneiss Terrains. Springer-Verlag, Berlin, Heidelberg, Germany, 150 p.

Paterson, S.R., and Fowler, Jr., T.K., 1993. Re-examining pluton emplacement processes. Journal of Structural Geology, **15**, 191-206.

Percival, J.A., and Skulski, T., 1998. Superior Province tectonics; new wrinkles on some old rocks. Geological Society of America Annual Meeting, Abstracts with Programs, **Vol. 30, No.7**, pp. 45-46.

Percival, J.A., Bleeker, W., Cook, F.A., Rivers, T., Ross, G., and van Staal, C., 2004. PanLITHOPROBE workshop IV; Intra-orogen correlations and comparative orogenic anatomy. Geoscience Canada, **Vol. 31, No. 1**, pp. 23-39.

Percival, J.A., Sanborn-Barrie, M., Skulski, T., Stott, G.M., and Helmstaedt, H., *submitted*. Tectonic evolution of the Western Superior Province from NATMAP and Lithoprobe studies.

Pidgeon, R.T., 1992. Recrystallisation of oscillatory zoned zircon: some geochronological and petrological implications. Contributions to Mineralogy and Petrology, **110**: 463-472.

Pidgeon, R.T., and Compston, W., 1992. A SHRIMP ion microprobe study of inherited and magmatic zircons from four Scottish Caledonian granites. Transactions of the Royal Society of Edinburgh: Earth Sciences, **83**: 473-483.

Skulski, T., Whalen, J.B., Stern, R.A., Stone, D., Corkery, M.T., 1999. Archean terranes and their boundaries in the northern Superior Province. *In* Lithoprobe Western Superior Transect Fifth Annual Workshop. *Edited by* R.M. Harrap and H.H. Helmstaedt. Lithoprobe Report **70**, pp. 163-165.

Skulski, T, Corkery, M.T., Stone, D., Whalen, J.B., and Stern, R.A., 2000. Geological and geochronological investigations in the Stull Lake-Edmund Lake greenstone belt and granitoid rocks of the northwestern Superior Province. *In* Report of Activities 2000. Manitoba Industry, Trade and Mines, Manitoba Geological Survey, Winnipeg, pp. 117–128.

Stauffer, M.R., 1984. Manikewan; an early Proterozoic ocean in central Canada, its igneous history and orogenic closure. Precambrian Research, **25**: 257-281.

Stern, R.A., 1997. The GSC Sensitive High Resolution Ion Microprobe (SHRIMP): analytical techniques of zircon U-Th-Pb age determinations and performance evaluation. *In* Radiogenic Age and Isotopic Studies; Report 10. Geological Survey of Canada, Current Research **1997-F**, pp.1-31.

Stern, R.A., and Amelin, Y., 2003. Assessment of errors in SIMS zircon U-Pb geochronology using a natural zircon standard and NIST SRM 610 glass. Chemical Geology, **197**: 111-142.

Stott, G.M., 1997. The Superior Province, Canada. *In* Greenstone belts. *Edited by* M.J. De Wit and L.D. Ashwal. Oxford Monographs on Geology and Geophysics, **Vol. 35**, pp.480-507.

Thurston, P.C., Osmani, I.A., and Stone, D., 1991. Northwestern Superior Province; review and terrane analysis. *In* Geology of Ontario. *Edited by* P.C. Thurston, H.R. Williams, and R.H. Sutcliffe. Ontario Geological Survey Special Volume, **Vol. 4, No. 1**, pp.81-142.

Vernon, R.H., 1986. K-feldspar megacrysts in granites; phenocrysts, not porphyroblasts. Earth-Science Reviews, **23**: 1-63.

Vernon, R.H., 1990. K-feldspar augen in felsic gneisses and mylonites; deformed phenocrysts or porphyroblasts? Geologiska Föreningens i Stockholm Förhandlingar, **Vol. 112, Part 2**, pp.157-167.

Weber, W., 1990. The Churchill-Superior boundary zone, southeast margin of the Trans-Hudson Orogen: a review. *In* The Early Proterozoic Trans-Hudson Orogen of North America. *Edited by* J.F. Lewry and M.R. Stauffer. Geological Association of Canada, Special Paper **37**, pp. 41-55.

Weber, W., and Scoates, R.F.J., 1978. Archean and Proterozoic metamorphism in the northwestern Superior Province and along the Churchill-Superior boundary, Manitoba. *In* Metamorphism in the Canadian Shield. *Edited by* J.A. Fraser and W.W. Heywood. Geological Survey of Canada, Paper **78-10**, pp. 5-16.

Weber, W., and Mezger, K., 1990. An oblique cross section of Archean continental crust at the northwestern margin of Superior Province, Manitoba, Canada. *In* Exposed cross-sections of the continental crust. *Edited by* M.H. Salisbury and D.M. Fountain. NATO ASI Series. Series C: Mathematical and Physical Sciences, **Vol. 317**, pp. 327-341.

White, D.J., Jones, A.G., Lucas, S.B., and Hajnal, Z., 1999. Tectonic evolution of the Superior boundary zone from coincident seismic reflection and magnetotelluric profiles. Tectonics, **18**: 430-451.

White, D.J., Lucas, S.B., Bleeker, W., Hajnal, Z., Lewry, J.F., and Zwanzig, H.V., 2002. Suture-zone geometry along an irregular Paleoproterozoic margin; the Superior boundary zone, Manitoba, Canada. Geology, **30**: 735-738.

Williams, I.S., and Claesson, S., 1987. Isotopic evidence for the Precambrian provenance and Caledonian metamorphism of high grade paragneisses from the Seve Nappes, Scandinavian Caledonides, II: Ion microprobe zircon U–Th–Pb. Contributions to Mineralogy and Petrology, **97**: 205-217.

Williams, I.S., 1992. Some observations on the use of zircon U-Pb geochronology in the study of granitic rocks. Transactions of the Royal Society of Edinburgh: Earth Sciences, **83**: 447-458.

Williams, I.S., Buick, I.S., and Cartwright, I., 1996. An extended episode of early Mesoproterozoic metamorphic fluid flow in the Reynolds Range, central Australia. Journal of Metamorphic Geology, **14**: 29-47.

Williams, P.F., and Jiang, D., 2001. The role of initial perturbations in the development of folds in a rock-analogue. Journal of Structural Geology, **23**: 845-856.

Yardley, B.W.D., 1989. An Introduction to Metamorphic Petrology. Longman Earth Science Series, Pearson Education Limited, Essex, England, 248 p.

Zwanzig, H.V., 1990. Kisseynew gneiss belt in Manitoba; stratigraphy, structure, and tectonic evolution. *In* The Early Proterozoic Trans-Hudson Orogen of North America. *Edited by* J.F. Lewry and M.R. Stauffer. Geological Association of Canada, Special Paper **37**, pp. 95-120.

Zwanzig, H.V., 1999. Structure and stratigraphy of the south flank of the Kisseynew Domain in the Trans-Hudson Orogen, Manitoba; implications for 1.845-1.77 Ga collision tectonics. Canadian Journal of Earth Sciences, **36**: 1859-1880.

Zwanzig, H.V., 2005. Hot, thin and mineral-rich – evolution of the Paleoproterozoic Trans-Hudson Orogen in western Canada. *Abstract and oral presentation for* 2004 Robinson Lecture Tour. Manitoba Geological Survey; Manitoba Industry, Economic Development and Mines.

Appendix A

Location map for geochronology samples mentioned in text

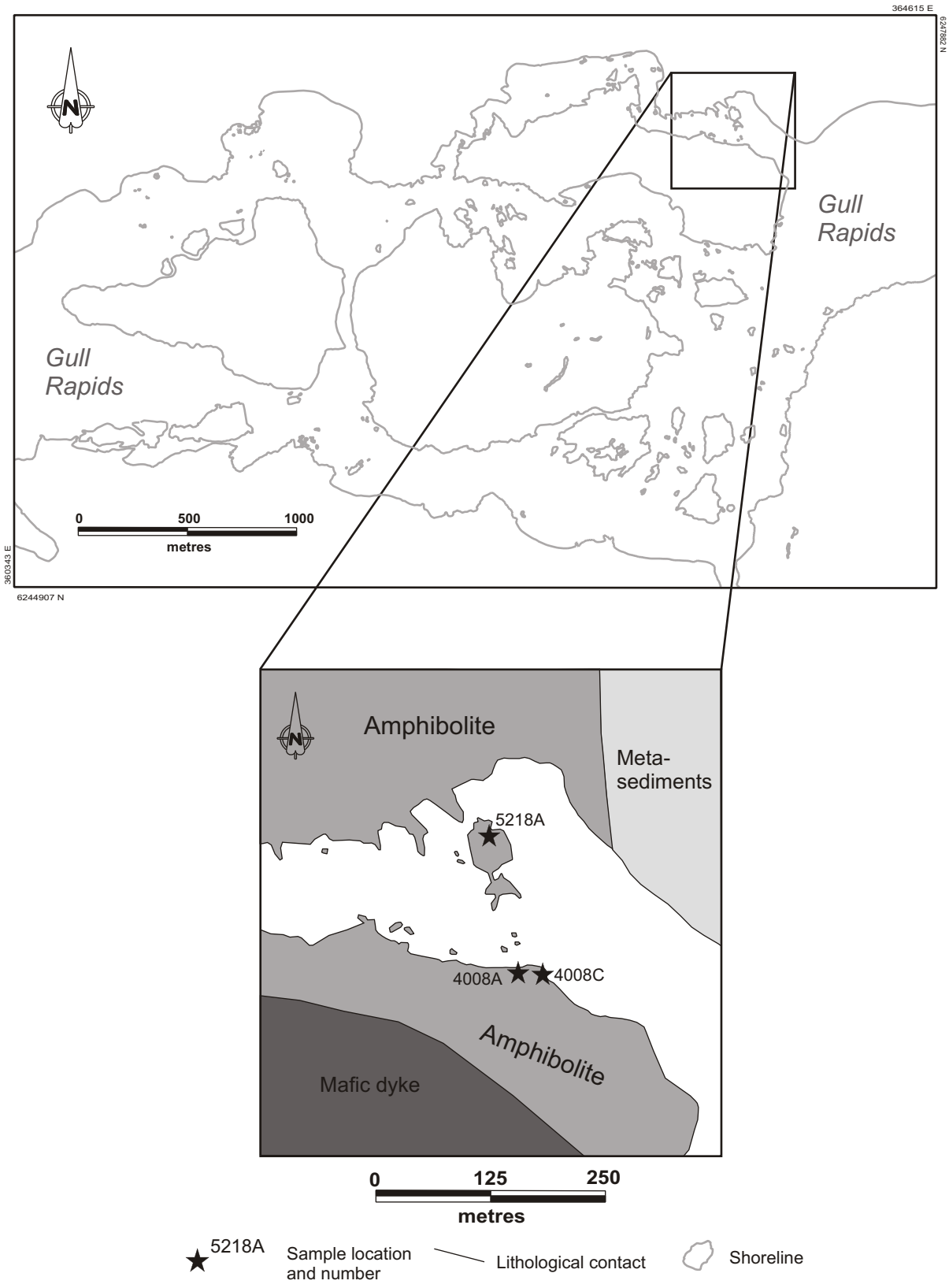

Appendix A: Sample location map, Gull Rapids northern portion of amphibolite. Refer to Figure 1.3.

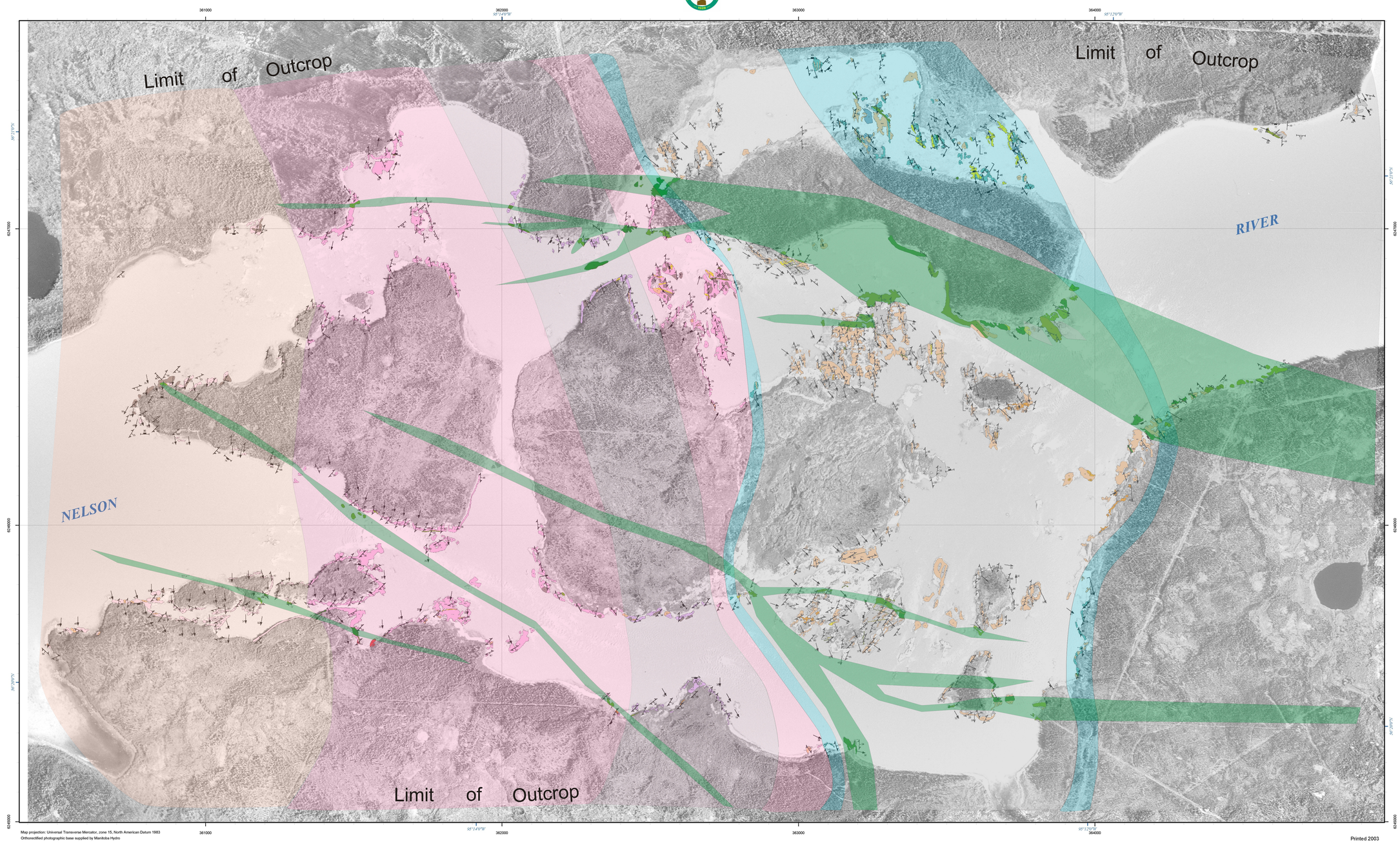

modified after Preliminary Map: PMAP2003-3

Geology of the Gull Rapids area, Manitoba (part of NTS 54D6)

Geology by:
C.O. Böhm, M.S. Bowerman[1] and M.W. Downey[2]

[1] Department of Earth and Atmospheric Sciences, University of Alberta, Edmonton, Alberta T6G 2E3
[2] Department of Earth Sciences, University of Waterloo, Waterloo, Ontario N2L 3G1

Logistical and financial support for this project was provided by Manitoba Hydro

Cartography by B. Lenton and P. Lenton

Published by:
Manitoba Industry, Economic Development and Mines
Manitoba Geological Survey, 2003

This map is a provisional summary of work carried out during the summer field season and is produced directly from the geologist's manuscript. It is not to be regarded as a final interpretation of the geology of the area.

SUGGESTED REFERENCE
Böhm, C.O., Bowerman, M.S. and Downey, M.W. 2003: Geology of the Gull Rapids area, Manitoba (part of NTS 54D6); Manitoba Industry, Economic Development and Mines, Manitoba Geological Survey, Preliminary Map PMAP2003-3, scale 1:5000.

0 100 200 300 400 500 Metres

1:5 000

Index Map

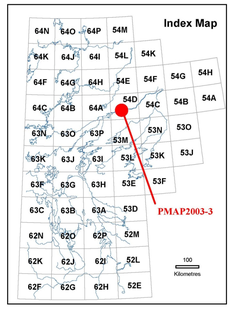

Legend

Mesoarchean granodiorite and derived gneissic rocks

- 1 — Mesoarchean granodiorite and derived gneissic rocks
- 1a — Granodiorite L-tectonite: strongly stretched, contains biotite±amphibole
- 1b — Leucogranodiorite and derived gneiss: contains biotite±amphibole, locally straight-layered to strongly foliated and sheared
- 1c — Granodiorite augen gneiss: locally up to 25% biotite±amphibole, strongly foliated

Archean mafic igneous rocks

- 2a — Amphibolite interpreted as metabasalt: massive to laminated and strongly foliated, composed of hornblende+ plagioclase±epidote±chlorite; interlayered with (and interpreted to be intruded by) unit 2B; contains intrusions of unit 4 and orthopyroxene-bearing leucosome
- 2b — Amphibolite interpreted as metagabbro: medium to coarse grained, strongly foliated; contains intrusions of unit 4 and orthopyroxene-bearing leucosome

Archean metasedimentary rocks

- 3a — Metagreywacke: interlayered pelite and psammite (centimetre to metre scaled), medium to dark grey and brown, Fe-rich, composed of quartz+biotite+feldspar±garnet±amphibole±pyroxene±staurolite±cordierite; locally arkosic with calc-silicate layers; contains up to 80% unit 4 as irregular bodies and foliation-parallel dikes and dikelets (locally orthopyroxene-bearing); primary bedding rarely preserved, moderately to strongly foliated, lineated, and folded
- 3b — Banded iron formation: oxide-, sulphide-, and silicate-facies; composed of quartz±chert±magnetite±hematite±garnet ±amphibole±pyroxene±biotite±sulphides; form discontinuous boudinaged foliation-parallel layers (few centimetres up to 3 metres wide) in unit 3A
- 3c — Ultramafic to mafic polymict metaconglomerate: forms rare lenses in unit 3A, lenses are moderately to strongly foliated and foliation-parallel

Neoarchean granitoid injection and pegmetite (veins and bodies in units 1-3)

- 4a — Granitic injection: as veins, sheets, leucosome pods, and irregular bodies; leucocratic, medium to coarse grained, locally contains aggregates (up to 5 cm) of biotite+garnet+amphibole±pyroxene partly retrogressed to chlorite (orthopyroxene retrogressed to clinopyroxene and amphibole)
- 4b — Grey tonalite: fine to medium grained, massive to weakly foliated
- 4c — Granitoid pegmatite: massive to layered, coarse to very coarse grained, forms dikes in units 1-3, 4A, and 4B

Paleoproterozoic mafic dikes

- 5 — Paleoproterozoic mafic rocks
- 5a — Gabbro dike: few metres up to 50 metres wide, medium to coarse grained, massive to locally weakly foliated in shear zones, composed of amphibole+plagioclase+pyroxene±sulphides
- 5b — Diabase dike: few centimetres to few metres wide, fine grained, massive to locally weakly foliated in shear zones; crosscuts unit 5A
- 5c — Mafic volcaniclastic rock
- A — Amphibolite rafts: hornblendite, metadiorite and rare metapyroxenite composition, form up to 10 metres wide discontinuous zones of angular to rounded xenoliths in unit 1; rafts are generally aligned to S1 and are moderately to weakly foliated
- G — Garnetite interpreted as iron formation: composed of garnet+feldspar±cordierite and heavy minerals (e.g. ilmenite, zircon, monazite), massive

Symbols

Layering
- bedding, topping unknown

Foliations
- foliation; generation unknown
- gneissocity; generation unknown

Shear zone
- dextral shear
- sinistral shear
- shear sense unknown

Fault
- dextral fault
- sinistral fault
- fault movement unknown

Lineation
- lineation

Minor fold
- minor fold axis
- axial plane of minor fold

Manitoba
Building for the Future